UNIVERSIDAD NACIONAL AUTÓNOMA DE MEXICO

POSGRADO EN CIENCIAS FÍSICAS

GEOMETRY OF MULTIPARTITE QUANTUM SYSTEMS

TESIS
QUE PARA OPTAR POR EL GRADO DE:
DOCTOR EN CIENCIAS (FÍSICA)

PRESENTA:
CHRISTIAN LOUIS HANOTEL PINZÓN

DR. CHRYSSOMALIS CHRYSSOMALAKOS
INSTITUTO DE CIENCIAS NUCLEARES

DR. DANIEL EDUARDO SUDARSKY SAIONZ
INSTITUTO DE CIENCIAS NUCLEARES

DR. ELIAS OKON GURVICH
INSTITUTO DE INVESTIGACIONES FILOSÓFICAS

CIUDAD DE MÉXICO, AGOSTO, 2022

Contents

Resumen

Nuestro entendimiento de las teorías físicas es, en buena medida, una cuestión de perspectivas. Dada una teoría física, un problema complejo puede reducirse a un problema trivial si lo apreciamos de la manera adecuada. Lo mismo ocurre con leyes físicas, teoremas y nociones físicas en general. Esto, sin duda, se aplica a la teoría de interés en esta tesis: la mecánica cuántica.

La mecánica cuántica en las últimas décadas ha comenzado a estudiarse desde una perspectiva geométrica, en contraparte con el enfoque algebraico tradicional. Este acercamiento ha permitido revelar sistemas cuánticos con propiedades excepcionales, nos ha dado una serie de herramientas para resolver problemas, así como un conjunto de conceptos que enriquecen nuestro entendimiento de la teoría misma. Estas aportaciones se han materializado en aplicaciones en campos como la computación cuántica o la metrología cuántica, como podremos ejemplificar en esta tesis.

Una ilustración de este enfoque está dada por la representación de Majorana, que es una manera de visualizar estados cuánticos de espín s como conjuntos de $2s$ puntos en la esfera unitaria, representando rotaciones de una manera conveniente, como explicaremos más adelante. A manera de ejemplo, considere el estado de espín 6 $|\psi\rangle = \frac{1}{5}\left(-\sqrt{7}|6,5\rangle + \sqrt{11}|6,0\rangle + \sqrt{7}|6,-5\rangle\right)$. A simple vista, sus propiedades rotacionales no son evidentes, mientras que por medio de la representación de Majorana este estado está representado por los vértices de un icosaedro, revelando las diversas simetrías que tiene este estado. De este modo, no sólo pudimos revelar las simetrías del estado, sino que tenemos una herramienta para visualizar estados que habitan en un espacio de Hilbert de dimensión alta.

Estas no son todas las consecuencias físicas que podemos obtener de esta perspectiva geométrica, sabemos también que estas simetrías nos dan información sobre valores esperados de ciertas observables, sobre ciertas fases geométricas del estado en evoluciones por medio de rotaciones y también sobre el enredamiento de algunos sistemas multipartitos. Con esto vemos que un enfoque geométrico en mecánica cuántica puede ser uno de los caminos para avanzar en nuestro conocimiento de la materia. Quizás este enfoque permita en un futuro tener un mayor conocimiento conjunto de la mecánica cuántica con otras teorías físicas con descripciones puramente geométricas, como ocurre con la relatividad general.

En esta tesis estudiaremos sistemas cuánticos multipartitos a través de una perspectiva geométrica. En particular, abordaremos algunos problemas geométricos relacionados con este tipo de sistemas. Veremos aspectos relacionados con rotaciones, fases geométricas, enredamiento, además de algunas herramientas para su visualización. Veremos también algunas aplicaciones relacionados con diversos temas en el contexto de información cuántica. También mostraremos algunos resultados de corte matemático que nos permiten entender de mejor manera las relaciones entre distintos resultados obtenidos.

Para poder dar un planteamiento preciso de los problemas estudiados y los resultados en las diferentes direcciones será necesario hacer una breve revisión de ciertas nociones fundamentales. En el capítulo 1 se presentan las ideas básicas sobre la mecánica cuántica, haciendo un énfasis particular en su estructura geométrica. En este capítulo presentamos el espacio proyectivo complejo y destacamos sus propiedades geométricas a distintos niveles: como variedad riemanniana, simpléctica, compleja y Kähler. También en este capítulo se presenta la representación de Majorana y su relación con rotaciones en mecánica cuántica.

El segundo capítulo da un panorama sobre la geometría de los sistemas cuánticos multipartitos. Este tipo de sistemas tienen correlaciones no locales que han mostrado ser de relevancia en diversos campos como computación cuántica, criptografía cuántica, metrología cuántica y un largo etcétera en el campo de las tecnologías cuánticas. Estas correlaciones suelen estudiarse a través del concepto de enredamiento, el cual tiene un origen algebraico. En este capítulo se discutirán estas ideas y también ejemplificaremos cómo los métodos geométricos nos permiten entender a las correlaciones de distintas maneras, llevándonos a conceptos más allá del enredamiento que son de utilidad en diversos contextos en información cuántica. Al

final del capítulo veremos cómo actúa el grupo de rotaciones en este tipo de sistemas, lo cuál será el punto de partida para el material de los capítulos 3 y 4.

En el capítulo 3 estudiamos aspectos geométricos de una clase particular de sistemas cuánticos multipartitos: sistemas de multiqudits simetrizados. Veremos cómo representar a los estados de este tipo de una manera fiel en lo que a rotaciones respecta, generalizando así los resultados de Majorana para el caso de sistemas de un espín. Veremos también una medida de enredamiento para este tipo de estados y algunas aplicaciones metrológicas en el contexto de detección de rotaciones.

El capítulo 4 está dedicado a la clase de estados antisimétricos. Además de una representación estelar para este tipo de estados, veremos algunas relaciones interesantes entre la estructura matemática de estos estados y los simétricos. También veremos aspectos de enredamiento, estados anticoherentes y aplicaciones en cómputo cuántico holonómico. En particular, veremos que las fases geométricas no abelianas adquiridas por estos estados por medio de evoluciones dadas por rotaciones dan lugar a compuertas lógicas robustas ante diferentes tipos de ruido, lo cual las hace una propuesta interesante en lo que respecta a cómputo libre de ruido.

En el capítulo 5 presentamos las conclusiones generales del trabajo y discutimos diversas direcciones para desarollar trabajo a futuro en las líneas de investigación desarrolladas en esta tesis.

Abstract

Our understanding of physical theories is, to a great extent, a matter of approaches. Given a physical theory, a complex problem can be reduced to a trivial one if we appreciate it in a proper way. The same applies to physical theories, theorems and physical notions in general. This, with no doubt, is the case for the theory of our interest in this thesis: quantum mechanics.

Quantum mechanics in the last decades has started to be studied from a geometric point of view, instead of the traditional algebraic approach. This approach led us to reveal quantum systems with exceptional properties, it had given to us a series of tools to solve problems, and a set of concepts that make richer our understanding of the theory itself. These contributions have been materialized in different applications in fields like quantum computation or quantum metrology, as we will exemplify in this thesis.

One example of this approach is given by the Majorana representation, which is a way to visualize quantum states of a given spin s as sets of $2s$ points on the unit sphere, representing rotations in a convenient way, as we will explain later. As a matter of example, consider the following spin-6 state $|\psi\rangle = \frac{1}{5}\left(-\sqrt{7}|6,5\rangle + \sqrt{11}|6,0\rangle + \sqrt{7}|6,-5\rangle\right)$. At a first glimpse, the rotational properties of this state are not evident, meanwhile through Majorana representation this state is represented by the vertices of an icosahedron, revealing the diverse symmetry properties of this state. In this way, we not only revealed the symmetries of the state but also were developed a tool to visualize states that live in a high-dimensional Hilbert space.

Those are not all the possible physical consequences that we can obtain from this geometric perspective, it is also well-known that these symmetries give us information about the expec-

tation values of some observables, geometric phases of the states under evolutions conducted by rotations and also about quantum entanglement of some multipartite systems. With this we see that a geometric approach in quantum mechanics can be one of the ways to advance our knowledge of the matter. Perhaps this approach will allow in the future to have a greater joint knowledge of quantum mechanics with other physical theories with purely geometric descriptions, as is the case with general relativity.

In this thesis we will study multipartite quantum systems through a geometric perspective. In particular, we will address some geometric problems related to this type of systems. We will explore aspects related to rotations, geometric phases, entanglement, as well as some tools for visualization. We will also see some applications related to various topics in the context of quantum information. We will also show some mathematical results that allow us to better understand the relationships between different results.

In order to give a precise description to the problems studied in this thesis and the results we obtained, it will be necessary to make a brief review of certain fundamental notions. Chapter 1 presents the basic ideas of quantum mechanics, with particular emphasis on its geometric structure. In this chapter we introduce the complex projective space and highlight its geometric properties at different levels: Riemannian, symplectic, complex, and as a Kähler manifold. Also in this chapter, the Majorana representation and its relation to rotations in quantum mechanics is presented.

The second chapter shows an overview of the geometry of multipartite quantum systems. This kind of quantum systems have non-local correlations that are relevant in different fields as quantum computation, quantum cryptography, quantum metrology, etc. These correlations are commonly studied through the concept of quantum entanglement, which has an algebraic origin. In this chapter, apart from those topics, we will exemplify how geometric methods can help us to understand the correlations in different ways. At the end of the chapter we will see how the rotation group acts in this type of systems, which will be the starting point for the material in chapters 3 and 4.

In chapter 3 we study geometrical aspects of a particular class of multipartite quantum systems: symmetrized multiqudit systems. We will see how to represent states of this type in a

faithful way as far as rotations are concerned, thus generalizing the Majorana results to the case of systems of one single spin. We will also see an entanglement measure for this category of states and some metrological applications in the context of rotation detection.

Chapter 4 is devoted to the class of antisymmetric states. Apart from a stellar representation, we wil seesome interesting relationships between the mathematical structure of these states and the symmetric ones. We will also investigate topics related to entanglement, anticoherent states and applications in holonomic quantum computation. Particularly, we will see that the non-abelian geometric factors that are acquired by those states by means of evolutions given by rotations induce robust quantum gates that are protected against different noise sources. This result will make this an interesting proposal in the field of noiseless quantum computation.

General concluding remarks and future directions of this work are discussed in chapter 5 .

Chapter 1

Prolegomena: Quantum mechanics and its geometric structure

1.1 Quantum mechanics

Quantum mechanics has its origin at the beginning of the last century as a response to a series of problems for which there was no satisfactory description in terms of the physics known until then. Problems such as the origin of atomic spectra, black body radiation and the specific heat of solids could not be understood until the introduction of the quantum ideas, which, beyond Planck's hypothesis, brought with them new knowledge of different aspects of the physical world that have drastically transformed our understanding of it.

Quantum mechanics is known to be one of the best physical theories in terms of the accuracy of its predictions, it is also known for its many counter-intuitive aspects such as the tunnelling phenomenon, the discretization of some physical quantities (quantization), for allowing superposition of states and by the non-local correlations that are described throught the concept of quantum entanglement. In addition to this, quantum mechanics has changed the way we understand all of physics, according to Messiah [1] "there hardly exists a branch of physics which one can seriously approach without a thorough knowledge of Quantum Mechanics". A series of examples of this are described in [2].

In a little more than its first centenary, quantum mechanics, in addition to its revolutionary role in fundamental physics, has been the departure point of various technological developments and applications, from the old tradition of nuclear science to modern quantum technologies in many fields such as ultracold matter, photonics, spintronics, quantum computing, quantum metrology, among many others, passing on its long journey through important discoveries that changed the way we live or promise to change it, such as lasers or high critical temperature superconductors.

The standard formalism of the theory is based on a series of principles that allow the mathematical abstraction of some physical notions. In the first place, the space of states of the system is represented by a Hilbert space $\mathcal{H}$, being each possible state of the system represented by a unit vector in $\mathcal{H}$. Physical observables are in correspondence with self-adjoint operators acting on $\mathcal{H}$.

The connection with the experimental results is given by means of the following rule: Consider a system in the state $|\psi\rangle$ from which we measure the value of a physical property A, represented by an operator $\hat{A}$, such that it has eigenvectors $|a_i\rangle$ with corresponding eigenvalues a_i, these eigenvalues are the possible results that can be obtained performing a measurement on the system. According to quantum mechanics, the result of this measurement will not have a deterministic result, we can only determine probabilities: the probability that the outcome is a_i is equal to $|\langle\psi|a_i\rangle|^2$, where $\langle\cdot|\cdot\rangle$ denotes the inner product of $\mathcal{H}$.

The dynamical aspects are expressed by the Schrödinger equation for almost all times, except at those times where measurements are performed, in those cases there is a non-linear evolution rule known as collapse. Expressed in this form, there are ambiguities about what is a measurement and when each of the evolution rules must be applied, this is one of the presentations of the *measurement problem*, which is currently subject to debate and is one of the most important conceptual problems of quantum mechanics.

As we can see from the above list of principles, the mathematical elements that appear in the theory have a noticeable algebraic flavor: vectors, Hilbert spaces, operators, etc. Phenomena like quantum superposition seem to have their ultimate origin in the linear structure of the theory. All this made the rich geometric structure of quantum mechanics go unnoticed, which

until before the last decades had not been explored in-depth. This structure reveals new horizons both in intrinsic aspects of the theory and in various applications. It is in this direction that this work brings new insights into the understanding of quantum mechanics through the eyes of geometry.

In the remaining part of this chapter, we will explore how interesting geometric structures arise even in the simplest of quantum systems. We will summarize the basic geometrical features of complex projective space, which plays an important role in this work and we will give some examples in which the geometric study of the quantum systems has been essential to understand fundamental aspects or to the development of applications.

Example 1. ***Space of states of a spin-*** $1/2$ ***particle.***

A two level system is probably the simplest example of quantum system, we can think of it as a spin $1/2$ *particle, whose Hilbert space is* $\mathbb{C}^2$ *and whose states can be written as* $|\psi\rangle = \alpha|\frac{1}{2},\frac{1}{2}\rangle + \beta|\frac{1}{2},-\frac{1}{2}\rangle$*, where* $|\frac{1}{2},\pm\frac{1}{2}\rangle$ *form a basis of common eigenvectors of* $\hat{S}_z$ *and* $\hat{S}^2$*, and* $\alpha,\beta \in \mathbb{C}$*. If the coefficients of the state are decomposed in their real and imaginary parts,* $\alpha = a + ib$ *and* $\beta = c + id$*, then the normalization condition leads to*

$$a^2 + b^2 + c^2 + d^2 = 1 \ , \tag{1.1}$$

which describes a 3*-sphere in* $\mathbb{R}^4$*. If we identify states that differ by a global phase (that are physically equivalent in the sense that all expectation values and probabilities are the same), we will obtain a* 2*-sphere; this is a classical well-known result in geometry: the Hopf fibration. See Figure 1.1 (Left).*

Therefore, the (pure) states are in correspondence with the points of the sphere, the so-called Bloch sphere*. The point with coordinates* (θ,ϕ) *represents the class of all states differing by a global phase with respect to the state* $|\psi\rangle = (\cos\frac{\theta}{2}\cos\phi, \sin\frac{\theta}{2}\sin\phi)^T$*, see Fig. 1.1 (Right). If we allow mixed states (i.e., convex linear combinations of pure states) we would have as space of states the three-ball that has the Bloch sphere as its boundary.* ■

We can see in this example that the state space of the simplest quantum system has a non-trivial geometry. If we consider a particle of spin 1, we will not have a sphere, but a space with a much more complex geometry, as we will see in the next section.

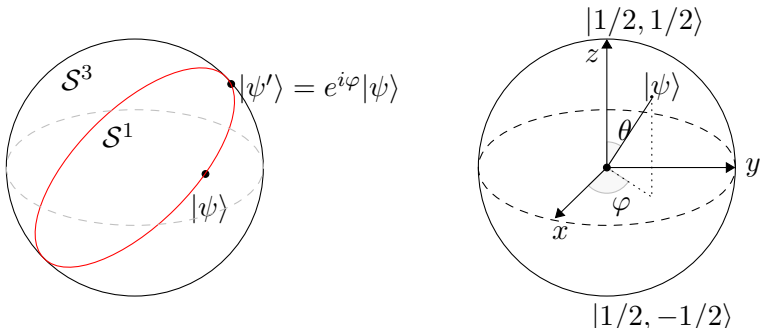

Figure 1.1: Left: Circle of states that differ by a phase factor. Right: Bloch sphere.

1.2 Geometry of Complex Projective Space

In this section, basic definitions and geometric properties of the complex projective space are presented, this will be the starting point for our geometric study of quantum mechanics because the space of pure quantum states of a spin is a complex projective space and not the usual Hilbert space, if we take into account the physical equivalence of states that only differ by a global phase factor, following a similar line of thought as in the example above.

Then, we conclude that the suitable space to study quantum mechanics is the quotient space $\mathcal{P}(\mathcal{H}) := \mathcal{S}(\mathcal{H})/\sim$, where $\mathcal{S}(\mathcal{H})$ is the unit sphere on Hilbert space and $\sim$ is an equivalence relation defined by

$$|\psi\rangle \sim |\phi\rangle \iff |\psi\rangle = e^{i\alpha}|\phi\rangle \;\; \alpha \in \mathbb{R} \; . \tag{1.2}$$

The space $\mathcal{P}(\mathcal{H})$ is known as *projective Hilbert space* and its points are equivalence classes of states, also known as *rays* in $\mathcal{H}$[1]. Rays are commonly described as density matrices of pure states $\rho_{|\psi\rangle} = |\psi\rangle\langle\psi|$ and they have all the information of the state $|\psi\rangle$ ignoring global phases. So, the ground where quantum mechanics takes place is not a linear space, but a space with a much more interesting geometry, that we will explore in this section.

1.2.1 Basic definitions

The complex projective space $\mathbb{CP}^n$ is the n-dimensional[2] space of lines through the origin in $\mathbb{C}^{n+1}$. Each point in $\mathbb{CP}^n$ corresponds to an equivalence class of points in $\mathbb{C}^{n+1}$, where two

[1] The class of a state $|\psi\rangle$ is defined as $[\psi] := \{\lambda|\psi\rangle \; , \lambda \in \mathbb{C}\backslash\{0\}\}$.

[2] Complex dimension.

points are identified if they lie on the same complex line. This space is physically relevant because $\mathbb{CP}^{2s}$ is the space of states of a spin s system (where $\mathcal{H} = \mathbb{C}^{2s+1}$).

This definition of projective space as lines through the origin, also called *rays*, is straightforwardly equivalent to the definition of the projective space in terms of projection operators. The point $[\psi] \in \mathbb{CP}^n$ can be regarded as the projector onto the normalized state $|\psi\rangle$, which in Dirac notation is written as $|\psi\rangle\langle\psi|$. This projector is known as *pure state density matrix of the state* $|\psi\rangle$ and it is usually denoted by $\rho_{|\psi\rangle}$. By definition, the density matrix is the same for any representative on the same equivalence class of states up to a global phase. In terms of components on a particular basis, if we consider $|\psi\rangle = \psi^i|e_i\rangle$ as a vector in $\mathbb{C}^{2s+1}$ then $\rho_{|\psi\rangle}$ is the $(2s+1)\times(2s+1)$ matrix given by the Kronecker product of $|\psi\rangle$ and $\langle\psi|$, whose entries are of the form $[\rho_{|\psi\rangle}]^i{}_j = \psi^i\bar{\psi}_j$.

It is easy to verify that pure state density matrices satisfy the following properties:

(i) $\mathrm{tr}\rho = 1$.

(ii) $\rho = \rho^\dagger$.

(iii) ρ has only non-negative eigenvalues.

(iv) $\rho^2 = \rho$.

In the case of mixed quantum states, properties (i)-(iii) hold but it happens that $\mathrm{tr}\rho^2 < 1$. States of this kind live in a greater space (which have the complex projective space as part of its boundary), but for now we will focus on the space of pure states.

To go further, the introduction of a coordinate system for $\mathbb{CP}^n$ is necessary. One of the most useful ones is that of *inhomogeneous coordinates*.

A state $|\psi\rangle = \psi^i|e_i\rangle \in \mathbb{C}^{n+1}$ can also represent a point on the projective space, the point $[\psi]$ with *homogeneous coordinates* ψ^i, commonly denoted by $[\psi^0 : \psi^1 : \cdots : \psi^n]$. These are not proper coordinates because they exceed the required number of parameters needed to specify a point on a n-dimensional manifold. Thus, we define the *inhomogeneous coordinates*, in the open set $U_0 = \{[\psi] \in \mathbb{CP}^n : \psi^0 \neq 0\}$ as $z_i^{(0)} := \psi^i/\psi^0$. Similarly, we can define inhomogeneous coordinates $z_i^{(j)} = \psi^i/\psi^j$ on the chart where $\psi^j \neq 0$. These coordinates are well defined and

they will be denoted simply by z_i unless more information about the chart is required.

Note that in the overlap of two charts with $U_k \cap U_l \neq \emptyset$, the transition function that relates the inhomogeneous coordinates given by each chart $\phi_{lk} : \mathbb{C}^n \to \mathbb{C}^n$ is given by

$$\phi_{lk}(z_i^{(k)}) = z_i^{(l)} = \frac{\psi^k}{\psi^l} z_i^{(k)} = z_i^{(k)} z_k^{(l)} \ , \tag{1.3}$$

this transition function is multiplication by $z_k^{(l)}$ which is a holomorphic map, this makes $\mathbb{CP}^n$ a n-dimensional complex manifold.

In $\mathbb{CP}^n$, we can define a $(1,1)$-tensor field

$$J = \sum_{r=1}^{n} i \frac{\partial}{\partial z^r} \otimes dz^r - i \frac{\partial}{\partial \bar{z}^r} \otimes d\bar{z}^r \ .$$

This tensor field is called *complex structure* and has the property that $J^2 = -I_{2n}$, hence it is a tensor field that generalizes the property $i^2 = -1$, it works like a imaginary unit. Any manifold of even dimension admits locally a tensor field with that property, but its global definition (integrability) is only allowed for complex manifolds[3].

In the subsections below we will explore some of the basic geometrical features of the complex projective space.

1.2.2 Riemannian, symplectic and Kähler structure

There is a natural notion of distance in $\mathbb{C}P^n$, inherited from the canonical hermitian inner product in $\mathbb{C}^n$.

This distance between two points $[\psi]$ and $[\phi]$ in the ray space $\mathbb{C}P^n$ is defined as

$$d_{FS}([\psi],[\phi]) := \arccos\left(\sqrt{\frac{\langle\psi|\phi\rangle\langle\phi|\psi\rangle}{\langle\psi|\psi\rangle\langle\phi|\phi\rangle}}\right) \ , \tag{1.4}$$

which is known as *Fubini-Study* distance, it is easy to show that it is in fact a distance function which is $U(1)$-invariant, hence, it is a well defined quantity on projective space.

If we take two infinitesimally separated points in $\mathbb{C}^n$, $|\psi\rangle$ and $|\phi\rangle = \phi^i|e_i\rangle = (\psi^i + d\psi^i)|e_i\rangle$, it is easy to show, expanding up to second order the squared cosine of the distance, that the

[3]This tensor field completely specifies the complex structure in the sense of atlases, it is interesting that for $n > 2$ it remains open the problem of classification of all the possible complex structures for $\mathbb{CP}^n$.

infinitesimal distance between two infinitesimally separated points is

$$ds^2_{FS} = \frac{\bar{\psi}^i\psi_i d\bar{\psi}^k d\psi_k - d\bar{\psi}^k\psi_k d\psi^i\bar{\psi}_i}{(\bar{\psi}^i\psi_i)^2} \ , \tag{1.5}$$

this is the *Fubini-Study metric* in homogeneous coordinates. If we change to inhomogeneous coordinates this metric takes the form

$$ds^2_{FS} = \frac{1}{1+|z|^2}\left(dz^a d\bar{z}_a - \frac{\bar{z}_a dz^a d\bar{z}_b z^b}{1+|z|^2}\right) \ . \tag{1.6}$$

In terms of matrices, the metric g_{FS} can be directly read from the line element $ds^2_{FS} = g_{ab}dz^a dz^b + 2g_{a\bar{b}}dz^a d\bar{z}^{\bar{b}} + g_{\bar{a}\bar{b}}d\bar{z}^{\bar{a}}d\bar{z}^{\bar{b}}$:

$$g_{FS} = \begin{pmatrix} 0 & g_{a\bar{b}} \\ g_{\bar{a}b} & 0 \end{pmatrix} \ , \tag{1.7}$$

where $\bar{g}_{a\bar{b}} = g_{\bar{a}b}$ and

$$g_{a\bar{b}} = \frac{1}{2}\cdot\frac{1}{1+|z|^2}\left(\delta_{a\bar{b}} - \frac{\bar{z}_a z_{\bar{b}}}{1+|z|^2}\right) = \frac{1}{2}\partial_a\partial_{\bar{b}}\ln(1+|z|^2) \ , \tag{1.8}$$

where we use the notation $\partial_a := \frac{\partial}{\partial z^a}$ and $\partial_{\bar{b}} := \frac{\partial}{\partial \bar{z}^b}$. We use this convention of putting bars in both z and the indices to clearly indicate that $g_{a\bar{b}}$ is only a sector of the full metric matrix (in fact, the entries with indices of the same type vanish).

The Fubini-Study metric is a hermitian metric, this means that g_{FS} is invariant under the action of the complex structure: $g_{FS}|_p(JX, JY) = g_{FS}|_p(X, Y)$,$\forall\ X, Y \in T_p\mathbb{C}P^n$, where we denote the tangent space of the projective space at the point p by $T_p\mathbb{C}P^n$. This gives $\mathbb{C}P^n$ the structure of a hermitian manifold. Given a hermitian manifold we can define a field of 2-forms Ω whose action satisfies the following condition

$$\Omega(X, Y) = g(JX, Y) \ . \tag{1.9}$$

To see that in fact is a 2-form is a straightforward consequence of the definition of hermitian metric and the definition of J. This 2-form is invariant under the action of J:

$$\Omega(JX, JY) = g(J^2X, JY) = g(J^3X, J^2Y) = \Omega(X, Y) \ . \tag{1.10}$$

The 2-form Ω is called a *Kähler form* and in the case of $\mathbb{C}P^n$ it can be written in terms of the components of the Fubini-Study metric as

$$\Omega = ig_{r\bar{s}}dz^r \wedge d\bar{z}^{\bar{s}} \ . \tag{1.11}$$

It is a classical result that $\Omega^{\wedge n}$ is a non-vanishing top form on $\mathbb{C}P^n$ and it defines a canonical volume form and therefore, $\mathbb{C}P^n$ is an oriented manifold (in fact, all complex manifolds are orientable).

In the case of $\mathbb{C}P^n$, the Kähler form is closed, i.e. $d\Omega = 0$, and for this reason $\mathbb{C}P^n$ is a Kähler manifold. This non-trivial property has some interesting consequences, for example, this implies that the metric can be found, locally, from a potential K, $g_{r\bar{s}} = \partial_r \partial_{\bar{s}} \ K$. In the case of the Fubini-Study metric, the potential is given by $K = \frac{1}{2}\ln\left(z_i \bar{z}^i\right)$. Other interesting consequences are extra symmetries of the Riemann tensor and simplifications of all the classical formulas for the Levi-Civita connection, Ricci tensor, Ricci scalar, etc. [3].

With this analysis we can see that complex projective space is a very particular space, with a metric, a symplectic and a complex structure. This illustrates the rich geometry underlying quantum mechanics. In the following sections we will see some results that shed light on the usefulness of geometric ideas in quantum mechanical scenarios.

Our first example concerns the visualization of spin states, which is difficult in general due to the high dimensionality of the involved spaces. One may insist and try to represent states of projective spaces on the sphere following the idea of Bloch sphere, and in fact there is a way to do that with a particularly useful property concerning rotations, as is shown in the next section.

1.3 Stars in Quantum Mechanics

Of the infinitely many maps that associate spin s states with sets of $2s$ points on the unit sphere, Majorana discovered that there is one particularly interesting, whose presentation, at least in the form given by Majorana in its relatively unknown 1932 paper, is as cryptic as it is elegant [4]. The Majorana representation was originally introduced to study spin systems

under the action of magnetic fields. After its appearance, the representation remained little known until its resurgence as central piece in Penrose's alternative proof of the Kochen-Specker Theorem. After this work, applications of it have appeared in various fields as in the study of quantum entanglement, quantum metrology, quantum computation, geometric phases, among many others. In the field of quantum information the Majorana representation is particularly useful because it provides a concept that extends the Bloch sphere representation to more general systems than qubits.

1.3.1 Construction

Consider a spin-s state, $|\psi\rangle$, given in the common eigenvector basis of the operators S^2 and S_z, this can be written as

$$|\psi\rangle = \sum_{m=-s}^{s} \psi_m |s,m\rangle \ , \ \psi_m \in \mathbb{C} \ . \tag{1.12}$$

To this state, following Majorana's prescription, we can associate $2s$ points on the unit sphere as follows. First, define a polynomial in the auxiliary complex variable ζ, $P_{|\psi\rangle}(\zeta)$, with coefficients that are linear in the components of the state, given by

$$P_{|\psi\rangle}(\zeta) = \sum_{m=-s}^{s} (-1)^m \sqrt{\binom{2s}{s-m}} \psi_m \zeta^{s+m} \ . \tag{1.13}$$

The $2s$ points on the complex plane that correspond to the roots of this polynomial, known as *Majorana polynomial*, must be stereographically projected to the unit sphere[4]. Each of these points is called a *star* and the set of all the stars, a (Majorana) *constellation*, following this nomenclature by its analogy with the celestial sphere. Note that this definition allows for degenerated constellations, i.e., with stars with multiplicity, this is due to the fact that the polynomial can have multiple roots.

Before analyzing the properties of this map, let us see how it works through a pair of examples.

Example 2. ***Determination of the Majorana constellation of a quantum state.***

Consider the spin-4 state

$$|\psi_{cub}\rangle = |4,4\rangle + \sqrt{\frac{14}{5}}|4,0\rangle + |4,-4\rangle \tag{1.14}$$

[4]Conventionally this projection is taken from the south pole.

By 1.13, its Majorana polynomial is

$$P_{|\psi\rangle} = z^8 + 14z^4 + 1 \ , \tag{1.15}$$

and its roots are given by

$$\begin{aligned}
z_1 &= \left(-\frac{1}{2} - \frac{i}{2}\right)\left(\sqrt{3}-1\right) \ , z_2 = \left(\frac{1}{2} - \frac{i}{2}\right)\left(\sqrt{3}-1\right) \ , \\
z_3 &= \left(-\frac{1}{2} + \frac{i}{2}\right)\left(\sqrt{3}-1\right) \ , z_4 = \left(\frac{1}{2} + \frac{i}{2}\right)\left(\sqrt{3}-1\right) \ , \\
z_5 &= \left(-\frac{1}{2} - \frac{i}{2}\right)\left(\sqrt{3}+1\right) \ , z_6 = \left(\frac{1}{2} - \frac{i}{2}\right)\left(\sqrt{3}+1\right) \ , \\
z_7 &= \left(-\frac{1}{2} + \frac{i}{2}\right)\left(\sqrt{3}+1\right) \ , z_8 = \left(\frac{1}{2} + \frac{i}{2}\right)\left(\sqrt{3}+1\right) \ .
\end{aligned}$$

Projecting the z_i's stereographically from the south pole to the unit sphere, we obtain the constellation

$$\left\{\pm\frac{1}{\sqrt{3}}, \pm\frac{1}{\sqrt{3}}, \pm\frac{1}{\sqrt{3}}\right\} \ ,$$

where all the possible combinations of signs must be considered, this corresponds to the set of the 8 vertices of a cube centered at the origin. ■.

Example 3. ***Determination of the state given the constellation.***

Consider the following constellation corresponding to the vertices of a regular tetrahedron:

$$\left\{\left(0, 0, \sqrt{\frac{2}{3}} - \frac{1}{2\sqrt{6}}\right), \left(-\frac{1}{2\sqrt{3}}, -\frac{1}{2}, -\frac{1}{2\sqrt{6}}\right), \left(-\frac{1}{2\sqrt{3}}, \frac{1}{2}, -\frac{1}{2\sqrt{6}}\right), \left(\frac{1}{\sqrt{3}}, 0, -\frac{1}{2\sqrt{6}}\right)\right\}$$

We project these points to the complex plane using the inverse stereographic projection from the south pole, this is the map

$$(x, y, z) \in \mathcal{S}^2 \to \frac{x + iy}{1 + z} \in \mathbb{C} \ , \tag{1.16}$$

obtaining the following set of points in the complex plane

$$\left\{0, -\frac{\sqrt{3} + 3i}{\sqrt{6}}, -\frac{\sqrt{3} - 3i}{\sqrt{6}}, \sqrt{2}\right\} \ . \tag{1.17}$$

These points are taken to be the roots r_i of the Majorana polynomial, then $P_{|\psi\rangle}(\zeta) = \prod_{i=1}^{4}(\zeta - r_i)$. In this example, we obtain the polynomial $z^4 - 2\sqrt{2}z$, and comparing with 1.13 for $s = 2$ (because the number of stars is $2s = 4$) we can read off, from the coefficients, the components of the states in the aforementioned standard basis, resulting that the normalized state for the spin-2 state associated, up to a phase, with the given tetrahedron is

$$|\psi_{tet}\rangle = \sqrt{\frac{2}{3}}|2,1\rangle + \frac{1}{\sqrt{3}}|2,-2\rangle \ . \quad \blacksquare \tag{1.18}$$

Remark 1. The singularity at the south pole of the stereographic projection and the possibility of multiple roots of the Majorana polynomial seem to obstruct the applicability of the stellar representation, to avoid confusion we will use the following rule: If $\psi_s = 0$, we will count this as a star at the south pole (this corresponds to take infinity as one root), moreover if the first k components of the state, i.e., $\psi_s, \psi_{s-1}, \ldots, \psi_{s-k+1}$ are all equal to zero we will assign a k-degenerated star at the south pole. Conversely, if given a constellation there is a k-fold degenerate star at the south pole the resulting state will have its first k entries equal to zero and the others will be found using the Majorana polynomial.

Example 4. ***Stars at the point at infinity on the Riemann sphere.***

(i) The state $|s,-s\rangle$ has its $2s$ stars at the south pole.

(ii) The state $|\psi_{oct}\rangle = \frac{1}{\sqrt{2}}(|3,2\rangle - |3,-2\rangle)$ must have one star at the south pole because of the lacking of a component along $|3,3\rangle$, in fact, the constellation of this state is an octahedron with stars at both poles. $\blacksquare$

1.3.2 Rotations of quantum states

How to perform a rotation on a quantum state of spin s, around the axis $\hat{n}$ by an angle θ, i.e., the rotation $R_{\hat{n},\theta}$? Quantum mechanics establishes that this operation corresponds to a unitary transformation, which can be obtained by taking the exponential of the hermitian generators of $\mathfrak{su}(2)$ in the spin s representation, i.e., the standard spin operators $\hat{S}_i^{(s)}$ with $i \in \{x, y, z\}$, this means that the evolution by means of rotations is represented by the $(2s+1)\times(2s+1)$ matrix $D^{(s)}(R_{\hat{n},\theta}) = e^{-i\theta\hat{n}\cdot\vec{S}^{(s)}}$. Equivalently, this rotation can be written as a

product of three successive particular rotations following the Euler angle representation[5], this is convenient since only one of the three rotations is non-trivial. In terms of the corresponding unitary $SU(2)$ operators this decomposition can be written as

$$D^{(s)}(\alpha,\beta,\gamma) = e^{-i\alpha\hat{S}_z^{(s)}} e^{-i\beta\hat{S}_y^{(s)}} e^{-i\gamma\hat{S}_z^{(s)}} \ . \tag{1.19}$$

The operator $D^{(s)}(\alpha,\beta,\gamma)$ applied to a state of the form 1.12 leads to a linear combination of the form

$$D^{(s)}(\alpha,\beta,\gamma)|\psi\rangle = \sum_{m,m'} D^{(s)}_{m'm}(\alpha,\beta,\gamma)\psi_m|s,m'\rangle \ , \tag{1.20}$$

and, by 1.19,

$$D^{(s)}_{m'm}(\alpha,\beta,\gamma) = \langle s,m'|e^{-i\alpha\hat{S}_z^{(s)}} e^{-i\beta\hat{S}_y^{(s)}} e^{-i\gamma\hat{S}_z^{(s)}}|s,m\rangle = e^{-i\alpha m'}\sigma^{(s)}_{m'm}(\beta)e^{-i\gamma m} \ , \tag{1.21}$$

where $\sigma^{(s)}_{m'm} := \langle s,m'|e^{-i\beta\hat{S}_y^{(s)}}|s,m\rangle$ is given by the well known Wigner Formula (D-Matrix) [5, 6]:

$$\begin{aligned}\sigma^{(s)}_{m'm}(\beta) = \sum_k (-1)^{k-m+m'} &\frac{\sqrt{(s+m)!(s-m)!(s+m')!(s-m')!}}{(s+m-k)!k!(s-k-m')!(k-m+m')!} \\ &\times \left(\cos\frac{\beta}{2}\right)^{2s-2k+m-m'} \left(\sin\frac{\beta}{2}\right)^{2k-m+m'} \ ,\end{aligned} \tag{1.22}$$

where the index k takes all the integer values where the factorials are well defined, i.e., when the value of the arguments of the factorials in 1.22 is non-negative.

1.3.3 Operational Definition

The Majorana constellation of a state is not only a pictorial representation of spin states, it has a concrete operational meaning. Physically, the constellation of a state corresponds to the $2s$ directions $\hat{n}_i$ (with possible degeneracy) in three-dimensional physical space in which the probability of measuring the minimal projection $|s,-s;\hat{n}_i\rangle$ is zero[6]. Measurements of this type can be made with a Stern-Gerlach apparatus.

[5] Any rotation can be written as a product of three rotations, by angles α,β and γ, along the z,y and z axes, respectively, of a fixed coordinate system.

[6] The notation $|s,m;\hat{n}\rangle$ stands for the common eigenvectors of $(S^s)^2$ and $\hat{n}\cdot\hat{S}^{(s)}$, e.g., $|s,m;\hat{z}\rangle = |s,m\rangle$.

To show this, first note that the state of minimal projection in an arbitrary direction $\hat{n}$ is

$$|s,-s;\hat{n}\rangle = D^{(s)}\left(R_{\vec{m}(\phi),\theta}\right)|s,-s;\hat{z}\rangle \ , \tag{1.23}$$

where the rotation that must be applied is the one that takes the vector $\hat{z}$ to the vector $\hat{n}$, i.e., the rotation around the axis $\vec{m}(\phi) = (-\sin\phi, \cos\theta, 0)$ by an angle θ.

In terms of Euler angles, it is easy to see that the corresponding rotation can be written as $D^{(s)}\left(R_{\vec{m}(\phi),\theta}\right) = e^{-i\phi S_z^{(s)}} e^{-i\theta S_y^{(s)}} e^{i\phi S_z^{(s)}}$. Using equation 1.22 we have

$$\begin{aligned} |s,-s;\hat{n}\rangle &= \mathcal{D}^{(s)}\left(R_{\vec{m}(\phi),\theta}\right)|s,-s;\hat{z}\rangle \\ &= e^{-i\phi S_z} e^{-i\theta S_y} e^{i\phi S_z}|s,-s;\hat{z}\rangle \\ &= \sum_{m=-s}^{s} \delta_{m-s} e^{-i\phi(s+m)} \\ &= \sum_{m=-s}^{s} e^{-i\phi(s+m)} \sqrt{\binom{2s}{s-m}} \cos^{s-m}\frac{\theta}{2} \sin^{s+m}\frac{\theta}{2} \ . \end{aligned} \tag{1.24}$$

Equation 1.24 in terms of $\zeta := \tan\frac{\theta}{2} e^{i\phi}$ can be rewritten as

$$|s,-s;\hat{n}\rangle = \left(\cos\frac{\theta}{2}\right)^{2s} \sum_{m=-s}^{s} (-1)^{s+m} \sqrt{\binom{2s}{s-m}} \bar{\zeta}^{s+m} \ . \tag{1.25}$$

Therefore, the directions in which the minimal projection of the state vanishes in a Stern-Gerlach measurement, are those in which $\langle s,-s;\hat{n}|\psi\rangle = 0$, this occurs when

$$(-1)^s \left(\cos\frac{\theta}{2}\right)^{2s} \sum_{m=-s}^{s} (-1)^m \sqrt{\binom{2s}{s-m}} \zeta^{s+m} \psi_m = 0 \ , \tag{1.26}$$

thus, when $P_{|\psi\rangle}(\zeta) = 0$, i.e., along the directions of the Majorana stars of the state.

Remark 2. In the case of states with degeneration of stars we can go further. Consider a state with a d-fold degenerate star along the direction $\hat{n}_d$, in this case not only the probability to find the state at $|s,-s;\hat{n}_d\rangle$ is zero, the same occurs for $|s,-s+1;\hat{n}_d\rangle, |s,-s+2;\hat{n}_d\rangle, \ldots, |s,-s+d-1;\hat{n}_d\rangle$. This can be easily shown by a recursive application of the operational definition we presented.

Summarizing, we have the following theorem.

Theorem 1. The Majorana constellation of a quantum state is constituted by the directions in space in which the probability of measuring the minimal projection of spin is zero. Moreover, if there is a star along direction $\hat{n}_d$ with degeneracy d, the probability of measuring the lowest projections $-s, -s+1, \ldots, -s+d-1$ is zero.

This result explains why the stellar representation is faithful in regards to rotations. Essentially, the Majorana stars capture a physical feature of quantum states. In the following diagram we summarize this correspondence of $SU(2)$ transformations acting on states in Hilbert space with rotations of constellations in physical space, $\mathcal{M}$ denotes the Majorana map from states to constellations and $\mathcal{M}^{-1}$ the map in the inverse sense. In this diagram the two paths from $|\psi\rangle$ to $D^{(s)}(R)|\psi\rangle$ are equivalent.

$$\begin{array}{ccc} |\psi\rangle & \xrightarrow{\quad\mathcal{M}\quad} & C_{|\psi\rangle} \\ {\scriptstyle D^{(s)}(R)}\downarrow & & \downarrow{\scriptstyle R} \\ D^{(s)}(R)|\psi\rangle & \xleftarrow[\mathcal{M}^{-1}]{} & R \triangleright C_{|\psi\rangle} \end{array}$$

Figure 1.2: Equivalence of rotations.

Remark 3. It is important to mention that the action of a general unitary transformation, not necessarily one in $SU(2)$, does not have, in principle, a transparent way to be understood in terms of stars, these can suffer complex motions. For example, the orthogonality of states in the Majorana representation can be cumbersome, even for small values of the spin. This means that the constellation of one state, in principle, does not give us an idea of how are the constellations of orthogonal states to it.

1.3.4 Symmetric configurations of stars and anticoherent spin states

Due to the transparency of the rotational properties provided by the stellar representation, states with rotational symmetries will have special symmetric configurations of stars as we will see in the following examples.

Example 5. ***Constellations of eigenvectors of*** $\hat{n} \cdot \vec{S}$.

From the definition of the Majorana polynomial 1.13, taking into account the details of Remark

1, it is easy to see that the state $|s,m\rangle$ has a constellation given by $s+m$ stars at the north pole and $s-m$ stars at the south pole. Therefore, the eigenstate $|s,m;\hat{n}\rangle$ of $\hat{n}\cdot\vec{S}$ has a constellation constituted by $s+m$ stars along the direction $\hat{n}$ and the remaining $s-m$ are in the antipodal direction.

Of particular interest are the coherent spin states*, defined as the states of maximal projection $|s,s;\hat{n}\rangle$. These states are important due to the property to be* the most classical quantum states *in the sense described in [7]. In terms of constellations, these are the states with maximally degenerated constellations in which the $2s$ stars coincide. The set of coherent states is topologically a sphere [7], as clearly appreciated in terms of the stellar representation, in the sense that $\hat{n}$ labels the coherent states and the set of all possible directions is a sphere.*
■

In opposition to coherent states, which are the *most classical* ones, one can ask for the *most quantum* states. Zimba [8] proposed a solution, leading to the concept of *anticoherent states*. Anticoherent states are those states $|\psi\rangle$ that have vanishing polarization vector, i.e., $\langle\psi|\hat{n}\cdot\vec{S}|\psi\rangle = 0$, in contrast, coherent states are those that maximize the norm of the polarization vector.

Examples of anticoherent states are $|\psi_{\text{tet}}\rangle, |\psi_{\text{cub}}\rangle$ and $|\psi_{\text{oct}}\rangle$, presented in the above sections, with constellations corresponding to a tetrahedron, a cube and an octahedron, respectively. In fact, as shown in [8], the states whose Majorana representation is a platonic solid are all anticoherent. The same occurs for the states whose constellations are the set of vertices of an Archimedean solid [9] . There are some other categories of polyhedra whose corresponding states are all anticoherent, e.g., Catalan or Kepler-Poinsot solids [9].

Looking at the above examples, it seems that discrete symmetries of the constellations and anticoherence of the corresponding states are related in some way. It was conjectured that anticoherence implied symmetry of the constellation [10] but counterexamples were found [11] and therefore, the conjecture was discarded. However, there is in fact a relation between symmetry and anticoherence. To explain this, it will be useful to introduce the concept of t-anticoherence [8].

We call a state $|\psi\rangle$ a t-anticoherent state if it is anticoherent and if $\left\langle \psi \left| \left(\hat{n}\cdot\vec{S}\right)^k \right| \psi \right\rangle$ is

independent of $\hat{n}$ for $k = 1, 2, \ldots, t$.

The following theorem [10] explains that if a constellation has a discrete symmetry group then there is a lower bound for its anticoherence order t.

Theorem 2. Let G be a t-homogeneous subgroup[7] of $O(3)$. Then, any state whose Majorana representation is an orbit of G is an anticoherent spin state of order greater or equal to t.

As a matter of fact, the tetrahedral, the octahedral and the icosahedral groups are the discrete subgroups of $O(3)$ of the symmetries that leave invariant the tetrahedron, the octahedron (or the cube), and the icosahedron, respectively. These groups are homogeneous of order $2, 3$ and 5, respectively, therefore, if a constellation has all the symmetries of one of these groups the corresponding state will be at least $2, 3$ or 5-anticoherent.

By Theorem 2, we know that the tetrahedral state (i.e., the state whose constellation is a tetrahedron) is at least 2-anticoherent, the octahedral and the cubical states are at least 3-anticoherent, and, also because of its symmetry group, the icosahedral and the dodecahedral states are at least 5-anticoherent.

By performing the computations in each case, it can be shown that the order of anticoherence of those states coincides exactly with the lower bound fixed by Theorem 2. The same occurs for all Archimedean states, where the symmetry directly corresponds to the order of anticoherence, but this is not the case in general for other solids, e.g., the triakistetrahedron (the dual of the truncated tetrahedron) is a Catalan solid with only tetrahedral symmetry but its anticoherence order is 3 and not 2, being the only one in its category that exceeds the bound set by the symmetry [9].

At this point, some details need to be clarified.

Remark 4. As can be noticed, e.g., in equations (1.14) and (1.18), many symmetric states have a spacing between their non-zero components when expressed in the standard $|s, m\rangle$ basis.

[7] A discrete subgroup of $O(3)$ is called t-homogeneous if all of its orbits are spherical t-designs. A spherical t-design is a finite set $X = \{x_1, x_2, \ldots, x_m \ : \ x_i \in \mathcal{S}^{n-1}\}$ such that

$$\frac{1}{\mathrm{vol}(\mathcal{S}^{n-1})} \int_{\mathcal{S}^{n-1}} p(x)dx = \frac{1}{m} \sum_{i=1}^{m} p(x_i) \ ,$$

for any homogeneous polynomial $p(x)$ in n variables, of degree lower or equal to t. See [12].

For example, the cubical state has non-vanishing components only along the projections $-4, 0$ and 4; similarly, the tetrahedral state has only non-vanishing projections -1 and 2. This is related to the symmetry, and in the former case the jumps by four are related to a symmetry under rotations around z axis by an angle of $2\pi/4$, in the latter case the jumps by three is an indicator of a rotational symmetry of the constellation by an angle $2\pi/3$ around z axis. This relation between symmetries and relationships among the components of the states is studied in detail in [13].

Remark 5. There is an intuition about anticoherent states besides symmetries. If coherent states are those with a pronounced directionality, having all the stars pointing along the same direction, it is reasonable to think that in the case of anticoherent states the stars are as spread out as possible (the condition of vanishing polarization vector can be interpreted as *spin is pointing nowhere*). Many of the polyhedra we considered as examples are also solutions to well known problems of maximal dispersion of points on the sphere, this reinforces the intuition. Nevertheless, it is easy to show that this intuition can lead us to mistakes, e.g., there are anticoherent states with degenerated constellations. For example, a platonic constellation with n stars at each vertex corresponds to an anticoherent state.

The Majorana representation constitutes a beautiful example of how the geometrical thinking of quantum mechanics has been essential to reveal physical properties of different quantum systems.

One of the main results of this thesis is a generalization of the Majorana stellar representation for more general quantum systems. The next chapter, about multipartite quantum systems will give us the necessary tools to introduce that generalization and other important concepts that will be useful along this work.

Chapter 2

Geometry of Multipartite Quantum Systems

2.1 Multipartite quantum systems and quantum entanglement

According to quantum mechanics, the space of states, $\mathcal{H}$, of a multipartite system composed by k subsystems is the tensor product of the Hilbert spaces of the corresponding subsystems,

$$\mathcal{H} = \bigotimes_{i=1}^{k} \mathcal{H}_i \ , \tag{2.1}$$

then $\dim \mathcal{H} = \prod_{i=1}^{k} \dim \mathcal{H}_i$.

One of the most remarkable aspects of these systems, in opposition with the classical case, is that correlations among the subsystems cannot be expressed only in terms of classical probabilities. This kind of non-classical correlations are described by the concept of *quantum entanglement*, which will be presented in what follows, standard references to this topic are [3, 14, 15]. As Schrödinger said, "I would not call that *one* but rather *the* characteristic trait of quantum mechanics, the one that enforces its entire departure from classical lines of thought" [16].

Quantum entanglement is an example of the intrinsic holism that pervades quantum theory, as Schrödinger explained [16]: "Another way of expressing the peculiar situation is: the best

possible knowledge of a whole does not necessarily include the best possible knowledge of all its parts, even though they may be entirely separate and therefore virtually capable of being 'best possibly known,' i.e., of possessing, each of them, a representative of its own."

The way in which we (mentally) divide a system into subsystems is arbitrary, then, entanglement can be manifested in different ways. In many cases, there is a more or less natural way of make that abstract partition, for example, systems of particles of a certain size r which are located in different distant places with separations $d >> r$.

To simplify the exposition, let us restrict our discussion to bipartite systems, i.e., systems whose space of states is of the form $\mathcal{H}_1 \otimes \mathcal{H}_2$.

Consider a state of the form $|\psi\rangle = |\psi_1\rangle \otimes |\psi_2\rangle$, with $|\psi_i\rangle \in \mathcal{H}_i$. If we compute the expectation value of a local observable on the first of the subsystems, that is, one of the form $\hat{A} \otimes \mathbb{I}$, we find that

$$\langle\psi|\hat{A} \otimes \mathbb{I}|\psi\rangle = (\langle\psi_1| \otimes \langle\psi_2|)(\hat{A} \otimes \mathbb{I})(|\psi_1\rangle \otimes |\psi_2\rangle) \tag{2.2}$$

$$= (\langle\psi_1| \otimes \langle\psi_2|)(\hat{A}|\psi_1\rangle \otimes |\psi_2\rangle) \tag{2.3}$$

$$= \langle\psi_1|\hat{A}|\psi_1\rangle \ \langle\psi_2|\psi_2\rangle \tag{2.4}$$

$$= \langle\psi_1|\hat{A}|\psi_1\rangle. \tag{2.5}$$

From this result (and the analogous one for a local observable in the second space) we can note that the measurements on a subsystem are not correlated with those of the other subsystem and depend only on the particular state of the corresponding subsystem. Therefore, the state $|\psi\rangle$ is said to be a non-entangled state.

States that cannot be expressed as the tensor product of a vector in each factor space, i.e. a linear combination of tensor products, in any possible basis, are said to be entangled or non-factorizable states.

In the case of entangled states we cannot define a pure state of the subsystem, we have only partial information encoded in a reduced density matrix and even in the case of local operations, results exhibit correlations involving the whole system. To show this, simply note

that if we take $|\psi\rangle = \frac{1}{\sqrt{2}}\left(|\psi_1\rangle \otimes |\psi_2\rangle + |\phi_1\rangle \otimes |\phi_2\rangle\right)$:

$$\langle\psi|\hat{A} \otimes \mathbb{I}|\psi\rangle = \mathrm{Tr}(\hat{A} \otimes \mathbb{I}|\psi\rangle\langle\psi|) \tag{2.6}$$

$$= \mathrm{Tr}_1\left(\hat{A}\mathrm{Tr}_2|\psi\rangle\langle\psi|\right) \tag{2.7}$$

$$= \mathrm{Tr}_1(\hat{A}\rho_1)\ , \tag{2.8}$$

where $\rho_1 := \mathrm{Tr}_2|\psi\rangle\langle\psi|$ is the partial trace with respect to the second space.

This happens for any $\hat{A}$, hence we can conclude that, in terms of measurements, ρ_1 behaves as the state of the first subsystem. Similarly, $\rho_2 = Tr_1|\psi\rangle\langle\psi|$ is said to be the state of the second subsystem. The ρ_i are known as reduced density matrices of the system.

This definition of entangled states as non-factorizable is straightforwardly extended to multipartite systems. There is also an extension of this definition in the context of mixed states, see [15, 14].

Given a particular quantum state it is not evident if it is entangled or not, sometimes the bases that we are using in the Hilbert spaces of the factors may lead to deceptive results as can be easily see in the following example: consider the state

$$|\psi\rangle = \frac{1}{5}\left(4|00\rangle - 2|01\rangle - 2|10\rangle + |11\rangle\right)\ , \tag{2.9}$$

that seems to be entangled, but it is not the case since $|\psi\rangle = |v\rangle \otimes |v\rangle$, where $|v\rangle = \frac{1}{\sqrt{5}}\left(2|0\rangle - |1\rangle\right)$, thus the state is in fact separable.

The complexity of the situation exemplified above increases with the dimension of the spaces and (perhaps most importantly) the number of factors.

The non-classical correlations observed among the different subsystems are not interpreted as a problem of the theory, rather as an opportunity to develop novel applications. Under this perspective, quantum entanglement is a kind of useful resource, this utility has been illustrated in many contexts, in quantum information, quantum computation or quantum metrology, with many examples in which protocols involving entangled states perform a task in the most efficient way.

As a resource, we would like to quantify how much entanglement we have or develop detectors of this valuable property. Horodecki et. al in its well known review [14] address some fundamental questions about entanglement in this direction:

- How to detect quantum entanglement?
- How to characterize, control and quantify quantum entanglement?
- How to avoid *the unavoidable process of degradation* of quantum entanglement?

An answer to these questions would require a classification and a quantification of entanglement. Let us study this in the simplest scenario: bipartite systems.

2.2 Bipartite systems and Schmidt decomposition

Consider a general bipartite state $|\psi\rangle \in \mathcal{H}_1 \otimes \mathcal{H}_2$, which can be written in the form

$$|\psi\rangle = \sum_{i,j=-s}^{s} \Gamma_{ij} |i\rangle \otimes |j\rangle \ . \tag{2.10}$$

It is guaranteed, by the Schmidt theorem, that there are bases $|\phi_i\rangle$ for $\mathcal{H}_1$ and $|\varphi_i\rangle$ for $\mathcal{H}_2$ in which $|\psi\rangle$ takes the form

$$|\psi\rangle = \sum_{k=1}^{2s+1} \lambda_k |\phi_k\rangle \otimes |\varphi_k\rangle \ . \tag{2.11}$$

where λ_k are real, non-negative and unique up to reordering. This way to write a quantum state is called *Schmidt decomposition* and it is closely related to the singular value decomposition of the matrix of coefficients Γ_{ij}.

The Schmidt decomposition allows us to detect entanglement, thorough the cardinality of the set of non-zero λ's, called *Schmidt rank*. Schmidt rank is 1 for separable states and at least two for entangled states. This quantity has been proposed as a discrete measure of entanglement.

There is a vast literature about the quantification of entanglement, and in many cases a refinement of the above measure is needed, this can be performed by using a continuous measure of entanglement. Probably, in terms of its reasonable properties, the best candidate

in the bipartite case is the Shannon information of the Schmidt coefficients:

$$S = -\sum_k \lambda_k \log \lambda_k \ , \tag{2.12}$$

being zero for separable states because $\lim_{x\to 0^+} x \log x = 0$, and reaching its maximum for the case of the uniform distribution $\lambda_k = 1/2 \ \forall k$. Those states that maximize S are called maximally entangled, for example, in the case of two qubits, the state $\frac{1}{\sqrt{2}}(|00\rangle + |11\rangle)$ is a maximally entangled quantum state.

The entanglement of pure bipartite systems is well understood using the Schmidt decomposition; however, there is not a clear generalization of this result for more complex systems and the detection and quantification of entanglement become hard tasks to accomplish.

Several attempts to generalize the aforementioned analysis have been carried out, as extensions in particular cases of the Schmidt decomposition [17, 18], entanglement witnesses, capable to detect entanglement although they do not give rise to an entanglement measure, or generalizations of the Schmidt rank like the *tensor rank* which measures the minimal number of factors needed to write a state in all the possible bases, this quantity in fact can be used as a discrete measure of entanglement.

For example, it can be shown that the minimal number of summands in any expression of the state $|W\rangle = \frac{1}{\sqrt{3}}(|100\rangle + |010\rangle + |001\rangle)$ is 3, i.e., its tensor rank is 3, this guarantees that this is not a factorizable state. The natural question at this point is how to find a better measure, e.g., a continuous measure of entanglement in the case of a N-partite system, for $N \geq 3$.

A reasonable approach to solve this problem came from an axiomatic perspective: which are the elementary requirements that we expect from a candidate of an entanglement measure?

As entanglement is a quantification of the non-local properties of the subsystems of a more complex quantum system, one of the basic features of a desirable measure of entanglement must be to be invariant under local unitary operations (LU), because local operations do not alter the global quantum correlations.

Due to its complexity, one usually considers a broader class of operations under which we expect entanglement to be al least non-increasing, these operations are called SLOCC (stochastic local operations and classical communication). Even in this case, the classification of

SLOCC-equivalent states is a difficult problem, with, in general, an infinite number of classes of equivalent states. The problem of the construction of a completely satisfactory measure remains unsolved. In this respect, geometric ideas have been useful to expand our horizons in our understanding and quantification of entanglement [19, 20, 21, 22, 23, 24, 25, 26, 27].

2.3 Separable state space, tensor rank and secant varieties

As we studied in the last section, entanglement is defined through the non-separability of a given quantum state. Then, for entangled states the number of elements in any linear combination that describes the state is at least two. The minimal number of terms in the linear combination of a state, considering all the possible bases, is called the *tensor rank* of the state. This quantity has been proposed as a discrete measure of entanglement [28]. For example, in the case of three qubits, the GHZ state, $|\psi_{\mathrm{GHZ}}\rangle = \frac{1}{\sqrt{2}}(|000\rangle + |111\rangle)$, is of rank two and the W state, $|\psi_{\mathrm{W}}\rangle = \frac{1}{\sqrt{3}}(|100\rangle + |010\rangle + |001\rangle)$, is of rank three. This varying amount of entanglement has been related with different physical properties. For example, the W state entanglement is more robust than that of the GHZ state, because, under projections on a particular qubit, GHZ entanglement disappear while in the W case, after a measurement on a particular factor, the resulting reduced state is still entangled.

This classification of quantum states in terms of their tensor rank, besides its apparent purely algebraic definition, has a deep geometrical meaning related to the concept of secant varieties.

The notion of secant variety is closely related to the concept of rank (in our context it will mean tensor rank). Denoting the rank of a state $[\psi]$ in projective space by $rk[\psi]$, define $\mathbb{X}_r := \{[\psi] \in \mathbb{P} \ : \ rk[\psi] = r\}$, for $r = 1, 2, \ldots$. It is easy to note that there exists a maximal possible rank r_m such that $\mathbb{X}_{r_m} \neq \emptyset$ and $\mathbb{X}_r = \emptyset$ for $r > r_m$. In general, $\mathbb{X}_r \subset \mathbb{P}$ are not closed sets in the Zarisky topology. We define the r-th secant variety of $\mathbb{X}_1$ (i.e., separable states) as

$$\sigma_r(\mathbb{X}_1) = \overline{\bigcup_{x_1,\ldots,x_r \in \mathbb{X}_1} \mathbb{P}_{x_1,\ldots,x_r}} \ , \tag{2.13}$$

where $\mathbb{P}_{x_1,\ldots,x_r}$ denotes the projective subspace of $\mathbb{P}$ spanned by the points $x_1, \ldots, x_r$ and the bar refers to the take the topological closure. They satisfy that $\sigma_1(\mathbb{X}_1) = \mathbb{X}_1$ and $\sigma_r(\mathbb{X}_1) \subset$

$\sigma_{r+1}(\mathbb{X}_1)$.

Separable states define a certain (projective) algebraic variety which, in general, has lower dimension than the full space of quantum states of the corresponding spin. The states of rank two lie in the first secant variety to the separable variety (which contain rank-2 states and the separable ones). The second secant variety, corresponding to rank-3 states, contains all the states whose rank is 3 or less, and so on. This onion-like structure continues until the maximal rank secant variety which corresponds to all projective space. A state has maximal rank (and therefore is maximally entangled with respect to the discrete measure) if it is not in any of the smaller secant varieties.

In some cases, the dimension of two consecutive secant varieties does not change, this is due to topological reasons and the concept of tangent varieties is useful to understand this point. In [29] a precise definition of these ideas and some formulas for the expected dimension of these varieties in some particular cases of interest are given. At this point, it will be useful to illustrate this in the simplest case: a bipartite system of spin 1/2. For rank 2, 3 and more, different geometric techniques will be necessary to describe the state spaces.

Let us see how the space of separable states of a bipartite system of spin 1/2 looks like. A bipartite state of spin s is of the form

$$|\Psi\rangle = \sum_{i,j=-s}^{s} \Gamma_{ij} |\psi_i\rangle \otimes |\phi_j\rangle \ , \tag{2.14}$$

where $|\psi_i\rangle$ and $|\phi_j\rangle$ denote bases in the corresponding spaces of the factors.

If this state is separable, it is the tensor product of two states

$$|\Psi\rangle = (a_0|\psi_0\rangle + a_1|\psi_1\rangle) \otimes (b_0|\phi_0\rangle + b_1|\phi_1\rangle) \ , \tag{2.15}$$

then for separable states $\Gamma_{ij} = a_i b_j$, and then the relation $\Gamma_{00}\Gamma_{11} - \Gamma_{01}\Gamma_{10} = 0$ is satisfied.

Geometrically, this complex (projective) variety is a doubly ruled surface (if the coordinates were taken real, this relation would describe a hyperboloid of one sheet).

In the general bipartite case, the space of separable states correspond to an embedding of

$\mathbb{C}P^n \times \mathbb{C}P^m$ into $\mathbb{C}P^{(n+1)(m+1)-1}$, which maps the pair $([\psi], [\phi])$ to $[\psi_0\phi_0 : \psi_0\phi_1 : \cdots : \psi_0\phi_m : \psi_1\phi_0 : \cdots : \psi_n\phi_m]$. This is a well known map in algebraic geometry, called *Segre embedding* [3, 30].

The most general space of quantum states (including mixed states), even for spin s states, remains barely explored until now, but some properties have been studied and summarized in [31, 3]. This space is the space of density matrices of dimension $N = 2s + 1$, hence its dimension is $N^2 - 1$ and it is a convex space. As pure separable states are part of this, it contains a complex projective space in its boundary. Its cross-sections and projections are related to numerical ranges of complex operators in the case of dimension two, and with joint numerical ranges of sets of operators in the three dimensional case [32]. Maximally entangled states also define an interesting lagrangian manifold of dimension half of the total dimension, the problem of a full understanding of this property remains open until today.

One of the main products derived from this thesis is related to rotational properties of multipartite systems, then, a brief description of rotations for those systems is necessary to present our results.

2.4 Rotations of multipartite systems

In this section we recall some general aspects of the action of the Lie group $SU(2)$ on tensor powers of $\mathcal{H}$ and some results on representation theory. This material will be essential to understand some generalizations of the Majorana representation, that will be useful to study different physical problems in areas like quantum computation and quantum metrology.

In 1.3.2 we studied how rotations act on quantum states by means of the Lie group $SU(2)$. Now we will see how this action is extended to tensor powers of $\mathcal{H}$ at the Lie algebra level.

If we apply a rotation to a multipartite system, each part will rotate by the same rotation. This means that if $g \in SU(2)$, its action over an element of the form $|\Psi\rangle = |\psi_1\rangle \otimes \cdots \otimes |\psi_k\rangle \in \mathcal{H}^{\otimes k}$ will be given by

$$g \triangleright (|\psi_1\rangle \otimes \cdots \otimes |\psi_k\rangle) = g \triangleright |\psi_1\rangle \otimes \cdots \otimes g \triangleright |\psi_k\rangle \ . \tag{2.16}$$

In practice, it is convenient to work with matrix representations of the group. If $\mathcal{H}_s$ is the Hilbert space of a spin-s state, i.e., $\mathcal{H}_s \sim \mathbb{C}^{2s+1}$, $g \in SU(2)$ acts on those states from the left by means of the matrix $D^{(s)}(g)$, regarding states as column vectors in this vector space. Hence, the group action is computed by

$$g \triangleright |\psi_1\rangle \otimes \cdots \otimes g \triangleright |\psi_k\rangle \to D^{(s)}(g)|\psi_1\rangle \otimes \cdots \otimes D^{(s)}(g)|\psi_k\rangle =: D^{(s,k)}(g)|\Psi\rangle \ , \tag{2.17}$$

where

$$D^{(s,k)}(g) := \underbrace{D^{(s)}(g) \otimes \cdots \otimes D^{(s)}(g)}_{k \text{ times}}$$

constitutes a $(2s+1)^k$-dimensional representation of $SU(2)$ on $\mathcal{H}_s^{\otimes k}$.

Each $g \in SU(2)$ can be written as an element of the form $g = e^{-i\alpha\hat{n}\cdot\mathbf{S}}$, where $S_i, i \in \{x, y, z\}$ denotes the generators of the Lie algebra $\mathfrak{su}(2)$, which satisfy the commutation relations $[S_i, S_j] = i\epsilon_{ijk}S_k$.

The action of the $SU(2)$ elements on states in $\mathcal{H}$ at the infinitesimal level is given through the action of $\mathfrak{su}(2)$ on $\mathcal{H}$. It is common to use matrix representations also for the Lie algebra elements, so that the element $S_n \in \mathfrak{su}(2)$ acts in $|\psi\rangle \in \mathcal{H}_s$ in the corresponding spin s representation, i.e.,

$$S_n \triangleright |\psi\rangle = S_n^{(s)}|\psi\rangle \ , \tag{2.18}$$

where $S_n^{(s)}$ is a hermitian matrix of dimension $2s+1$. It is a very well known result that in the case of this group (and algebra) there exists irreducible representations for all dimensions, this is a highly non-trivial situation, that does not happen in other groups, e.g., $SU(3)$.

The corresponding action of the algebra on the tensor powers of $\mathcal{H}_s$, denoted by $S_n \triangleright |\psi_1\rangle \otimes \cdots \otimes |\psi_k\rangle$, is given in terms of representations as

$$S_a \triangleright (|\psi_1\rangle \otimes \cdots \otimes |\psi_k\rangle) = \sum_{m=1}^{k} |\psi_1\rangle \otimes \cdots \otimes S_a^{(s)}|\psi_m\rangle \otimes \cdots \otimes |\psi_k\rangle \ =: S_n^{(s,k)}|\Psi\rangle \ , \tag{2.19}$$

defining a representation of $\mathfrak{su}(2)$ in $\mathcal{H}_s^{\otimes k}$.

We see in this case that the elements of the Lie algebra act as derivations, i.e., satisfying Leibniz rule. This is so because in this way, when the generators are exponentiated to obtain the group elements, their action complies with (2.16). In terms of spin-s representations we have then the following relations between the matrices that represent group elements and those representing algebra elements:

$$D^{(s)}(g) = e^{-it\hat{n}\cdot\mathbf{S}^{(s)}} \ , \ \hat{n}\cdot\mathbf{S}^{(s)} = i\frac{\partial}{\partial t}D^{(s)}(g)|_{t=0} \ , \tag{2.20}$$

that in the case of the action on tensor powers of $\mathcal{H}_s$ take the form

$$D^{(s,k)}(g) = e^{-it\hat{n}\cdot\mathbf{S}^{(s,k)}} \ , \ \hat{n}\cdot\mathbf{S}^{(s,k)} = i\frac{\partial}{\partial t}D^{(s.k)}(g)|_{t=0} \ . \tag{2.21}$$

2.5 Symmetric and antisymmetric states

In $\mathcal{H}^{\otimes k} = \mathcal{H}\otimes\cdots\otimes\mathcal{H}$, there are two particularly interesting subspaces: the subspace of totally symmetric tensors $\mathcal{H}^{\vee k}$ and the subspace $\mathcal{H}^{\wedge k}$ of totally antisymmetric tensors. These spaces are defined as the images of $\mathcal{H}^{\otimes k}$ under the action of the corresponding projectors $\pi_k^{\vee} : \mathcal{H}^{\otimes k} \to \mathcal{H}^{\vee k}$ and $\pi_k^{\wedge} : \mathcal{H}^{\otimes k} \to \mathcal{H}^{\wedge k}$, respectively, whose action on the element $f_1 \otimes \cdots \otimes f_k \in \mathcal{H}^{\otimes k}$ is given by:

$$\pi_k^{\vee}\left(f_1 \otimes \cdots \otimes f_k\right) = \frac{1}{k!}\sum_{\sigma\in S_k} f_{\sigma(1)} \otimes \cdots \otimes f_{\sigma(k)} \ , \tag{2.22}$$

and

$$\pi_k^{\wedge}\left(f_1 \otimes \cdots \otimes f_k\right) = \frac{1}{k!}\sum_{\sigma\in S_k} (-1)^{\sigma} f_{\sigma(1)} \otimes \cdots \otimes f_{\sigma(k)} \ , \tag{2.23}$$

respectively. In these expressions, S_k denotes the permutation group of k elements and $(-1)^{\sigma}$ denotes the sign of the permutation σ. We will write $f_1 \vee \cdots \vee f_k$ to represent $\pi_k^{\vee}\left(f_1 \otimes \cdots \otimes f_k\right)$ and similarly, $f_1 \wedge \cdots \wedge f_k = \pi_k^{\wedge}\left(f_1 \otimes \cdots \otimes f_k\right)$.

It is easy to show that $\dim\mathcal{H}^{\vee k} = \binom{n+k-1}{k}$ and that $\dim\mathcal{H}^{\wedge k} = \binom{n}{k}$.

The inner product $\langle \cdot \mid \cdot \rangle$ of $\mathcal{H}$ induces one in $\mathcal{H}^{\otimes k}$,

$$\langle \phi_1 \otimes \cdots \otimes \phi_k | \psi_1 \otimes \cdots \otimes \psi_k \rangle = \langle \phi_1 | \psi_1 \rangle \cdots \langle \phi_k | \psi_k \rangle \ , \tag{2.24}$$

and this one induces another on the symmetric subspace

$$\begin{aligned}
\langle \phi_1 \vee \cdots \vee \phi_k | \psi_1 \vee \cdots \vee \psi_k \rangle &= \frac{1}{(k!)^2} \sum_{\sigma,\sigma' \in S_k} \langle \phi_{\sigma(1)} \otimes \cdots \otimes \phi_{\sigma(k)} | \psi_{\sigma'(1)} \otimes \cdots \otimes \psi_{\sigma'(k)} \rangle && (2.25) \\
&= \frac{1}{k!} \sum_{\sigma \in S_k} \langle \phi_1 \otimes \cdots \otimes \phi_k | \psi_{\sigma(1)} \otimes \cdots \otimes \psi_{\sigma(k)} \rangle && (2.26) \\
&= \frac{1}{k!} \sum_{\sigma \in S_k} \langle \phi_1 | \psi_{\sigma(1)} \rangle \cdots \langle \phi_k | \psi_{\sigma(k)} \rangle && (2.27) \\
&= \frac{1}{k!} \mathrm{perm}((\langle \phi_i | \psi_j \rangle)) \ . && (2.28)
\end{aligned}$$

Analogously, for the antisymmetric subspace we have

$$\langle \phi_1 \wedge \cdots \wedge \phi_k | \psi_1 \wedge \cdots \wedge \psi_k \rangle = \frac{1}{k!} \det((\langle \phi_i | \psi_j \rangle)) \ . \tag{2.29}$$

An inner product is not the only geometric structure induced by the original Hilbert space, there also are induced orthonormal bases. Given an orthonormal basis in $\mathcal{H}$ by the ordered set of vectors $e_1, e_2, \ldots, e_n$, the following orthonormal bases for $\mathcal{H}^{\vee k}$ y $\mathcal{H}^{\wedge k}$ are induced, respectively:

$$\sqrt{\frac{k!}{k_1! \cdots k_n!}} \ e_1^{k_1} \vee \cdots \vee e_n^{k_n} \ , \ k_1 + \cdots + k_n = k, \tag{2.30}$$

with $k_1 \leq k_2 \leq \cdots \leq k_n$, and for $\mathcal{H}^{\wedge k}$:

$$\sqrt{k!} \ e_{i_1} \wedge \cdots \wedge e_{i_k} \ , \ 1 \leq i_1 < i_2 < \cdots < i_k \leq n \ . \tag{2.31}$$

Example 6. *Induced bases.*

Let $\{e_i\}$, with $i = 1, 2, 3$, be a basis for the space of states of spin 1; $\mathcal{H} \sim \mathbb{C}^3$. In this case $n = k = 3$, $\dim \mathcal{H}^{\wedge 3} = 1$ and $\dim \mathcal{H}^{\vee 3} = 10$.

The basis vector for $\mathcal{H}^{\wedge 3}$ is given by $e_1 \wedge e_2 \wedge e_3$, which is not normalized, the corresponding normalized vector, with respect to the above inner product, is $\hat{e}_{123} := \sqrt{3} e_1 \wedge e_2 \wedge e_3$.

For $\mathcal{H}^{\vee 3}$, denoting by e_{ijk} the element $e_i \vee e_j \vee e_k$, the induced basis is given by the vectors e_{111}, e_{112}, e_{113}, e_{122}, e_{123}, e_{133}, e_{222}, e_{223}, e_{233}, e_{333}, which are not normalized. The standard basis corresponds to the normalization of those vectors, namely

$$\{\hat{e}_{111}, \hat{e}_{112}, \hat{e}_{113}, \hat{e}_{122}, \hat{e}_{123}, \hat{e}_{133}, \hat{e}_{222}, \hat{e}_{223}, \hat{e}_{233}, \hat{e}_{333}\} = \tag{2.32}$$

$$\{e_{111}, \sqrt{3}e_{112}, \sqrt{3}e_{113}, \sqrt{3}e_{122}, \sqrt{6}e_{123}, \sqrt{3}e_{133}, e_{222}, \sqrt{3}e_{223}, \sqrt{3}e_{233}, e_{333}\} \ . \quad \blacksquare \tag{2.33}$$

2.6 Rotating symmetric and antisymmetric states

The $SU(2)$ action on tensor powers of states, described in 2.4, leads to an action on symmetric and antisymmetric tensor powers.

In one case, we will have that the totally antisymmetric part of $D^{(s,k)}$ defines a representation $D^{(s,k)}_{\wedge}$ of $SU(2)$ over $\mathcal{H}^{\wedge k}$ of dimension $\binom{2s+1}{k}$; in the other case, the totally symmetric part defines a representation $D^{(s,k)}_{\vee}$ of $SU(2)$ over $\mathcal{H}^{\vee k}$ of dimension $\binom{2s+1+k}{k}$. That means that if $|\Psi\rangle \in \mathcal{H}^{\wedge k}$ is a column vector expressed in the induced basis (the so-called *Plücker basis* in this case), the action of $SU(2)$ is given by

$$g \triangleright |\Psi\rangle = g \triangleright (|\psi_1\rangle \wedge \cdots \wedge |\psi_k\rangle) = D^{(s)}(g)|\psi_1\rangle \wedge \cdots \wedge D^{(s)}(g)|\psi_k\rangle \equiv D^{(s,k)}_{\wedge}(g)|\Psi\rangle \ , \tag{2.34}$$

meanwhile, in the symmetric case, if $|\Psi\rangle \in \mathcal{H}^{\vee k}$ represents a column vector in the induced basis,then the actions of $SU(2)$ is given by

$$g \triangleright |\Psi\rangle = g \triangleright (|\psi_1\rangle \vee \cdots \vee |\psi_k\rangle) = D^{(s)}(g)|\psi_1\rangle \vee \cdots \vee D^{(s)}(g)|\psi_k\rangle \equiv D^{(s,k)}_{\vee}(g)|\Psi\rangle \ . \tag{2.35}$$

The corresponding generators act as

$$S_a \triangleright (|\psi_1\rangle \vee \cdots \vee |\psi_k\rangle) = \sum_{m=1}^{k} |\psi_1\rangle \vee \cdots \vee S^{(s)}_a|\psi_m\rangle \vee \cdots \vee |\psi_k\rangle =: S^{(s,k)}_{\vee\ a}|\Psi\rangle \tag{2.36}$$

and

$$S_a \triangleright (|\psi_1\rangle \wedge \cdots \wedge |\psi_k\rangle) = \sum_{m=1}^{k} |\psi_1\rangle \wedge \cdots \wedge S^{(s)}_a|\psi_m\rangle \wedge \cdots \wedge |\psi_k\rangle =: S^{(s,k)}_{\wedge\ a}|\Psi\rangle \ . \tag{2.37}$$

Note that (2.36) implies that a symmetric product of eigenvectors of S_z is an eigenvector of $S^{(s,k)}_{\vee\ a}$ with eigenvalue equal to the sum of the eigenvalues of each of the factors, namely,

$$S_a \triangleright (|s, m_1\rangle \vee \cdots \vee |s, m_k\rangle) = \sum_{i=1}^{k} m_i \, (|s, m_1\rangle \vee \cdots \vee |s, m_k\rangle) \ , \tag{2.38}$$

analogously, the antisymmetric products of eigenvectors of angular momentum gives us eigenvectors of the representation $S_{\wedge}^{(s,k)}$ with eigenvalue given by the sum of the eigenvalues of the factors.

These induced representations in the symmetric and antisymmetric tensor powers of the Hilbert space are not, in general, irreducible. In the following chapters we will see how to find a decomposition into irreducible components and how to use this decomposition to extend the idea of stellar representation to these classes of multipartite states.

To end this chapter we will present some aspects of multipartite entanglement, which will be useful in chapter 3 in our study of entanglement of multipartite symmetric systems and in the last chapter for some discussions about possible future directions of this work.

2.7 Multipartite entanglement and the momentum map

There are several approaches to the classification of multipartite entanglement. Instead of a review of the extensive literature on this topic I will present some ideas that will be useful in our study.

In particular, I will introduce concepts of two different approaches to multipartite entanglement: on the one hand, the theory of invariant polynomials, in particular the hyperdeterminants that generalize in a natural way some well-known entanglement measures, as the concurrence or the 3-tangle. On the other hand, the momentum map, a concept that generalizes the notion of conserved quantity in physics and makes the study of multipartite entanglement a subject with plenty of deep geometrical insights.

2.7.1 Invariant polynomials and quantum entanglement

Apart from entanglement witnesses that allow for the detection of entanglement and entanglement measures that quantify entanglement, there exists a qualitative description of entanglement by means of SLOCC-invariant polynomials, which have the same value for states that differ by a SLOCC operation. If an invariant gives different values for two states, they cannot be equivalent under SLOCC. Let us describe some examples.

Example 7. *Two qubit entanglement*

A general state of two qubits can be written as

$$|\psi\rangle = \sum_{i,j} \Gamma_{ij} |i\rangle \otimes |j\rangle \ , \tag{2.39}$$

where i, j *run from* 0 *to* 1.

The determinant of the matrix $\Gamma = [\Gamma_{ij}]$ *is a degree-2 polynomial, in the components of the state, invariant under SLOCC (and it is essentially the only one), this makes* $\det \Gamma$ *a characteristic feature of the entanglement of this type of systems. This quantity is related to the Shannon entropy of Schmidt coefficients and the entanglement of formation, which is an entanglement measure based on the concurrence* C*, which is related with our polynomial by* $C = 2|\det \Gamma|$.

This shows that, essentially, there is only one way in which two qubits can be entangled, in the sense that all the above measures can be written in terms of the Schmidt coefficients. The non-trivial and very interesting feature of concurrence is that it can be straightforwardly extended to mixed states. ■

Example 8. *Three-qubit entanglement*

In the case of three qubits, the general state can be expanded as

$$|\psi\rangle = \sum_{i,j,k} \Gamma_{ijk} |i\rangle \otimes |j\rangle \otimes |k\rangle \ , \tag{2.40}$$

where i, j, k *run from* 0 *to* 1.

In this case, there also exists a SLOCC-invariant polynomial, that we will call $\det_3 \Gamma$*, closely related to the* 3*-tangle or residual entanglement* τ*, precisely,* $\tau = 4|\det_3 \Gamma|$*. This SLOCC-invariant polynomial is given by [33]*

$$\det_3 \Gamma = (\mathrm{tr} A \mathrm{tr} B - \mathrm{tr} AB)^2 - 4 \det A \det B \ , \tag{2.41}$$

where

$$A = \begin{pmatrix} \Gamma_{000} & \Gamma_{001} \\ \Gamma_{010} & \Gamma_{011} \end{pmatrix} \text{ and } B = \begin{pmatrix} \Gamma_{100} & \Gamma_{101} \\ \Gamma_{110} & \Gamma_{111} \end{pmatrix} . \tag{2.42}$$

Hence, for three qubits we have an invariant polynomial of degree four, instead of one of degree two in the two-qubit case.

This particular way to measure entanglement differs from others because it is a measure of global entanglement, this measure is invariant with respect permutations of the parties that constitute the system. This explain the name residual entanglement*, because it quantifies the fraction of entanglement non described by any two-party measures [3].* ■

These examples can be generalized thanks to the notion of Cayley's hyperdeterminant, for a system of n-qubits there is a SLOCC-invariant polynomial $\det_n \Gamma$, but in general it is difficult to compute. It is known that the degree of the polynomial grows very fast [34], for $n = 2, \ldots, 15$ qubits the degrees are $2, 4, 24, 128, 880, 6816, 60032, 589312, 6384384, 75630080, 972387328, 13483769856, 200571078656, 3185540657152$, respectively.

There are generalizations of this notion of hyperdeterminant for systems of different levels (not only qubits) in each of the factors, and the SLOCC-invariant polynomials are homogeneous of known degree. This complexity of multipartite entanglement has been conjectured to have some relation with the growing complexity of braids as the number of strands increases [35].

2.7.2 Momentum Map

The momemtum map is a geometrical object that generalizes the concept of conserved quantity and has its origin in the study of the relationship between symmetry and conserved quantities in the context of classical mechanics. It is common to state this relationship in the form of a theorem, the celebrated Noether's theorem, usually stated in the Lagrangian formulation of mechanics. On the other hand, the most suitable formulation of mechanics to reveal its geometric structure is the Hamiltonian formulation, in which the dynamics is expressed in terms of the symplectic structure of the phase space. If one wants to translate Noether's theorem into this formulation, the momentum map will come as an elegant and practical tool to state the theorem and to explore conserved quantities in different physical scenarios, even

in a broader context than classical mechanics.

Conserved quantities like linear momentum, angular momentum, electric charge, are different momentum maps but even in quantum mechanical context there are some momentum maps that, besides their complexity, are promising quantities to understand purely quantum phenomena as quantum entanglement. The geometry of momentum map is closely related to the intrinsic convex geometry of quantum mechanics, as we will explore in this section.

I will discuss the definition of momentum map and the related geometric ideas and I will give some examples in the context of classical mechanics. Next, we will explore some momentum maps that naturally arise in quantum mechanics and we will discuss their relevance in physical problems like the classification of quantum entanglement.

Momentum map is a generalization of momentum and angular momentum for more general Lie group actions on symplectic manifolds than simple rigid transformations like translations or rotations. More than a practical tool to describe conserved quantitites in Hamiltonian mechanics, it is a geometric object that carries a lot of physical information to be revealed.

To define a momentum map three basic ingredients are needed:

- A symplectic manifold (M, ω),
- a Lie group G,
- and an action of G over M by symplectomorphisms:

$$\forall\ g \in G\ ,\ \Phi_g : M \to M \text{ such that } \Phi_g^* \omega = \omega\ . \tag{2.43}$$

Once we have a Lie group acting on a manifold, symplectic or not, there is a naturally induced vector field on M, known as fundamental field. Take an element $\xi \in \mathfrak{g}$, where $\mathfrak{g}$ denotes the correspondent Lie algebra associated with G, and define a curve starting on the identity of G with tangent vector ξ. This is always possible, at least locally because the Lie algebra is by definition the vector space of tangent vectors at the identity of the Lie group.

For each $x \in M$ we can define a curve on M, with x as starting point, using the action of G on M, applying to x all the elements belonging to the curve on G generated by ξ. Taking

the tangent vector at x of this curve we define a tangent vector on T_xM. Repeating this procedure for all the points of M we have a well defined vector field, which is denoted by ξ_M and this is the fundamental vector field.

$$x \to \Phi_{e^{t\xi}}(x) \ , \tag{2.44}$$

$$\xi_M(x) = \frac{d}{dt}\left(\Phi_{e^{t\xi}}(x)\right)|_{t=0} \ . \tag{2.45}$$

Now, we are ready to define the momentum map. Let us consider a map $\mu : M \to \mathfrak{g}^*$. For every $x \in M$, $\mu(x)$ is an element of the dual of the Lie algebra and by the usual pairing with vectors

$$\langle \mu(x), \xi \rangle \in \mathbb{R} \ , \tag{2.46}$$

for all $\xi \in \mathfrak{g}$ we define

$$\mu^{\xi}(\cdot) = \langle \mu(\cdot), \xi \rangle : M \to \mathbb{R} \tag{2.47}$$

The function $\mu : M \to \mathfrak{g}^*$ is a momentum map for the action of G on (M, ω) if and only if for all $\xi \in \mathfrak{g}$ it is true that

$$\omega(\xi_M, \cdot) = -d\mu^{\xi}(\cdot) \ . \tag{2.48}$$

This means that we will have different momentum maps if we change the action or the group, or if we change the symplectic structure defined on M. Some examples will be useful to clarify this definition.

Example 9. *Translation on phase space.*

Consider the action of the group of spatial translations in three-dimensional Euclidean space and take as symplectic manifold the phase space of two point particles with the standard symplectic structure. In terms of coordinates we have

$$G = (\mathbb{R}^3, +), \quad M = \{(\vec{r}_1, \vec{r}_2, \vec{p}_1, \vec{p}_2)\}, \quad \omega = d\vec{p}_1 \wedge d\vec{r}_1 + d\vec{p}_2 \wedge d\vec{r}_2 \ . \tag{2.49}$$

The action of G on M is the usual one, $(\vec{r}_1, \vec{r}_2, \vec{p}_1, \vec{p}_2) \to (\vec{r}_1 + \vec{g}, \vec{r}_2 + \vec{g}, \vec{p}_1, \vec{p}_2)$.

The fundamental vector field associated with this action is

$$\xi_M = \xi_x \left(\frac{\partial}{\partial r_{1x}} + \frac{\partial}{\partial r_{2x}} \right) + \xi_y \left(\frac{\partial}{\partial r_{1y}} + \frac{\partial}{\partial r_{2y}} \right) + \xi_z \left(\frac{\partial}{\partial r_{1z}} + \frac{\partial}{\partial r_{2z}} \right) \ . \tag{2.50}$$

Then,

$$\omega(\xi_M, \cdot) = -d(\vec{p}_1 + \vec{p}_2) \cdot \vec{\xi} \ , \tag{2.51}$$

therefore,

$$\mu = \vec{p}_1 + \vec{p}_2 \ . \tag{2.52}$$

In this example, momentum map is just the total linear momentum of the system (this explains the name of this object). I would like to emphasize that this is a function that evaluated in a point on the phase space gives us an element of the dual of the Lie algebra, being in this case $(\mathbb{R}^3)^* \sim \mathbb{R}^3$, i.e. , $\vec{p}_i$ acts on a vector $\vec{\xi}$ by $\vec{p}_i(\vec{\xi}) = p_{1x}\xi_x + p_{1y}\xi_y + p_{1z}\xi_z$. ■

Example 10. *Angular momentum. (Taken from [36]) If now we take as Lie group $SO(3)$, this is spatial rotations in three dimensions and M a phase space with the standard symplectic structure*

$$M = \{(\vec{r}, \vec{p})\}, \quad \omega = d\vec{p} \wedge d\vec{r} \ . \tag{2.53}$$

It can be shown, following a similar procedure that

$$\mu \sim \vec{L} \tag{2.54}$$

Hence, angular momentum is the momentum map that results from the action of rotations on phase space. ■

One of the most important properties of the momentum map are the convex structures that arise from it, this is one of the points that besides to be non-evident from our intuition

of classical conserved quantities, will be very important to understand momentum map in quantum mechanics. Useful references for this topic are [37, 38, 39, 40].

The first convexity theorem states that if G is a Lie group acting by symplectomorphisms on M with momentum map μ, and if G is abelian, then $\mu(M)$ is a convex polytope whose extremal points are the fixed points by the group action. This theorem was proven by Atiyah and by Guillemin and Sternberg, independently.

For example, consider as symplectic manifold $M = \mathbb{C}P^n$ with the usual Fubini-Study symplectic form. Let $G = T^{n+1}$, the diagonal subgroup of the unitary group, act on M. Note also that $\mathfrak{g} \sim \mathbb{R}^{n+1}$.

In this case,

$$\mu([z_0, z_1, \ldots, z_n]) = \frac{1}{\sum_i |z_i|^2} \left(|z_0|^2, |z_1|^2, \cdots, |z_n|^2\right) \ , \tag{2.55}$$

from this we conclude that the image of the entire complex projective space, under the momentum map, is the classical probability simplex, which is obviously convex.

The natural question to address at this point is, what if G is non-abelian? This was answered by Kirwan by showing the following theorem. To state it, define $\Psi(M)$ as the intersection of the image of the momentum map of an orbit in M and the positive Weyl chamber $\mathfrak{t}_+^*$, defined as the Weyl chamber[1] of vectors of positive entries in decreasing order.

Theorem. Let G be a compact, connected Lie group acting on a compact and symplectic manifold M with momentum map μ. If G is non-abelian then $\Psi(M)$ ($\Psi : M \to \mathfrak{t}_+^*$) is a convex polytope[2], known as Kirwan polytope.

There are some particular theorems about the momentum map in the case where $M = \mathbb{C}P^n$:

- The set $\Psi(\overline{G \triangleright x})$ is a convex polytope, where the bar denotes the topological closure of the G-orbit of x.
- The collection of all possible polytopes that can be obtained by mapping all the orbits

[1] Weyl chambers are defined as the spaces of orbits under the action of the unitary group.

[2] A convex polytope is defined as the convex hull of a finite set of points.

from every $x \in \mathbb{C}P^n$ is finite.

Example 11. *Momentum map for a multipartite quantum system*

Consider a multipartite quantum system under the action of the special unitary group. Call G the complexification of this group (this is the one that will be used to compute the momentum map)

$$\mathcal{H} = \mathbb{C}^N \otimes \cdots \otimes \mathbb{C}^N \ , \ G = SL(N,\mathbb{C})^{\times L} \text{ and } K = SU(N)^{\times L}, \text{ with } G = K^{\mathbb{C}}.$$

The momentum map is given by [40]

$$\mu([\phi]) = \left(\rho_1([\phi]) - \frac{1}{N}, \rho_2([\phi]) - \frac{1}{N}, \ldots, \rho_L([\phi]) - \frac{1}{N}\right) \ , \tag{2.56}$$

whose entries contain the information of the reduced density matrices of the system. This appearance of the reduced density matrix is what primarily suggests the relationship between momentum map and entanglement. More specifically, as discussed in [40], maximally entangled states correspond to critical states of the square modulus of momentum map, conclusions of this type are related to geometric invariant theory and methods of Morse functions. ■

2.7.3 Kirwan polytopes in Quantum Mechanics

The image of the momentum map, appropriately restricted under Kirwan' s theorem considerations will be a convex polytope. In the case of M qubits ($N = 2$) this is the polytope defined by the polygonal inequalities:

$$\lambda_k \leq \lambda_1 + \cdots + \lambda_{k-1} + \lambda_{k+1} + \cdots + \lambda_M. \tag{2.57}$$

With $0 \leq \lambda_k \leq 1/2$, denoting by λ_k the minimal eigenvalue of the k-th reduced density matrix $\rho_k([\phi])$. This is a very important result because it shows that we can obtain information about the entanglement of the system by local information, in the sense that is the information encoded by the reduced density matrices. Let's exemplify the Kirwan polytopes in the case of a three qubit system.

Example 12. *Kirwan polytopes for three qubits (taken from [3])*

In this case we have 6 classes of entanglement, each one defined as the SLOCC orbit of the following representative states:

$$|\psi_{sep}\rangle = |000\rangle \tag{2.58}$$

$$|\psi_1\rangle = \frac{1}{\sqrt{2}}\left(|001\rangle - |010\rangle\right) \quad |\psi_2\rangle = \frac{1}{\sqrt{2}}\left(|001\rangle - |100\rangle\right) \quad |\psi_3\rangle = \frac{1}{\sqrt{2}}\left(|010\rangle - |100\rangle\right) \tag{2.59}$$

$$|\psi_{GHZ}\rangle = \frac{1}{\sqrt{2}}\left(|000\rangle + |111\rangle\right) \quad |\psi_W\rangle = \frac{1}{\sqrt{3}}\left(|001\rangle + |010\rangle + |100\rangle\right) \ . \tag{2.60}$$

For the separable state we have that Kirwan polytope is only a single point (see Figure 2.1 (a)), for biseparable states (i.e., $|\psi_1\rangle, |\psi_2\rangle, |\psi_3\rangle$ defined above) the polytopes are segments (see Figure 2.1 (b)), all the SLOCC-equivalent states to the W state belong to the pyramid and the whole space, including the class of GHZ state has as Kirwan polytope the bipyramid that contains all the above figures. Figure 2.1 (d) shows the nested Kirwan polytopes for this example.

In the case of n qubits it is known that the Kirwan polytope is the convex hull of $2^n - n$ extreme points.

For systems of higher dimensionality the structure of these polytopes is as follows [3, 41]:

n=3 : 5 vertices and 6 faces

n=4 : 12 vertices and 12 facets

n=5 : 27 vertices and 15 facets

This exemplifies how the momentum map can help us to understand multipartite entanglement . Even if SLOCC classes are infinite, the number of Kirwan polytopes remains finite, then, we have a finite number of families in which we can classify states according to a meaningful criterion related to its SLOCC equivalence.

In the following chapter we will focus on the study of a particular class of multipartite systems, those with a very particular symmetry property.

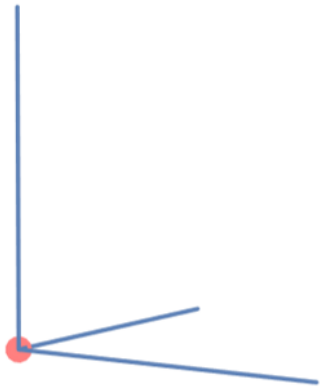

(a) Separable state.

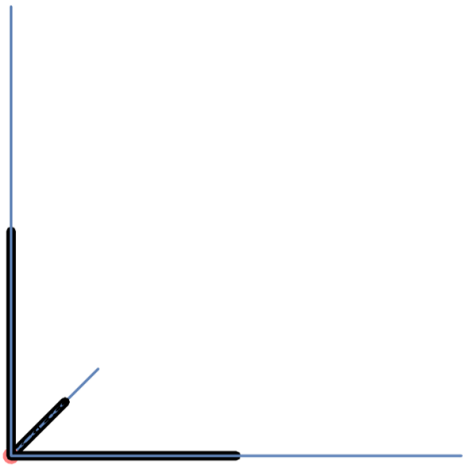

(b) Biseparable states.

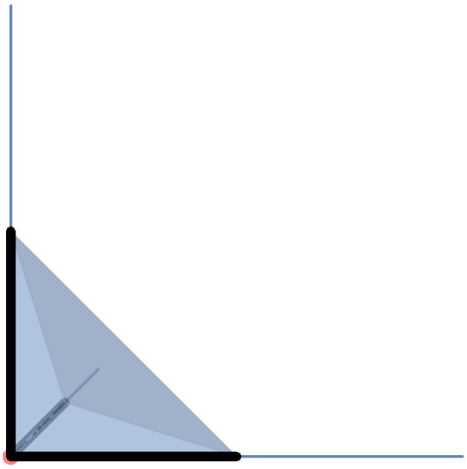

(c) Pyramid of states
SLOCC equivalent to W

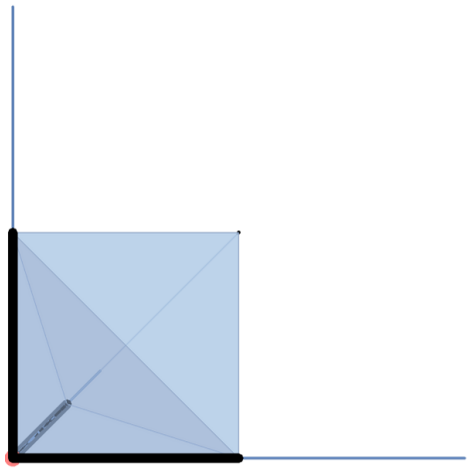

(d) Bipyramid of states
SLOCC equivalent to GHZ

Figure 2.1: Kirwan polytopes for three-qubit systems.

Chapter 3

Geometry of symmetric multiqudit systems

Symmetric multiqudit states are an interesting starting point to explore the geometry and the physical properties of multipartite quantum states. Due to its symmetry properties, the dimension of the spaces is noticeably reduced and this can diminish the complexity of several questions about those states, apart from this, we know that in the multiqubit case, we recover the well known theory of single spins in the sense that a spin s state can be understood as a symmetrized state of $2s$ two-level systems.

Some symmetric states of three and four qutrits and states of two qudits have been useful for processes of quantum error correction, and some states of this class are absolutely maximally entangled states, this means that are multipartite states that carry the maximal possible amount of entanglement in all possible partitions, those states are relevant in different tasks in quantum information contexts [42, 3]. The entanglement properties of this class of quantum states will be explored in a geometric way in the applications part of this chapter as well as some metrological aplications in the problem of quantum detection of rotations.

3.1 Stellar representation of symmetric multiqudit states

In this section we develop a generalization of the Majorana stellar representation to the case of symmetric multiqudit states, which naturally reduces to Majorana representation when the system is composed by qubits in all the tensor factors. This will be useful to clarify the rotational properties of this class of multipartite quantum states. As we show below, in this case there is no way to associate a constellation with each state in a one-to-one form, rather we must associate a collection of constellations, a *multiconstellation*, that reveals those properties. This will be useful to find some states with interesting metrological properties. In order to construct this multiconstellation, we must analyze how the $\mathfrak{su}(2)$ action on the totally symmetric subspace of a tensor power of Hilbert space is decomposed into irreducible components, this action was introduced in section 2.6.

3.1.1 Irreducible components of the $\mathfrak{su}(2)$ action

To decompose the matrices representing the action of the element $g \in \mathfrak{su}(2)$ on tensor powers of $\mathcal{H}$ as a direct sum of irreducible representations , $D_{\vee}^{(s,k)}(g)$, we must block-diagonalize those matrices. In other words, we want to express

$$D_{\vee}^{(s,k)}(g) = \bigoplus_{i=s_{\min}}^{s_{\max}} m_i^{(s,k)} D^{(i)}(g) \ , \tag{3.1}$$

where i increases by integer steps (as we will show later) and $m_i^{(s,k)}$ is the multiplicity of $D^{(i)}$ in the decomposition of $D_{\vee}^{(s,k)}$. Notice that there is no ambiguity in labelling the irreducible components by a single number, since there is a canonical choice (in fact, essentially unique) of representation for each i.

Therefore, we must find $s_{\min}$, $s_{\max}$, and the multiplicities $m_i^{(s,k)}$ and the basis that performs the change of basis to the block-diagonal one.

Following the standard procedure, to find the block-diagonal basis we must find the vector of maximum weight and then apply the lowering operator to find the first multiplet. Subsequently, using orthogonality, the maximum weight vector corresponding to the next block is generated and with the lowering operator the entire second multiplet is generated and so on. By (2.38) we know that the eigenstate of maximal eigenvalue corresponds to the symmetrized

product of the vectors of maximal spin in each factor, i.e.,

$$|s_{\max}, s_{\max}\rangle = |s, s\rangle \vee \cdots \vee |s, s\rangle \ , \tag{3.2}$$

so, from this expression the spin of the highest representation is determined, $s_{\max} = ks$.

To generate the basis we must apply the lowering operator, if we apply it once we will obtain (normalizing) the second state of the block-diagonalized basis under consideration, which is given by

$$|s_{\max}, s_{\max} - 1\rangle = \sqrt{k}|s, s\rangle \vee \cdots \vee |s, s\rangle \vee |s, s-1\rangle \ , \tag{3.3}$$

If we apply the lowering operator once more, a new basis vector will be generated, which is in a two-dimensional space generated by the states E_1 and E_2, the linear combination orthogonal to this vector will serve as a vector of maximum weight for the generation of the representation of the second block, continuing in this way it is possible to construct the entire basis that diagonalizes the original representation by blocks.

From this it is clear that $m^{(s,k)}_{s_{\max}} = 1$ and that $m^{(s,k)}_{s_{\max}-1} = 0$ and that the next block appears until after two applications of the lowering operator to the maximum weight state. Since the operator lowers the spin in integer steps, we know that if we start with integer spin, all the representations that appear in the block decomposition will be of integer spin and if we begin with maximum half-integer spin, the representations that appear in the decomposition will all be of half-integer spin.

From this we see that then $s_{\min} = 0$ except in the case of k odd and s half-integer in which $s_{\min} = 1/2$, although it may be the case that not all the representations appear and the one of $s_{\min}$ is not reached.

Although the multiplicities of the different representations can be read from this algorithm, there is a more efficient way of calculating them if we are only interested in these and not the whole change of basis. This technique, based on character theory, will be presented in subsection 3.1.2.

Let us see the simplest example, apart from the case of symmetrized qubits that leads to the well-known result that $2s$ spins $1/2$ are rotationally indistinguishable from a single spin-s.

Example. Symmetric state of two qutrits.

First, we must notice that the dimension of the symmetric tensor space in this case is 6 with a basis given by:

$$e_{11} = e_1 \vee e_1, \quad e_{12} = e_1 \vee e_2, \quad e_{13} = e_1 \vee e_3,$$
$$e_{22} = e_2 \vee e_2, \quad e_{23} = e_2 \vee e_3, \quad e_{33} = e_3 \vee e_3.$$

This is an orthogonal but not orthonormal basis, normalizing this basis we obtain the following orthonormal basis:

$$\hat{e}_{11} = e_1 \vee e_1, \quad \hat{e}_{12} = \sqrt{2}e_1 \vee e_2, \quad \hat{e}_{13} = \sqrt{2}e_1 \vee e_3,$$
$$\hat{e}_{22} = e_2 \vee e_2, \quad \hat{e}_{23} = \sqrt{2}e_2 \vee e_3, \quad \hat{e}_{33} = e_3 \vee e_3.$$

Now we must find an adequate basis for rotations, i.e., the block-diagonal basis which in this case gives us a natural decomposition in a spin 2 subspace and a spin 0, each one transforming with its corresponding representation of rotations when the original state is rotated, as explained above. In this case, the orthonormal basis that block-diagonalizes the action of rotations is found by successive applications of the lowering operator starting with the state

$\hat{e}_{11}$ and it is given by

$$\text{for the spin 2 :}$$

$$e_{(2,2)} = \hat{e}_{11} \ ,$$

$$e_{(2,1)} = \hat{e}_{12} \ ,$$

$$e_{(2,0)} = \sqrt{\frac{2}{3}} \left(e_2 \vee e_2 + e_1 \vee e_3 \right) \ ,$$

$$e_{(2,-1)} = \hat{e}_{23} \ ,$$

$$e_{(2,-2)} = \hat{e}_{33} \ ,$$

$$\text{and for the spin 0 :}$$

$$e_{(0,0)} = \frac{1}{\sqrt{3}} \left(e_2 \vee e_2 - 2 e_1 \vee e_3 \right) ,$$

where the spin 0 component was found taking a linear combination orthogonal to $e_{(2,0)}$.

We can collect the information of the new basis in a matrix $U_{(1,2)}$, in this case given by

$$U_{(1,2)} = \begin{pmatrix} 1 & 0 & 0 & 0 & 0 & 0 \\ 0 & 1 & 0 & 0 & 0 & 0 \\ 0 & 0 & \frac{1}{\sqrt{3}} & \sqrt{\frac{2}{3}} & 0 & 0 \\ 0 & 0 & 0 & 0 & 1 & 0 \\ 0 & 0 & 0 & 0 & 0 & 1 \\ 0 & 0 & -\sqrt{\frac{2}{3}} & \frac{1}{\sqrt{3}} & 0 & 0 \end{pmatrix} . \tag{3.4}$$

This change of basis, acting on states by simple multiplication and on operators by conjugation, allows to express the $\mathfrak{su}(2)$ matrices in a block-diagonal form consisting of a five-dimensional block in which appears the spin-2 representation of the algebra and a spin 0 one-dimensional block. Thus, when one applies this matrix to a state written as a column vector whose components are given by the projections of the state along the induced basis vectors the result is a new column vector that have the components in the block-diagonal basis.

In the general case of k-symmetric states of spin s, our construction procedure will result in a matrix $U_{(s,k)}$ that block-diagonalizes the action as in the last example. Then, if we denote by a subscript S the standard induced basis, with the proper normalization and by BD the block-diagonal one, then $|\Psi\rangle_{BD}^T = U_{(s,k)}|\Psi_S\rangle$ and

$$|\Psi\rangle_{BD}^T = \left(|\psi^{s_{max}}\rangle^T, |\psi^{s_{max}-2}\rangle^T, \cdots\right) \ , \tag{3.5}$$

where we denote by T the usual operation of transposition.

In general, some blocks will be repeated and the appearing representations in the decomposition will have particular multiplicities. This point will be clarified in the following subsection.

3.1.2 Multiplicities and characters

Character theory is a useful tool to study the representations of a Lie group. Let us introduce some basic definitions and results that will be useful in our study of the irreducible representations that appear in the decomposition of $D_\vee^{(s,k)}$.

Given a group G and a representation $\rho_V : G \to GL(V)$, we define the character of the representation as a function from G to $\mathbb{R}$ that is given in the element $g \in G$ by the trace of the matrix that represents g. That means, if the element $g \in G$ is represented by $\rho_V(g) \in GL(V)$, then

$$\chi_V(g) := \mathrm{tr}\left(\rho_V(g)\right) \ . \tag{3.6}$$

It is easy to see, by the cyclicity of the trace and by the definition of a representation, that χ_V is a class-function on G, i.e., a function which is invariant under conjugation. As noticed above, we commonly refer to the representation by its carrier space, this is the space in which it acts.

For example, if we take $G = SU(2)$ and we take the spin s representation, it suffices to compute the character of a rotation of angle α with respect to z-axis, because any other can be found by conjugation with other group elements.

In this case, the computation simply reduces to

$$\chi_s(\alpha) = \mathrm{tr\ diag}\left(e^{-i\alpha s}, e^{-i\alpha(s-1)}, \ldots, e^{i\alpha s}\right) = e^{-i\alpha s} + e^{-i\alpha(s-1)} + \cdots + e^{i\alpha s} = \frac{\sin\left(\frac{2s+1}{2}\alpha\right)}{\sin\frac{\alpha}{2}} \ , \tag{3.7}$$

note that there is an abuse of notation because we label the character with s instead of the vector space where the spin-s representation of $SU(2)$ is acting.

Given representations of a Lie group, we can deduce from them new representations, e.g., taking direct sums or tensor products. In these cases, characters of the derived representations are related to the old ones: $\chi_{V\oplus W} = \chi_V + \chi_W$, $\chi_{V\otimes W} = \chi_V \chi_W$, etc.

Characters encode many information about a representation, including invariant subspaces and information about irreducible components. If W is a completely reducible representation $W = \bigoplus_{i=1}^{n} V_i^{m_i}$, it is easy to see, by the above properties, that $\chi_W = \sum_{i=1}^{n} m_i \ \chi_{V_i}$.

The multiplicities m_i of the blocks can be computed using the orthogonality property of the characters under the invariant inner product defined through the Haar measure $d\mu(g)$ on the group:

$$\int_G d\mu(g)\chi_A^*(g)\chi_B(g) = \begin{cases} 1 \text{ if } A = B \\ 0 \text{ if } A \neq B \end{cases} . \tag{3.8}$$

Hence,

$$m_i = \int_G d\mu(g)\chi_{V_i}^*(g)\chi_W(g) \ . \tag{3.9}$$

Now we will use these ideas to compute the multiplicities of the blocks that appear in the block-diagonal decomposition of the induced representation in the symmetric tensor product space. Let us start by an example in the simplest case.

Example 13. *Characters of $W \vee W$.*

Consider an element $g \in G$. Its eigenvalues are λ_i with corresponding eigenvectors $|e_i\rangle$, i.e., $g \triangleright |e_i\rangle = \lambda_i |e_i\rangle$ (no sum). In $W \vee W$, the eigenvectors will be of the form $|e_i\rangle \vee |e_j\rangle$, and the eigenvalues are $\lambda_i\lambda_j$, with $i \leq j$. Then,

$$\chi_{W\vee W}(g) = \text{tr } \rho_{W\vee W}(g) \tag{3.10}$$

$$= \sum_{i\leq j} \lambda_i\lambda_j = \sum_{i=j} \lambda_i\lambda_j + \sum_{i<j} \lambda_i\lambda_j \ , \tag{3.11}$$

using that

$$\sum_{i<j} \lambda_i \lambda_j = \frac{(\sum_i \lambda_i)^2 - \sum_i \lambda_i^2}{2} \ , \tag{3.12}$$

$$\chi_{W\vee W}(g) = \sum_i \lambda_i^2 + \frac{(\sum_i \lambda_i)^2 - \sum_i \lambda_i^2}{2} \tag{3.13}$$

$$= \frac{1}{2}\left(\sum_i \lambda_i^2 + \left(\sum_i \lambda_i\right)^2\right) \tag{3.14}$$

$$= \frac{1}{2}\left(\chi_V(g^2) + \chi_V(g)^2\right) \ . \tag{3.15}$$

In the particular case of our interest, take g as a rotation by an angle α, then

$$\chi_\vee^{(s,2)}(\alpha) = \frac{1}{2}\left(\chi_s(2\alpha) + \chi_s(\alpha)^2\right) \tag{3.16}$$

$$= \frac{\sin((s+1)\alpha)\sin((s+\frac{1}{2})\alpha)}{\sin\alpha \sin\frac{\alpha}{2}} \ , \tag{3.17}$$

where we are denoting by $\chi_\vee^{(s,k)}(\alpha)$ the character associated with $D_\vee^{(s,k)}(R_{\hat{n},\alpha})$. ■

This result can be generalized as follows.

An element $R_{\hat{n},\alpha}$ in the spin s representation, is given by a matrix $D^{(s)}(R_{\hat{n},\alpha})$, whose eigenvalues are $\lambda_m = e^{im\alpha}$ for $-s \leq m \leq s$.

Then, generalizing (3.10), $\chi_\vee^{(s,k)}(R_{\hat{n},\alpha})$ can be written as the k-th complete symmetric polynomial $H_k(\lambda_{-s}, \cdots, \lambda_s)$, this is:

$$\chi_\vee^{(s,k)}(R_{\hat{n},\alpha}) = H_k(\lambda_{-s}, \cdots, \lambda_s) = \sum_{m_1 \leq \cdots \leq m_k} \lambda_{m_1} \cdots \lambda_{m_k} \ , \tag{3.18}$$

this means that $\chi_\vee^{(s,k)}(R_{\hat{n},\alpha})$ is given by the sum of all the possible products of k eigenvalues, allowing repetitions.

As we appreciate in the example above, the result depend on $\chi_s(\alpha)$ and on $\chi_s(2\alpha)$ as well. For this reason will be convenient to introduce the Newton polynomials

$$P_r(\lambda_{-s} \cdots, \lambda s) = \sum_{m=-s}^{s} \lambda_m^r = \chi_s(r\alpha) \ . \tag{3.19}$$

In the general case, the decomposition of the terms in the symmetric polynomial become more complicated, this relation between Newton and symmetric polynomials [43] is given by

$$H_k = \sum_{(m_1,\cdots,m_k)}^{*} \frac{P_1^{m_1}\cdots P_k^{m_k}}{1^{m_1}m_1!2^{m_2}m_2!\cdots k^{m_k}m_k!}\ , \tag{3.20}$$

where the sum $\sum^{*}_{(m_1,\cdots,m_k)}$ is restricted to the k-tuples of nonnegative integers that satisfy $\sum_{r=1}^{k} rm_r = k$.

With this, regarding (3.18) and (3.19), we conclude that

$$\chi_{\vee}^{(s,k)} = \sum_{(m_1,\cdots,m_k)}^{*} \frac{(\chi_s(\alpha))^{m_1}\cdots(\chi_s(k\alpha))^{m_k}}{1^{m_1}m_1!2^{m_2}m_2!\cdots k^{m_k}m_k!}\ . \tag{3.21}$$

Example 14. *2-symmetric system*

In this case, the constraint for the pairs (m_1, m_2) appearing in the sum is $m_1 + 2m_2 = 2$, its valid solutions are $(m_1, m_2) = (2, 0)$ or $(m_1, m_2) = (0, 1)$, which gives the two terms of (3.16). ■

Now, we can find the multiplicities as follows. By (3.9), and using that the Haar measure for this group is given, having integrated over the adjoint orbit, by $d\mu = \sin^2\frac{\alpha}{2}d\alpha$, we conclude that

$$m_i^{(s,k)} = \int_0^{2\pi} \sin^2\frac{\alpha}{2}\chi_i^*(\alpha)\chi_{\vee}^{(s,k)}(\alpha)d\alpha = \int_0^{2\pi} \sin^2\frac{\alpha}{2}\chi_i^*(\alpha) \sum_{(m_1,\cdots,m_k)}^{*} \frac{(\chi_s(\alpha))^{m_1}\cdots(\chi_s(k\alpha))^{m_k}}{1^{m_1}m_1!2^{m_2}m_2!\cdots k^{m_k}m_k!}d\alpha\ . \tag{3.22}$$

There are other approaches to find these multiplicities, mainly based on generating functions [44, 45]. It can be shown that the multiplicities $m_i^{(s,k)}$ are given by the coefficient of x^j, for $0 \le j \le s_{max}$, in the Laurent series, around zero, of the function

$$\zeta_{\vee}^{(s,k)}(x) = (1 - x^{-1})\prod_{r=1}^{2s} \frac{x^{\frac{k}{2}+r} - x^{-\frac{k}{2}}}{x^r - 1}\ . \tag{3.23}$$

Example 15. *Three spin 2 symmetrized states.*

To analyze the irreducible components appearing in the decomposition of $\mathcal{H}_{s=2}^{\vee 3}$ let us apply our results of this section.

The character is given by

$$\chi_{\vee}^{(2,3)} = \frac{1}{6}\left(\chi_2(\alpha)^3 + 3\chi_2(\alpha)\chi_2(2\alpha) + 2\chi_2(3\alpha)\right) \ , \tag{3.24}$$

then we can compute the multiplicities. The number of cases is simplified by the fact that we only need to check for integer spins and from $s_{max} = ks$ to zero. In this example, the multiplicities are 1,0,1,1,1,0,1 for spin 0,1,2,3,4,5,6 , respectively.

Then, the decomposition has the form

$$\mathbf{5}^{\vee 3} = \mathbf{13} \oplus \mathbf{9} \oplus \mathbf{7} \oplus \mathbf{5} \oplus \mathbf{1} \ , \tag{3.25}$$

where the spin-s irreducible components are denoted by their dimension $2s + 1$.

In general, multiplicities can take any value and are not necessarily one or zero as in this case, for example, in the case of a symmetrized state of 6 ququarts one of the irreducible components appears twice, namely

$$\mathbf{4}^{\vee 6} = \mathbf{19} \oplus \mathbf{15} \oplus \mathbf{13} \oplus \mathbf{11} \oplus \mathbf{9} \oplus 2 \times \mathbf{7} \oplus \mathbf{3} \ . \quad \blacksquare \tag{3.26}$$

3.1.3 Multiconstellations

Following the above discussion, a general system can be expressed in the block-diagonal basis that makes explicit its rotational properties. Following the last example, the state $|\psi\rangle = \hat{e}_{12}$ written in the block-diagonal basis takes the form

$$|\psi\rangle_{BD} = U_{(1,2)}|\psi\rangle = \frac{1}{\sqrt{3}}\left(e_{(2,0)} - \sqrt{2}e_{(0,0)}\right) \ , \tag{3.27}$$

this shows that the first five components of the state transform as a spin 2 state without mixing with the last (spin 0) component.

In the general case, each k-symmetric state of spin s can be regarded as a collection of spins (of different s, with possible degeneracy) in the sense that when we act on the states by rotations, each part behaves as a single spin with the same dimension of the block acting on it.

With this at hand, we may build a generalization of the Majorana representation: If a k-symmetric state of spin s is "composed" by a collection of spins, assign to it a multiconstellation that is a list of the Majorana constellations of each of the component spins.

This prescription has the problem that there is information lost in each block because when taking Majorana constellations of the component spins we ignore its norm and the relative phases among the different blocks. This information can be codified in a list $(n_1 e^{i\alpha_1}, \ldots, n_{2r+1} e^{i\alpha_{2r+1}})$, which can be regarded as a spin-r state and will be called *spectator spinor*, its Majorana constellation will be called the *spectator constellation*.

This is possible only when a reference state is defined to each block, otherwise there is no way to define the phases of the entries of the spectator spinor, which in fact is not a true spinor, because it does not transform in the same way. Once fixed this point, the full multiconstellation that contains all the rotational information of the state will be given by the collection of the particular Majorana constellations and the spectator constellation.

There are various ways to define a reference state to each block, and there is one that makes the spectator constellation invariant under rotations for almost all states. Let us describe this particular choice.

In order to do this, it will be useful to see the space of states as a fiber bundle with a base space called shape space formed by possible forms (of Majorana constellations of the states) with a $SU(2)$ archetypical fiber describing the possible orientations of the state. Hence, we can describe a state by choosing a point on the space of shapes and another on space of orientations. A section on this fiber bundle will correspond to a choice of a particular orientation for any possible shape on the base space. Then a section essentially specifies a reference constellation in each possible $SU(2)$-orbit.

Another way to describe this is the following: two forms are said to be equivalent if they differ only by a rotation, this means that if C is one possible constellation, all the constellations $C' = R(C)$ belong to the same equivalence class, where R is a rotation. We define a section on this fibre bundle by making the choice of one representative of each form in this $SU(2)$-bundle. Therefore, given a constellation C there will be a constellation C' that differ of C by a rigid rotation of all its points.

Of the infinitely many possible choices of representatives we will define one that will be particularly useful later. This will be defined for all the constellations C whose associated states via the inverse Majorana representation $|\psi_C\rangle$ are such that are not 1-anticoherent, that is $\langle\vec{S}\rangle_C \neq \vec{0}$. If this is the case, define R_1 as one of the rotations that takes this expectation value to $\hat{z}$. Define the rotated state $\rho = D(R_1)\rho_{|\psi_C\rangle}D(R_1)^{-1}$, where $D(R_1)$ is the representation of spin s of the rotation R_1, where s is the spin of $|\psi_C\rangle$, obviously this state will have expectation value along $\hat{z}$.

Decomposing this matrix in terms of polarization tensors, we obtain the following linear combination

$$\rho = \sum_{l=0}^{2s} \sum_{m=-l}^{l} c_{lm}\hat{T}_{lm} \ . \tag{3.28}$$

We use the first non-zero coefficient with $m \neq 0$, say $c_{\tilde{l}\tilde{m}}$, to define a rotation R_2 along $\hat{z}$ by an angle $\arg(c_{\tilde{l}\tilde{m}})/\tilde{m}$. The resulting ρ will have its first non-zero coefficient in the expansion in polarization tensors real and positive.

Then, the reference constellation will be defined as $\tilde{C} = R_2(R_1(C))$. This particular election will be necessary to have a rotational invariant spectator constellation.

Now, we return to the problem of the definition of a reference state for each block in the block-diagonal basis. Suppose that the state corresponding to one of the blocks is $|\psi\rangle$. Consider its uniquely defined Majorana constellation C. C is an element on the fiber, diffeomorphic to $SU(2)$, and can be obtained from the reference constellation associated with that shape, i.e., $C = R(\tilde{C})$, for some $R \in SU(2)$. Then, we define the reference state $|\psi_C\rangle = D(R)|\psi_{C'}\rangle$, where $|\psi_{C'}\rangle$ is the state associated with the reference constellation by the inverse Majorana mapping, whose global phase is such that its first non-zero entry is real and positive.

Then, each $|\psi^{(i)}\rangle$ that appear in the block-diagonal decomposition is related by a complex number with its corresponding reference state, $|\psi^{(i)}\rangle = z^{(i)}|\psi_C^{(i)}\rangle$, where i goes from 1 to the total number of blocks (counted with multiplicity). Those complex numbers $z^{(i)} = n_i e^{i\alpha_i}$ are the components of the spectator spinor.

Now we proceed to prove that this particular definition leads to a rotationally invariant specta-

tor spinor. Consider the action of a rotation R_0 on a state $|\Psi\rangle_{BD}$ in the block-diagonal basis. This rotated state is $|\Psi'\rangle_{BD} = D^{s,k}_{\vee}(R_0)|\Psi\rangle_{BD}$, in terms of each block this transformation looks like

$$|\psi^{(i')}\rangle = D^{(s)}(R_0)|\psi^{(i)}\rangle \ , \tag{3.29}$$

where s is the spin of the corresponding block labelled by i. The constellations are also rotationally related: $\mathcal{C} = R_0(C)$.

This implies that

$$\begin{aligned} |\psi^{(i')}\rangle &= D^{(s)}(R_0)|\psi^{(i)}\rangle && (3.30)\\ &= z^{(i)}D^{(s)}(R_0)|\psi_C\rangle && (3.31)\\ &= z^{(i)}D^{(s)}(R_0)D^{(s)}(R)|\psi_{C'}\rangle && (3.32)\\ &= z^{(i)}D^{(s)}(R_0 \circ R)|\psi_{C'}\rangle && (3.33)\\ &= z^{(i)}|\psi_{\mathcal{C}}\rangle \ , && (3.34) \end{aligned}$$

therefore, $z^{(i')} = z^{(i)}$, and the proof is completed.

Now, let us see some examples of multiconstellations.

Example 16. ***Multiconstellations of a symmetric state of three qutrits***

Consider a symmetric state of three qutrits. Here the dimension of the symmetric space is 10 with a basis given by

$$\begin{aligned} &e_{111} = e_1 \vee e_1 \vee e_1, \quad e_{112} = e_1 \vee e_1 \vee e_2, \quad e_{113} = e_1 \vee e_1 \vee e_3, \quad e_{122} = e_1 \vee e_2 \vee e_2,\\ &e_{123} = e_1 \vee e_2 \vee e_3, \quad e_{133} = e_1 \vee e_3 \vee e_3, \quad e_{222} = e_2 \vee e_2 \vee e_2, \quad e_{223} = e_2 \vee e_2 \vee e_3,\\ &e_{233} = e_2 \vee e_3 \vee e_2, \quad e_{333} = e_3 \vee e_3 \vee e_3. \end{aligned}$$

This is an orthogonal but not orthonormal basis, normalizing this basis we obtain the following orthonormal basis:

$\hat{e}_{111} = e_1 \vee e_1 \vee e_1$, $\hat{e}_{112} = \sqrt{3}e_1 \vee e_1 \vee e_2$, $\hat{e}_{113} = \sqrt{3}e_1 \vee e_1 \vee e_3$, $\hat{e}_{122} = \sqrt{3}e_1 \vee e_2 \vee e_2$, $\hat{e}_{123} = \sqrt{6}e_1 \vee e_2 \vee e_3$, $\hat{e}_{133} = \sqrt{3}e_1 \vee e_3 \vee e_3$, $\hat{e}_{222} = e_2 \vee e_2 \vee e_2$, $\hat{e}_{223} = \sqrt{3}e_2 \vee e_2 \vee e_3$, $\hat{e}_{233} = \sqrt{3}e_2 \vee e_3 \vee e_2$, $\hat{e}_{333} = e_3 \vee e_3 \vee e_3$.

*Now we must find an adequate basis for rotations, i.e., the block-diagonal basis which in this case gives us a natural decomposition into a spin-*3 *subspace and a spin-*1*, each one transforming with its corresponding representation of rotations when the original state is rotated. In this case, this basis is one whose spin-*3 *part is given by*

$$
\begin{aligned}
e_{(3,3)} &= \hat{e}_{111} \ , \\
e_{(3,2)} &= \hat{e}_{112} \ , \\
e_{(3,1)} &= \frac{1}{\sqrt{5}} \left(\hat{e}_{113} + 2\hat{e}_{122}\right) \ , \\
e_{(3,0)} &= \frac{1}{\sqrt{5}} \left(\sqrt{3}\hat{e}_{123} + \sqrt{2}\hat{e}_{222}\right) \ , \\
e_{(3,-1)} &= \frac{1}{\sqrt{5}} \left(2\hat{e}_{223} + \hat{e}_{133}\right) \ , \\
e_{(3,-2)} &= \hat{e}_{233} \ , \\
e_{(3,-3)} &= \hat{e}_{333} \ ,
\end{aligned}
$$

*and whose spin-*1 *component is*

$$
\begin{aligned}
e_{(1,1)} &= \frac{1}{\sqrt{5}} \left(2\hat{e}_{113} - \hat{e}_{122}\right) \ , \\
e_{(1,0)} &= \frac{1}{\sqrt{5}} \left(\sqrt{2}\hat{e}_{123} - \sqrt{3}\hat{e}_{222}\right) \ , \\
e_{(1,-1)} &= \frac{1}{\sqrt{5}} \left(2\hat{e}_{133} - \hat{e}_{223}\right) \ .
\end{aligned}
$$

Now, consider the state $|\psi\rangle := \frac{1}{\sqrt{3}} \left(e_{111} + e_{222} + e_{333}\right)$*, this in the above basis can be written as*

$$
|\psi\rangle = \frac{1}{\sqrt{3}} \left(e_{(3,3)} + e_{(3,-3)} + \sqrt{2/5}e_{(3,0)} - \sqrt{3/5}e_{(1,0)}\right) \ . \tag{3.35}
$$

From this equation we can see that the corresponding (non-normalized) spin-3 state is $\psi_2 = \left(\frac{1}{\sqrt{3}}, 0, 0, \sqrt{\frac{2}{5}}, 0, 0, \frac{1}{\sqrt{3}}\right)$ *(whose constellation consists of two parallel equilateral triangles) and the state of spin-1 is* $\left(0, -\sqrt{\frac{3}{5}}, 0\right)$ *(with a pair of antipodal points as constellation).*

To give a complete description it will be necessary to find the spin-1/2 spectator constellation (z_3, z_1)*, which in this case is given by* $(1/(2\sqrt{3}))\left(\sqrt{5}(i-1), -(i+1)\right)$*.*

Let us compute z_1 *with the algorithm provided above. We start by computing the spin expectation value of* $|\psi^{(1)}\rangle$*, which is* $\langle\psi^{(1)}|\vec{S}|\psi^{(1)}\rangle = (0, 0, 1/10)$*. In this case, it is already pointing in the direction of the z axis, then the first rotation of the algorithm (which rotates the direction of the spin expectation value to the z axis) is the identity matrix, i.e.,* $R_1 = I$*. Then, the rotated density matrix is*

$$\rho_1^{'} = \rho_1 = \begin{pmatrix} \frac{2}{15} & 0 & -\frac{i}{15} \\ 0 & 0 & 0 \\ \frac{i}{15} & 0 & \frac{1}{30} \end{pmatrix} . \tag{3.36}$$

Expanding this density matrix in the basis of polarization operators we find

$$\rho_1^{'} = \frac{1}{6\sqrt{3}}T_{00} + \frac{1}{10\sqrt{2}}T_{10} - \frac{i}{15}T_{22} + \frac{1}{6\sqrt{6}}T_{20} + \frac{i}{15}T_{2-2} \ ,$$

where the first $m \neq 0$ *component is* $c_{22} = -\frac{i}{15}$ *(taking an order starting by the higher m), then the second rotation,* R_2*, is along z axis by an angle* $\alpha = \arg(c_{22})/2 = \arg\left(-\frac{i}{30}\right) = -\frac{\pi}{4}$*.*

Then, a state whose constellation has the reference orientation is the one given by the successive application of R_1 *and* R_2 *to our spin-1 state associated with the spin-1 block:*

$$|\psi_{ref}^{(1)}\rangle = D^{(1)}(R_2)D^{(1)}(R_1)|\psi^{(1)}\rangle = \left(-\frac{1-i}{\sqrt{15}}, 0, -\frac{\frac{1}{2}-\frac{i}{2}}{\sqrt{15}}\right) .$$

following our convention for fixing the phase (taking the first non-negative entry real and positive), the state with the correct phase is

$$|\psi_{\tilde{C}_1}\rangle = \frac{1}{\sqrt{5}}(2, 0, 1) \ ,$$

which is obtained from (16) *multiplying by the inverse phase factor of its first entry.*

With this at hand, the canonical ket is given by

$$D^{(1)}(R_2 \circ R_1)^{-1}|\psi_{\tilde{C}_1}\rangle = \left((1-i)\sqrt{\frac{2}{5}}, 0, \frac{1+i}{\sqrt{10}}\right) .$$

Multiplying this by z_1 will give us $|\psi^{(1)}\rangle$, then comparing (16) with $|\psi^{(1)}\rangle$ we obtain $z_1 = \frac{1}{\sqrt{6}}e^{i\frac{3\pi}{4}}$. Following a similar procedure we can find the given z_3.

■

Example 17. ***Multiconstellations of maximally entangled states of two qutrits.***

Let us consider the Bell-like state[1]

$$\psi = |1,\ 1\rangle + |0,\ 0\rangle + |-1,\ -1\rangle\ , \tag{3.37}$$

which is normalized under the corresponding induced inner product. This can be written in the basis of e_{ij} as

$$\psi = e_{11} + e_{22} + e_{33} = \hat{e}_{11} + \hat{e}_{22} + \hat{e}_{33}\ , \tag{3.38}$$

following the notation of the notes for the associated orthonormal basis in $\mathcal{H}^{\vee 2}$.

We know that in this case the decomposition in irreducible components is $\mathbf{3}^{\vee 2} = \mathbf{5} \oplus \mathbf{1}$, therefore, we have a spin-2 constellation and another one of spin-0.

The change of basis is the following:

$$\{\hat{e}_{(2,2)}, \hat{e}_{(2,1)}, \hat{e}_{(2,0)}, \hat{e}_{(2,-1)}, \hat{e}_{(2,-2)}\} = \{\hat{e}_{11}, \hat{e}_{12}, \frac{1}{\sqrt{3}}\left(\hat{e}_{13} + \sqrt{2}\hat{e}_{22}\right), \hat{e}_{23}, \hat{e}_{33}\}$$

and

$$\hat{e}_{(0,0)} = \frac{1}{\sqrt{3}}\left(\sqrt{2}\hat{e}_{13} - \hat{e}_{22}\right)\ .$$

Applying this change of basis, we find that the spin-2 state associated to the Bell-like state is $\psi_1 = (1, 0, \sqrt{2/3}, 0, 1)^T$. Its Majorana constellation, two pair of antipodal points along the y axis is shown in Figure 3.1.

We can repeat the procedure for the state

$$\tilde{\psi} = |1,\ 1\rangle - |0,\ 0\rangle + |-1,\ -1\rangle\ , \tag{3.39}$$

[1] We call that state a Bell-like state because it is maximally entangled. This non-trivial property comes from the anticoherence of the spin 2 components. The relationship between maximally entangled states and anticoherence is discussed, in terms of polarization operators in [46].

and we obtain that the corresponding spin-2 state is given by $\psi_2 = (1, 0, -\sqrt{2/3}, 0, 1)^T$. *Its Majorana constellation, two pair of antipodal points along the* x *axis is shown in Figure 3.2 .*

Now, let us consider the state

$$\bar{\psi} = |1,\ 1\rangle + |0,\ 0\rangle - |-1,\ -1\rangle\ , \tag{3.40}$$

repeating we obtain $\psi_3 = (1, 0, \sqrt{2/3}, 0, -1)^T$. *Its Majorana constellation is not as in the previous cases, it has a tetrahedral form. It is interesting to note in Figure 3.3 that this constellation has a rotational symmetry along the* z *axis by an angle of* π *(the* z *axis in the figure corresponds to the blue line).*

We can explain these symmetries by recalling the results that relate the symmetries of a state with the shape *of its expansion in the* $\hat{S}_z$ *eigenbasis.* ψ_1 *must have symmetry along the* z *axis by* π *because of the pattern of vanishing entries of the state (i.e., it is of the form* $(\alpha, 0, \beta, 0, \gamma)^T$*). In addition to this, the state must by symmetric by an angle of* π *along the* x *axis because is of the form* $(\alpha, \beta, \gamma, \beta, \alpha)^T$. *Those symmetry restrictions explain why we have such a constellation. All the entries of this state are real and this is related to the fact that the state has a reflection symmetry with respect to the* xz *plane.*

In the case of ψ_3 *we have the spacing of zeroes and the constellation is symmetric along the* z *axis by an angle of* π. *The entries are all real and this implies the* xz*-reflection symmetry of the constellation (the plane of symmetry is the plane that contains the blue and the green lines), in these plots we follow the convention RGB for the coloring of the* x,y,z *axes, respectively, then the red line represents* x*-axis, and so on.*

Example 18. ***Multiconstellations of degenerated tetrahedra formed by coherent states.***

I list below the multiconstellations of the symmetrized state of four coherent states in the directions of the vertices of a tetrahedron (with $k = 2, 3$ *stars per vertex, i.e., coherent states of spin* 1 *and spin* $3/2$*, respectively). The first three constellations of the case* $k = 4$ *are also described.*

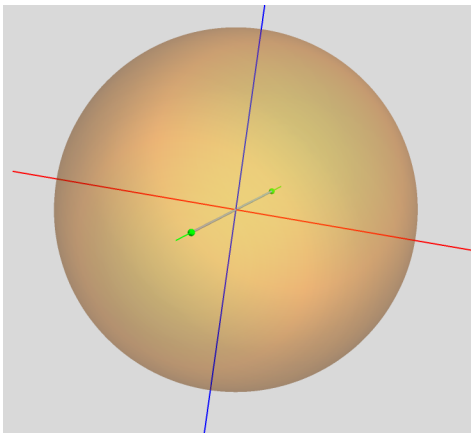

Figure 3.1: Constellation of the spin-2 part of ψ_1

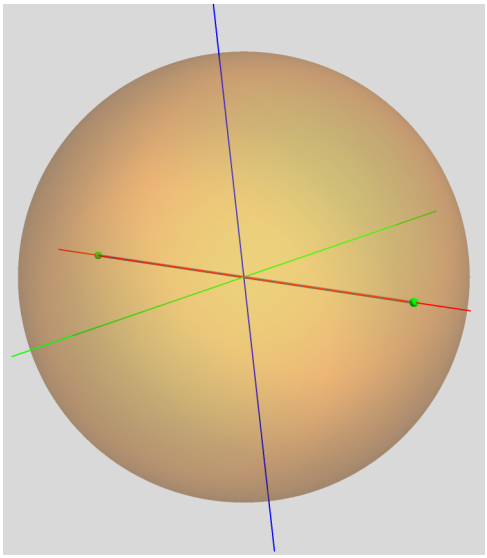

Figure 3.2: Constellation of the spin-2 part of ψ_2

k=2

In this case, the state is given by

$$|\hat{n}_1\rangle \vee |\hat{n}_2\rangle \vee |\hat{n}_3\rangle \vee |\hat{n}_4\rangle \ ,$$

where $|\hat{n}_i\rangle$*, for* $i = 1, \ldots, 4$*, denotes the spin-*1 *coherent state along the direction* $\hat{n}_i$*, being these the directions of the vertices of the tetrahedron. Those states have degenerated Majorana constellations constituted by two superimposed stars, e.g.,* $|\hat{n}_1\rangle = |1, 1\rangle$*, whose Majorana constellation is given by two points at the north pole.*

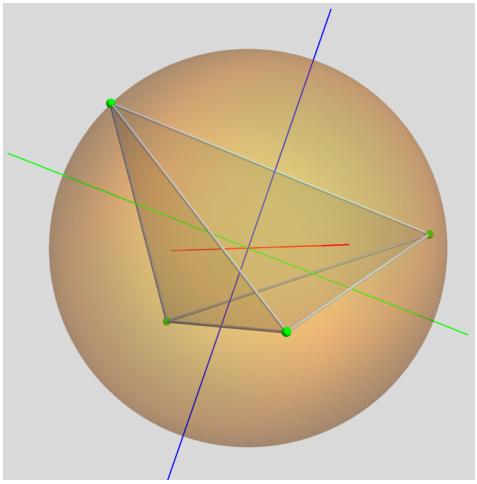

Figure 3.3: Constellation of the spin-2 part of ψ_3

Decomposition: $\mathbf{3}^{\vee 4} = \mathbf{9} \oplus \mathbf{5} \oplus \mathbf{1}$.

Constellations:

- *Spin* 4*: Double tetrahedron*
- *Spin* 2*: Tetrahedron*
- *Spin* 0*: 0*

k=3

Decomposition: $\mathbf{4}^{\vee 4} = \mathbf{13} \oplus \mathbf{9} \oplus \mathbf{7} \oplus \mathbf{5} \oplus \mathbf{1}$.

Constellations:

- *Spin* 6*: Triple tetrahedron*
- *Spin* 4*: Cube (= tetrahedron + inverted tetrahedron)*
- *Spin* 3*: Octahedron*
- *Spin* 2*:* $\emptyset$
- *Spin* 0*:* $18\sqrt{\frac{2}{1295}}$

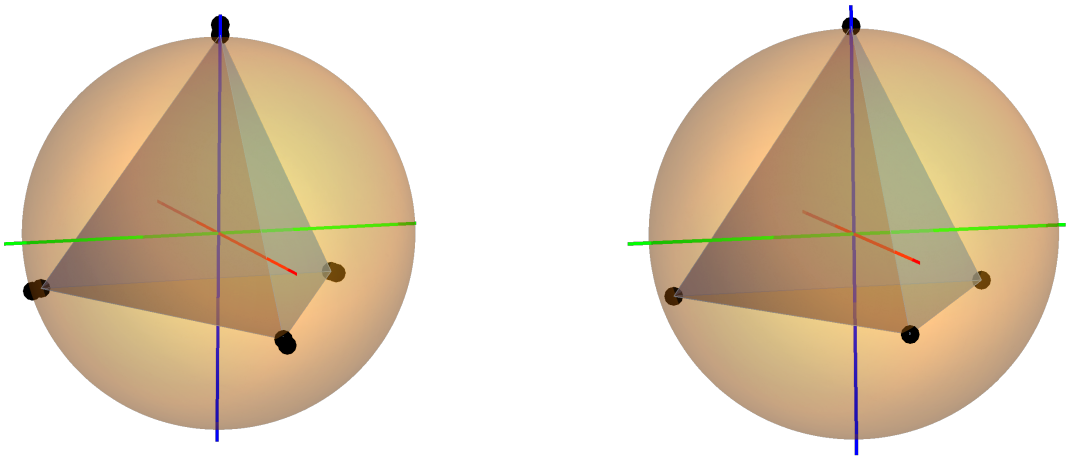

(a) $k = 2$, $s = 4$ (I put 2 dots to show the degeneracy of the stars)

(b) $k = 2$, $s = 2$

Figure 3.4: Multiconstellation for $k = 2$

k=4

Decomposition: $\mathbf{5}^{\vee 4} = \mathbf{17} \oplus \mathbf{13} \oplus \mathbf{11} \oplus 2 \times \mathbf{9} \oplus 2 \times \mathbf{5} \oplus \mathbf{1}$.

Constellations (first three):

- *Spin* 8*: Quadruple tetrahedron*
- *Spin* 6*: Double tetrahedron + inverted tetrahedron (its convex hull is again a cube)*
- *Spin* 5*: Tetrahedron + octahedron*

This construction can be used to study some practical problems in quantum mechanics, as we will explore in next section. Let us conclude this part with one more example of multiconstellations to visualize a set of mutually unbiased bases. Mutually unbiased bases (MUB) are a particular set of orthonormal N-dimensional bases characterized by the property that the square modulus of the inner product of any two elements of different bases is $1/N$. MUBs are important in quantum tomography and have applications in many areas, for example, in quantum cryptography. See, e.g., [47].

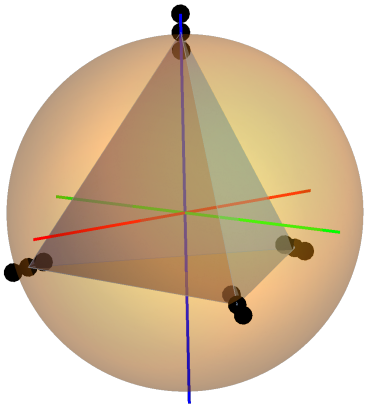

Figure 3.5: $k = 3$, $s = 6$

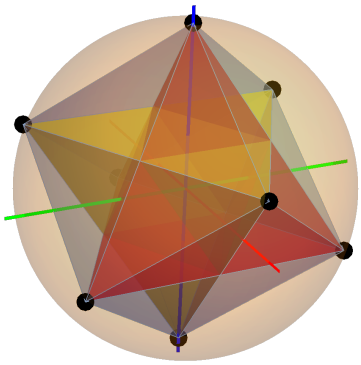

Figure 3.6: $k = 3$, $s = 4$

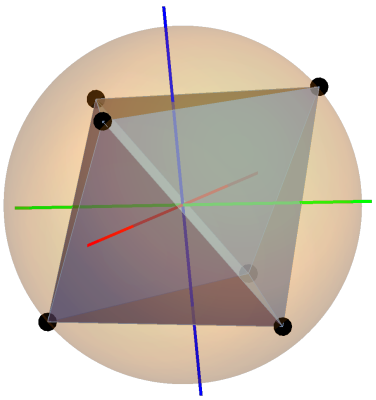

Figure 3.7: $k = 3$, $s = 3$

Example 19. ***MUB's in four dimensions using symmetrized ququarts***

In the case of ququarts, i.e. states of a four-level system or spin 3/2 *states, there are five mutually unbiased bases, in [48] the following set of MUB's is given (I will follow the notation*

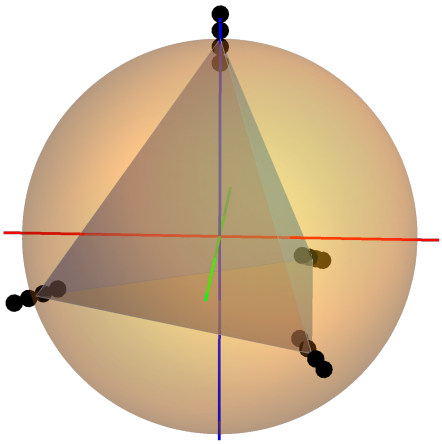

Figure 3.8: $k = 4$, $s = 8$

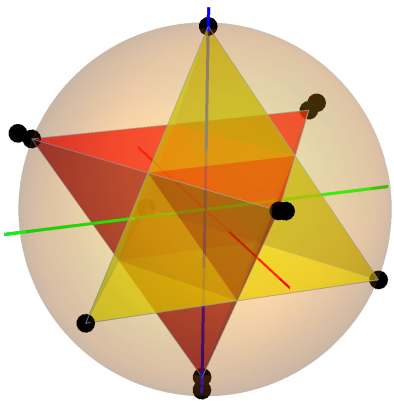

Figure 3.9: $k = 4$, $s = 6$

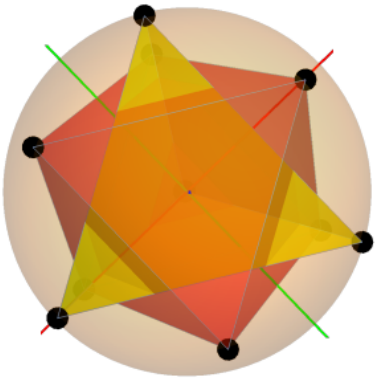

Figure 3.10: $k = 4$, $s = 5$ (Viewpoint $(0, 0, 1)$)

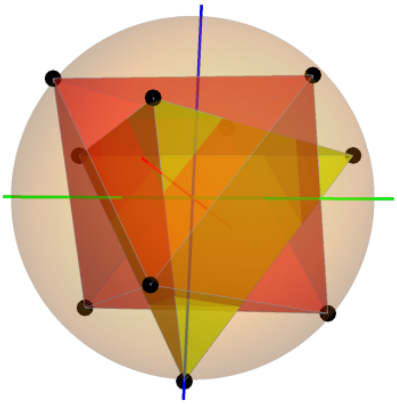

Figure 3.11: $k = 4$, $s = 5$

of that article in which each basis is given by the columns of the matrices):

$$\mathcal{B}_1 = \begin{pmatrix} 1 & 0 & 0 & 0 \\ 0 & 1 & 0 & 0 \\ 0 & 0 & 1 & 0 \\ 0 & 0 & 0 & 1 \end{pmatrix}, \quad \mathcal{B}_2 = \frac{1}{2}\begin{pmatrix} 1 & 1 & 1 & 1 \\ 1 & 1 & -1 & -1 \\ 1 & -1 & -1 & 1 \\ 1 & -1 & 1 & -1 \end{pmatrix}, \quad \mathcal{B}_3 = \frac{1}{2}\begin{pmatrix} 1 & 1 & 1 & 1 \\ 1 & 1 & -1 & -1 \\ -i & i & i & ,-i \\ i & -i & i & -i \end{pmatrix},$$

$$\mathcal{B}_4 = \frac{1}{2}\begin{pmatrix} 1 & 1 & 1 & 1 \\ i & -i & i & -i \\ -1 & -1 & 1 & 1 \\ i & -i & -i & i \end{pmatrix} \quad , \quad \mathcal{B}_5 = \frac{1}{2}\begin{pmatrix} 1 & 1 & 1 & 1 \\ i & -i & i & -i \\ i & -i & -i & i \\ -1 & -1 & 1 & 1 \end{pmatrix} .$$

The symmetrized states of 4 ququarts associated to each basis were computed. In the following table I describe qualitatively the shape of each of the constellations of each state. For each basis we have a multiconstellation composed of 4 constellations since $\mathbf{4}^{\vee 4} = \mathbf{13} \oplus \mathbf{9} \oplus \mathbf{7} \oplus \mathbf{5} \oplus \mathbf{1}$ *(in fact, are five considering the spin zero). Some of the shapes can be described differently*[2] *but I think that is interesting that in all cases such symmetric figures are obtained. Denote by AP an antipodal pair (of stars) and by* † *the corresponding multiplicity. In the following figure we plot the corresponding multiconstellation for* $\mathcal{B}_2$ *as an example.* ■

Basis	Spin-6 Const.	Spin-4 Const.	Spin-3 Const.	Spin-2 Const.
$\mathcal{B}_1$	6 AP z-axis	4 AP along z-axis	$\emptyset$	$\emptyset$
$\mathcal{B}_2$	Hexagon and two pairs of points†	Octagon (irreg.)	octahedron	2 AP along z-axis
$\mathcal{B}_3$	Hexagon and two pairs of points†	Cube	$\emptyset$	2 AP along y-axis
$\mathcal{B}_4$	Parallel hexagons	Parallelogram†	octahedron	2 AP along z-axis
$\mathcal{B}_5$	Parallel hexagons	Parallelogram†	$\emptyset$	2 AP along x-axis

3.2 Entanglement

3.2.1 Geometric measure of entanglement

In this section we will use our representation of symmetrized states to study a geometric measure of entanglement. For these systems several measures have been investigated [49, 42, 50, 51, 52].

Due to symmetrization, all the symmetrized multiqudit states are entangled following the usual definition, except in the case of diagonal states which are conformed by copies of the same state in all the factors. There are some notions of entanglement that can be defined in

[2] For example, the hexagon and the two pairs of stars can be interpreted as the union of a parallelogram and an antipodal pair, as can be checked looking at Figure 3.12.

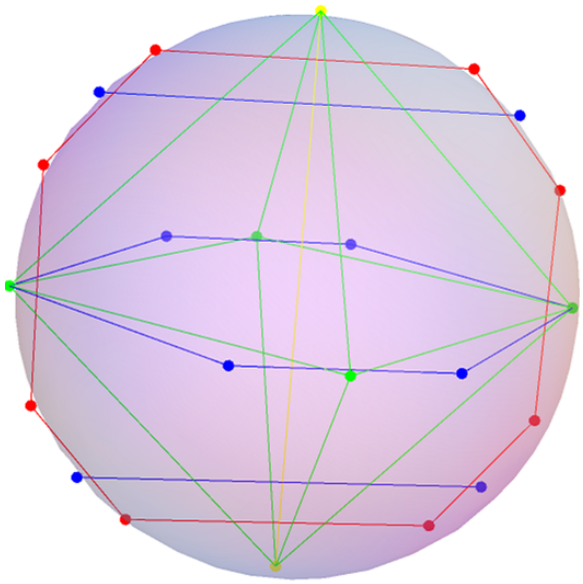

Figure 3.12: Multiconstellation for the basis $\mathcal{B}_2$ where blue corresponds to spin 6, red to spin 4, green to spin 3 and yellow to spin 2.

the symmetrized case, as the *symmetric tensor rank* [53] which counts the minimal number of symmetrized tensor factors with respect to vee product (i.e., the symmetrized tensor product), this is a discrete measure.

In this section we will study a (continuous) geometric measure defined as the distance, in the sense of Fubini-Study, between the state and a diagonal one, minimized over all the states in the diagonal subspace, which plays the role of separable states in the sense that the measure will vanish for diagonal states. In particular, we will study the class of $\vee$-factorizable states, i.e., k-partite states of the form

$$|\Psi\rangle = \bigvee_{a=0}^{k-1} |\psi_a\rangle \ . \tag{3.41}$$

The geometric measure of entanglement $E(|\Psi\rangle)$ is defined as the distance of $|\Psi\rangle$ to the set of factorizable states using the Fubini-Study metric. If we call $\mathbb{F}$ the set of factorizable states,

$$E(|\Psi\rangle) = \min_{|\Phi\rangle \in \mathbb{F}} d_{FS}(|\Psi\rangle, |\Phi\rangle) \ . \tag{3.42}$$

It is known [52] that the states that minimize the above quantity lies in the diagonal submanifold, defined as the space of all states of the form $|\Phi\rangle = |\phi\rangle \otimes \cdots \otimes |\phi\rangle$.

Hence,

$$E(|\Psi\rangle) = \min_{|\phi\rangle\in\mathcal{H}} \arccos |^{\otimes k}\langle\phi|\Psi\rangle|. \tag{3.43}$$

Another measure is given by

$$\tilde{E}(|\Psi\rangle) = \min_{|\phi\rangle\in\mathcal{S}(\mathcal{H})} \left(1 - |^{\otimes k}\langle\phi|\Psi\rangle|^2\right) \ , \tag{3.44}$$

where $\mathcal{S}(\mathcal{H})$ denotes the unit sphere on $\mathcal{H}$.

The search for the state $|\phi\rangle$ that minimizes the above measures is simplified noting that this state must be expressed as a linear combination of the factor states $|\psi_0\rangle,\ |\psi_1\rangle,\ \ldots,\ |\psi_{k-1}\rangle$, because all the components outside the plane Π generated by those factor states do not contribute to the final result when computing the geometric measure of entanglement.

In the case in which the factor states are linearly independent, those generate a plane of the maximal possible dimension ($\dim\Pi = k$). In this case, the optimization problem is naturally translated to the problem of maximizing

$^{\otimes k}\langle\phi|\Psi\rangle$ with $|\phi\rangle \in \mathcal{S}(\mathcal{H})$, or equivalently, to compute

$$\max_{|\phi\rangle\in\mathcal{H}} \prod_{I=0}^{k-1} \frac{\langle\phi|\psi_I\rangle}{\langle\phi|\phi\rangle^k} \ , \tag{3.45}$$

where the last expression can be found by explicitly writing the state $|\phi\rangle$ as a linear combination of the basis of the plane $|\psi_I\rangle$ and dropping $|\phi\rangle$-dependent normalization factors which are not relevant to the optimization problem.

It will be useful to introduce the Gramian matrix G that encodes the inner products of the factor states $|\psi_I\rangle$,

$$G_{IJ} := \langle\psi_I|\psi_J\rangle \ , I, J = 0, 1, \ldots, k-1 \ , \tag{3.46}$$

with inverse given by $G^{IJ} = \langle\psi^I|\psi^J\rangle$, where $\{|\psi^I\rangle\}$ is the dual basis, which satisfies $\langle\psi^I|\psi_J\rangle = \delta^I_J$.

Expanding $|\phi\rangle$ in the basis of the plane, we have

$$|\phi\rangle = \langle\psi^I|\phi\rangle|\psi_I\rangle := \phi^I|\psi_I\rangle \ , \tag{3.47}$$

then,

$$\langle\phi|\phi\rangle = \bar{\phi}^I\langle\psi_I|\psi_J\rangle\phi^J = \bar{\phi}^I G_{IJ}\phi^J = \bar{\phi}_I G^{IJ}\phi_J \ . \tag{3.48}$$

Therefore, if we define the inhomogeneous coordinates $z_i = \frac{\phi_i}{\phi_0}$ with $i = 1, \ldots, k-1$ and $z_0 = 1$, the function to be maximized is

$$f(z, \bar{z}) = \frac{|z_1 \ldots z_{k-1}|^2}{(\bar{z}_I G^{IJ} z_J)^k} \ . \tag{3.49}$$

A necessary condition to have a maximum is the vanishing of the first partial derivatives $\frac{\partial f}{\partial z}$ and $\frac{\partial f}{\partial \bar{z}}$. Implying this that the maximum is subject to the following system of equations

$$\bar{z}_I G^{IJ} Z_J - k\bar{z}_M G^{Mi} Z_i = 0 \ , \tag{3.50}$$

and

$$\bar{z}_I G^{IJ} Z_J - k\bar{z}_I G^{iM} Z_M = 0 \ , \tag{3.51}$$

where $i = 1, \ldots, k-1$, notice that there is no sum over the index i. We consider the case $z_i \neq 0$, because if it is not the case we are in a critical point that is a minimum (which is naturally degenerated).

Example 20. *Geometric measure of entanglement*

Consider the $\vee$*-factorizable* 3*-symmetric state of spin* 1 *given by* $|\Psi\rangle \sim |\psi_0\rangle \vee |\psi_1\rangle \vee |\psi_2\rangle$*, with*

$$|\psi_0\rangle = \frac{1}{\sqrt{2}}(1, 0, 1)^T \ , \tag{3.52}$$

$$|\psi_1\rangle = \frac{1}{\sqrt{2}}(1, 0, i)^T \ , \tag{3.53}$$

$$|\psi_2\rangle = \frac{1}{\sqrt{2}}(1, 1, 1)^T \ . \tag{3.54}$$

As there are linearly independent, those states generate a 3*-plane. The above conditions* (3.50) *and* (3.51) *give us a system of equations in which one of the solutions, namely* $z_1 = 0.907899 - 1.112441i, z2 = 1.569411 + 0.467862i$*, corresponds to the maximum (*$f = 0.424016$*). The eigenvalues of the Hessian matrix of* f *evaluated at this point are all negative confirming that this is in fact a local maximum.*

With this solution we find that $|\phi\rangle = (0.604248, 0.390835 - 0.390835i, 0.573916)$, $|\phi\rangle^{\otimes 3}$ *is therefore the closest state, in the diagonal embedding, to* $|\Psi\rangle$. *By* (3.44), *the entanglement is* $\tilde{E} \approx 0.8$. ■

In the case in which the dimension of the plane generated by the factor states is lower than k we must have a linearly dependent set of factors. In this case the problem can be reduced to a lower dimensional one as we will describe now.

Suppose that the k factor states are $|\psi_0\rangle, \ldots, |\psi_{k-1}\rangle$, and suppose that the plane generated by them is of dimension $\dim \Pi = r < k$. We can also suppose that the first r are linearly independent.

A useful basis will be the following. Take $|e_0\rangle = |\psi_0\rangle$, $|e_1\rangle$ in the space generated by $|\psi_0\rangle$ and $|\psi_1\rangle$, $|e_2\rangle$ in the space generated by $|\psi_0\rangle$, $|\psi_1\rangle$ and $|\psi_2\rangle$, and so on. In this way, in the first r steps we will have a basis $|e_0\rangle, |e_1\rangle \ldots, |e_{r-1}\rangle$ for Π.

By construction, the factor states written in this basis for the plane, have their last components equal to zero, more precisely, the state $|\psi_i\rangle$ has its last $r - i - 1$ components equal to zero. By the same construction the states $|\psi_{r-1}\rangle, |\psi_r\rangle, \ldots, |\psi_{k-1}\rangle$ when written in this basis are, in general, full vectors. This basis can be extended to one of $\mathcal{H}$ adding $2s + 1 - r$ zeroes to the right at each vector.

The basis $\{|e_i\rangle\}$ may be extended to one of $\mathcal{H}$ by adding $2s + 1 - r$ zeros to each vector and completing the basis with unit vectors along these new $2s + 1 - r$ directions.

There exists a unitary matrix U such that this basis in $\mathcal{H}$ is mapped to the canonical basis of common eigenvectors of S_z and S^2, $\{|s, m\rangle\}$, with $m = -s, -s + 1, \ldots, s - 1, s$. In this way, U maps $|e_0\rangle = |\psi_0\rangle \to |s, s\rangle$, $|e_1\rangle = \alpha|\psi_0\rangle + \beta|\psi_1\rangle \to |s, s - 1\rangle$, etc.

This construction guarantees that all the factor states will have $2s + 1 - r$ trailing zeros and therefore $U|\phi\rangle$ will also have them.

Then, we can solve the problem ignoring those extra zeros, i.e., we can reduce the problem to one of lower spin, if we have a state with only r components then the effective spin is $(r - 1)/2$. To recover the solution to the original problem, after solving the reduced optimization problem, one must add $2s + 1 - r$ zeros and map the result back to the original basis with

$U^{-1} = U^{\dagger}$.

3.2.2 Gramian matrix of a factorizable symmetric state vs geometric entanglement

The system of equations that appear in the solution of the optimization problem involved in the computation of the geometric measure of entanglement for a $\vee$-factorizable state is fully determined by the matrix of inner products, the Gramian matrix G. We will see that the eigenvalues of G are related to the geometric measure of entanglement in an interesting way.

Let us start by considering the simplest case, a 2-symmetric state of spin 1/2, i.e., $|\Psi\rangle \sim |\psi_0\rangle \vee |\psi_1\rangle$ with $|\psi_i\rangle \in \mathcal{H}_{1/2}$, where $\mathcal{H}_{1/2}$ denotes the Hilbert space of a two-level system. In this case the Gramian matrix is given by

$$G = \begin{pmatrix} 1 & a \\ \bar{a} & 1 \end{pmatrix} ,$$

where $a := \langle\psi_0|\psi_1\rangle$. Its eigenvalues are $\lambda_{\pm} = 1 \pm |a|$, as expected its eigenvalues are real since G is hermitian, greater or equal to zero since G is a positive semidefinite matrix.

The geometric measure of entanglement $\tilde{E}$ is computed by finding first the state $|\phi\rangle$ such that $|\langle\phi| \otimes \langle\phi|\Psi\rangle|^2$ is maximal.

A symmetric state of two qubits can be regarded as a single spin-1 state living in the projective space $\mathbb{C}P^2$, whose real dimension is 4. This projective space can be thought as fiber bundle, where the *shape space* $\mathcal{S}$ serves as base space and a fiber diffeomorphic to $SU(2)$, that captures the rotational degrees of freedom. This means that, given a particular shape, in the fiber reside all its posible orientations. Since the dimension of the generic rotational orbit is three, the dimension of the shape space in this case is 1.

In the case of a spin 1, the shape space can be parametrized by the angle 2θ between the two Majorana stars of the state. As we are dealing with rotationally invariant quantities, the geometric measure of entanglement and the eigenvalues of the Gramian matrix are in fact constant along the $SU(2)$-orbits, hence, functions on the shape space.

In terms of this parameter θ, we can compute the above quantities obtaining (the a above is

$\cos\theta$)

$$\lambda = 1 - \cos\theta \ , \quad \tilde{E} = 1 - \left(1 + \tan^4 \frac{\theta}{2}\right)^{-1} \ ,$$

where λ denotes the minimal eigenvalue of the Gramian matrix and the last expression can be obtained by solving the optimization problem, to do this we can describe the spin-1 state as a symmetrized state of two states, e.g., we can give a particular orientation because the function is invariant on the shape space, taking the first state in the symmetrized tensor product as $|\psi_1\rangle = |\frac{1}{2}, \frac{1}{2}\rangle$ and the second one making an angle 2θ with respect to the first, i.e., on the xz-plane, namely $|\psi_2\rangle = \cos\theta|\frac{1}{2}, \frac{1}{2}\rangle + \sin\theta e^{i\phi}|\frac{1}{2}, -\frac{1}{2}\rangle$. The result of the optimization procedure is a state having a star at half of the angle in the same plane. From the expression of this the above given expression for $\tilde{E}$ can be derived.

The one-to-one relation of those quantities is shown in Figure 3.13, which is a parametric plot $(\lambda(\theta), \tilde{E}(\theta))$, where θ runs from 0 to $\pi/2$. The maximal value of the geometric measure of entanglement is $1/2$ reached at $\lambda = 1(\theta = \frac{\pi}{2})$ and the minimum is zero at $\theta = 0$, i.e., at the coherent states (whose Majorana constellation is degenerated at a single point on the sphere).

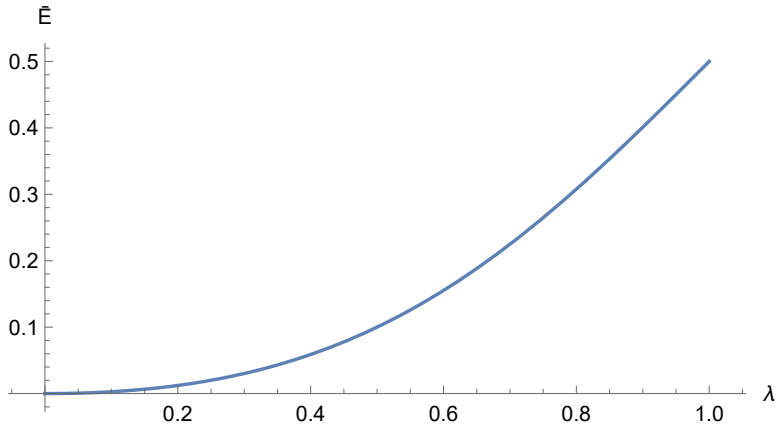

Figure 3.13: Geometric measure of entanglement vs λ for symmetrized states ($k = 2$).

Now, we will describe the relationship between $\tilde{E}$ and the eigenvalues of the Gramian matrix in the case of symmetrized states of three qubits ($k = 3$, $s = 1/2$). In this case, the two non-vanishing eigenvalues of the Gramian matrix sum 3, because for a generic state there are two non-vanishing eigenvalues λ_i such that $\lambda_1 + \lambda_2 = k$, this is a consequence of the general properties of the Gramian:

- The Gramian has $k - r$ vanishing eigenvalues, where r is the rank of the symmetrized state.
- The diagonal elements of the Gramian are equal to 1, then, the sum of its eigenvalues (the trace) is equal to the number of factors.

Plotting the geometric measure of entanglement versus the smaller eigenvalue λ for $30,000$ randomly chosen states we have the set of points shown in Figure 3.14 (E_G denotes $\tilde{E}$ in the plot).

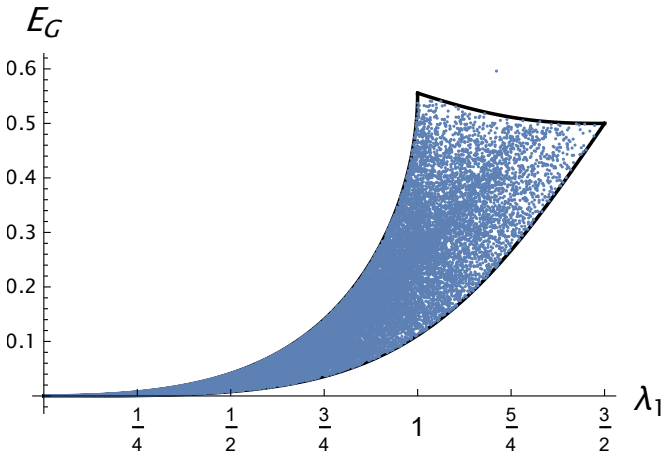

Figure 3.14: Geometric measure of entanglement vs λ for symmetrized states of three qubits.

Those points are on a region that we conjecture that it is limited by the curves shown in the figure, which are superimposed to the scatter plot. The extra point outside the region may correspond to a numerical error, but this statement has to be proved. Those curves connect three *vertices*, which correspond, respectively, to a coherent state, the GHZ and the W state. The coherent state corresponds to the origin in the plot, the W state to the upper-left vertex and the GHZ state to the upper-right vertex.

It is interesting that the GHZ and the W state came out as vertices in this figure. It is well known that the entanglement properties of these two states behave in radically different ways, for example, the W state is more robust under measurements but in terms of Kirwan polytopes, GHZ-like entanglement seems to be more special in the sense that it is represented by the maximal polytope containing all the others.

The curves that we conjecture that delimit the region correspond to three geodesics. Recall that if $|\psi_1\rangle$ and $|\psi_2\rangle$ are two states such that $\langle\psi_1|\psi_2\rangle \geq 0$, a geodesic curve that connects them has the form [3]

$$|\psi(t)\rangle = \cos t|\psi_1\rangle + \frac{\sin t}{\sqrt{1-(\langle\psi_1|\psi_2\rangle)^2}}\left(|\psi_2\rangle - \langle\psi_2|\psi_1\rangle|\psi_1\rangle\right) \ .$$

The black lines in the above figure correspond to three geodeiscs: the geodesic that goes from the coherent state to GHZ-state, one from GHZ to W and the third one from W to the coherent state. The first on these curves, regarded through the Majorana representation, starts at the north pole of the sphere with triple degeneration and goes to an equilateral triangle on the equator and as the parameter of the curve increases, the triangle is continuously increasing its size and lies on a plane that is parallel to the equator al each value $t > 0$ of its parameter. The other two geodesics can be easily found geometrically using the Majorana representation.

3.3 Metrological applications

Quantum metrology is a field of quantum technologies devoted to the creation of quantum states able to extract metrological information in a given setting. Roughly speaking, there are quantum states that help us in the process of making measurements and sometimes with a noticeable advantage in comparison with the accessible information by classical means. A measure of this advantage is encoded in the so-called metrological power of the state.

To be concise, we will not try to give a quantification of the metrological power, instead, we will study how symmetrized multiqudit states are useful in a series of problems in the context of quantum detection of rotations.

We will proceed as follows: first, we will motivate our study by a brief presentation of the classical and quantum approaches to the parameter estimation problem, based mainly on [54], next we will make use of some of these results and ours to find symmetric quantum rotosensors, in three different contexts, as we will explain along this section.

3.3.1 The parameter estimation problem

One of the most representative problems in metrology is that of the estimation of an unknown physical parameter.

Let us consider first the classical approach. Suppose that θ is an unknown parameter which we want to estimate. The only accessible information is obtained performing measurements and reading their outcomes $\{x\}$. For a given value of θ, the outcomes follow a probability distribution $f(x|\theta)$ which naturally satisfies $\int dx f(x|\theta) = 1$.

Suppose that we perform an experiment and the outcome is x_1. Based on the results of this measurement, we need to guess the value of θ, which is represented by $t(x_1)$. The function $t(x)$ is known as estimator.

Given that we try to estimate θ, if θ has a fixed value, our guess must be correct, in average, if we repeat the experiment by a suitable number of times, that means that we should have

$$\langle t \rangle_\theta := \int dx f(x|\theta) t(x) = \theta \ , \tag{3.55}$$

an estimator satisfying that $\langle t \rangle_\theta = \theta$ is called unbiased estimator.

The main result in this problem is that our capability to estimate the value of the parameter θ is, in a large extent, determined by the Fisher information $I(\theta)$, defined as

$$I(\theta) := \left\langle \left(\frac{\partial}{\partial \theta} \log f(x|\theta) \right)^2 \right\rangle_\theta = \int dx f(x|\theta) \left(\frac{\partial}{\partial \theta} \log f(x|\theta) \right)^2 \ , \tag{3.56}$$

this is the case because there exists an important bound for the variance of the estimator, as described in the following theorem.

Theorem 4. Cramér-Rao bound

Let $t(x)$ be an unbiased estimator, i.e., $\langle t \rangle_\theta = \theta$. Then,

$$\Delta^2 t \geq \frac{1}{n I(\theta)} \ , \tag{3.57}$$

where n denotes the number of independent experiments (repetitions) and $\Delta^2 t$ the variance of the estimation.

The Cramér-Rao bound sets fundamental limits to our capacity to extract information about an external parameter θ, for any possible unbiased estimator $t(x)$. The natural question that arises at this point is can we really saturate this bound? In simple terms the answer is yes if the number of measurements is large, the details of this asymptotic reachability of the Cramér-Rao bound can be found in [55, 54].

In the quantum version of this problem, the parameter to be estimated θ is encoded in a quantum channel Φ_θ. In quantum metrology a probe is required, the probe is a density matrix ρ which help us to extract the information by passing this state through the channel,leading to the state $\rho_\theta := \Phi_\theta(\rho)$. In order to extract the information about the parameter we need to perform measurements. Consider a set of positive operator valued measurements(POVM) $M := \{\Pi_x\}$ satisfying $\int dx \Pi_x = 1$ and Π_x is positive. Performing a measurement we obtain a distribution $f(x|\theta) := \mathrm{tr}(\Pi_x \rho_\theta)$. Once we found this statistical distribution the problem has been reduced to the classical one.

One of the challenges in quantum metrology is to find an optimal POVM to be applied to ρ_θ. To understand this point, it will be useful to review some definitions and results.

The symmetric logarithmic derivative of ρ_θ is the operator D_θ that satisfies

$$\frac{\partial \rho_\theta}{\partial \theta} = \{\rho_\theta, D_\theta\}/2 \ , \tag{3.58}$$

where $\{\cdot,\cdot\}$ denotes the anticommutator. It is a well defined quantity and it always has a solution, this can be verified by substitution $D_\theta = 2\sum_{i,j} \left(A_{ij}/(\lambda_i + \lambda_j)\right) |i\rangle\langle j|$, where $A = \{\rho_\theta, D_\theta\}/2$, and $\rho = \sum_i \lambda_i |i\rangle\langle i|$.

In terms of this, the quantum Fisher Information (QFI) is defined. For a given symmetric logarithmic derivative D_θ, the QFI is given by

$$I_Q(\rho, \theta) := \mathrm{tr}(\rho_\theta D_\theta^2) \ . \tag{3.59}$$

As in the classical case, there is a Cramér-Rao bound. Denote by $I(\theta|\rho, M)$ the Fisher information of the probability distribution $f(x|\theta)$, given a probe ρ and a POVM M. Then, for any M is satisfied

$$I(\theta|\rho, M) \leq I_Q(\rho, \theta) = \mathrm{tr}(\rho_\theta D_\theta^2) \ , \tag{3.60}$$

in consequence, for any unbiased estimator $t(x)$

$$\Delta^2 t \geq \frac{1}{nI_Q(\rho,\theta)} \ , \tag{3.61}$$

being n the number of repetitions of the experiment.

This bound is an extension of the classical Cramér-Rao bound to the quantum regime and sets limitations on how much information about θ can be extracted through any set POVM. Despite of this measurement independence, this bound depends on the probe state and the value of θ , which is the unkonwn quantity. This implies that in practice one must work with iterative-adaptative methods in both cases. Another important point to address is that there is no universal probe, as θ changes, the optimal probe in general also changes. In the case of unitary evolutions this is not an issue as discussed below.

Another way to avoid the dependence on θ is working in the local estimation approach, physically related to high precision measurements, in which we can suppose that the variation of the parameter is small around a fixed value θ_0 and the QFI is a function only of the probe.

If instead of a general quantum channel encoding the parameter, we use a unitary encoding, i.e., $\Phi_\theta(\rho) = U_\theta \rho U_\theta^\dagger$, where $U = e^{-i\theta G}$, with G Hermitian, then QFI is reduced to

$$I_Q(\rho, G) := 2\sum_{i,j} \frac{(\lambda_i - \lambda_j)^2}{\lambda_i + \lambda_j} |\langle i|G|j\rangle|^2 \ . \tag{3.62}$$

This quantity is independent on θ because U_θ commutes with its generator G.

3.3.2 Symmetric Quantum Rotosensors

Quantum rotosensors are states that can detect rotations by quantum means. Our study of the decomposition of symmetric states into different spins will be useful to find *optimal* quantum rotosensors in a sense of optimality that we make precise in this section. These extremal quantum states might be useful in the context of high precision measurements.

There are three instances in which we will study optimal detection:

(i) Small rotations about a given axis.

(ii) Small rotations averaging over all the axes.

(iii) Finite rotations averaging over all the axes.

Optimal rotosensors for infinitesimal rotations around a given axis

In this case we are looking for the optimal detectors of small rotations given a fixed axis $\hat{n}$. Detection of infinitesimal rotations is a local unitary estimation problem, then QFI is only dependent on the probe state and unitarity implies that we can make use of (3.62). This equation is essentially a generalized notion of variance, which in the case of a pure state is proportional to the variance [56, 57]. If $\rho = |\psi\rangle\langle\psi|$, then

$$I_Q(\psi, G) := 4\mathrm{Var}_\psi G = 4\mathrm{Var}_\psi(\hat{n} \cdot \vec{S}) \ , \tag{3.63}$$

then the optimal rotosensors for infinitesimal rotations along a given axis $\hat{n}$ are those that maximize the variance of the spin operator along the axis direction [58]. This class of states would be useful, for example, in problems of magnetometry.

The small angle case is also interesting because is related to the distinguishability problem of quantum states. Suppose that we want to make high-precision measurements detecting a weak signal. This signal makes a small change on the state of the system, then our ability to measure the signal is translated to our ability to distinguish two very close quantum states. There are several ways to measure the distinguishability between two quantum states, one of the most used is the *Bures distance* defined as

$$D_B(\rho_1, \rho_2) = \sqrt{1 - F(\rho_1, \rho_2)} \ , \tag{3.64}$$

where $F(\rho_1, \rho_2) = \mathrm{tr}\left(\sqrt{\sqrt{\rho_1}\rho_2\sqrt{\rho_1}}\right)^2$ is known as fidelity [59].

The interesting result is that QFI is related to this distinguishability measure, if ρ_θ and $\rho_{\theta+\delta\theta}$ are states that differ by a small change in the parameter θ then [57]

$$D_B^2(\rho_\theta|\rho_{\theta+\delta\theta}) = \frac{1}{8} I_Q(\rho, \theta)(\delta\theta)^2 \ . \tag{3.65}$$

The small variation of a parameter θ of the state will generate a curve on the projective space. Geometrically, to find optimal states for detection of variations of the parameter we can look for states that have maximal squared modulus of its tangent vector. In the case of our interest, a curve on $SU(2)$ will be mapped to the projective space by its action on it. If we take, without loss of generality, $\hat{n} = \hat{z}$ then the curve takes the form $\rho_t = e^{-itS_z}\rho_0 e^{itS_z}$.

We will study this in the case of symmetrized multiqudit states, then all the curve lies on $\mathbb{P}(\mathcal{H}_s^{\vee k})$. The tangent vector at $t = 0$ is

$$V_z := \frac{\partial}{\partial t}\rho_t|_{t=0} = i[S_z^{(s,k)}, \rho_0] \ , \tag{3.66}$$

we compute the square modulus using the Fubini-Study metric, if $\rho = |\Psi\rangle\langle\Psi| \in \mathbb{P}(\mathcal{H}_s^{\vee k})$ then

$$|V_z|^2 = F_{|\Psi\rangle}(V_z, V_z) = \langle\Psi| \left(S_z^{(s,k)}\right)^2 |\Psi\rangle - \langle\Psi|S_z^{(s,k)}|\Psi\rangle^2 = \mathrm{Var}_{|\Psi\rangle}\left(S_z^{(s,k)}\right) \ , \tag{3.67}$$

then, geometrically we have the same condition of optimality, maximization of variance, as in the analysis of the QFI.

If we write the last expression in terms of the states of each block in the block-diagonal decomposition, we have that the quantity to be maximized is

$$|V_z|^2 = \sum_j |z_j|^2 \langle\psi^{(j)}| \left(S_z^{(j)}\right)^2 |\psi^{(j)}\rangle - \left(\sum_j |z_j|^2 \langle\psi^{(j)}|S_z^{(j)}|\psi^{(j)}\rangle\right)^2 \ , \tag{3.68}$$

where j runs over the irreducible spins that appear in the decomposition. Note that this quantity does not depend on the particular phases of the z_j.

It is easy to see that in this case the state that maximizes $|V_z|^2$ is the GHZ state

$$|\Psi\rangle_{GHZ} = \frac{1}{\sqrt{2}}\left(|s,s\rangle^{\vee k} + e^{i\theta}|s,-s\rangle^{\vee k}\right) = \frac{1}{\sqrt{2}}\left(|s,s\rangle^{\otimes k} + e^{i\theta}|s,-s\rangle^{\otimes k}\right) \ , \tag{3.69}$$

with $|V_z|^2 = ks(1+ks)$. This state has only top constellation, this means that the only non-vanishing z_j is $z_{s_{max}} = z_{ks}$. The top spinor $|\psi^{ks}\rangle$, i.e. the state corresponding to the largest irreducible block, has as constellation an equatorial regular $2ks$-agon, where the parameter θ translates into a rotation of the shape around the z-axis. The corresponding spectator spinor is a coherent state with all the stars pointing along the positive z-axis, this is an orthogonal direction to the polygon described by the principal (and sole) constellation of the state. It is easy to see that this is the unique optimal solution in this case.

Let us now consider the case in which we look for optimal solutions when we take the average on the axial directions.

Optimal rotosensors for infinitesimal rotations around an averaged axis

In this case, we are looking for the state $|\Psi\rangle$ that maximizes the squared modulus of the tangent vector averaged over all possible axes $\hat{n}$, this generalizes the result of [57],namely the quantity

$$I(|\Psi\rangle) = \int_{\mathcal{S}^2} d\hat{n}|V_{\hat{n}}|^2 = \frac{1}{3}\sum_{i=x,y,z}(\Delta_{|\Psi\rangle}S_i)^2, \tag{3.70}$$

that in the block-diagonal basis takes the form

$$I(|\Psi\rangle) = \left(\sum_{r=1}^{t}|z_r|^2 s_r(s_r+1) - \sum_{i=x,y,z}\left(\sum_{r=1}^{t}|z_r|^2\langle\psi^{(s_r)}|S_i^{(s_r)}|\psi^{(s_r)}\rangle\right)^2\right) . \tag{3.71}$$

In the last expression t counts the number of the irreducible blocks with multiplicity and r is an index over the blocks (with an abuse of notation because in the cases with repeated spins there must be an extra index indicating in which of them we are).

To maximize the overall quantity one strategy may be maximize the first term which is strictly positive and minimize the contribution of the second (and negative) term. This can be done using states that only have principal constellation, i.e., that the only non-vanishing z_j is z_1 with $|z_1| = 1$ and such that $|\psi^{(ks)}\rangle$ is an 1-anticoherent state, to minimize the second factor in (3.71).

For example, a candidate of optimal rotosensor in this case is given by the following state of four qutrits

$$|\Psi\rangle = e_{1111} + \frac{1}{5}e_{1133} + \frac{2}{5}e_{1223} + \frac{4}{5}e_{2222} + e_{3333} , \tag{3.72}$$

because in the block diagonal basis has only principal constelation and it is an anticoherent state (in fact, a state whose Majorana constellation is a cube).

Let us see the case for symmetric states of two qutrits.

Example 21. 2-*qutrit optimal symmetric rotosensor*

Let $|\Psi\rangle$ *be a* 2*-symmetric qutrit state. When it is written in the block-diagonal basis it has a*

spin-2 and a spin-0 component, namely

$$|\Psi\rangle = (z_2|\psi^{(2)}\rangle, z_0|\psi^{(0)}\rangle)^T \ ,$$

then we can find optimal solutions taking $z_0 = 0, |z_2| = 1$ *with* $|\psi^{(2)}\rangle$ *a 1-anticoherent state. For example, the GHZ-state or the tetrahedral state leads to optimal solutions.*

In general, it is known [60] that all the spin-2 anticoherent states are, up to rigid rotations, equivalent to one of the states of the family

$$|\psi_2(\nu)\rangle = \sqrt{\frac{3}{6+2|\nu|^2}}\left(1, 0, \sqrt{\frac{2}{3}}\nu, 0, 1\right) \ , \tag{3.73}$$

where ν *is a complex variable with domain* $D = \{\nu \in \mathbb{C} | \mathrm{Re}(\nu) \geq 0 \ , \ \mathrm{Im}(\nu) \geq 0 \text{ and } |\nu - 1| \leq 2\}$.

Optimal rotosensors for finite rotations around an averaged axis

Now let us consider the case in which the angle is not infinitesimal but a finite one η. In this case, we have not a local estimation problem and optimal solutions are in general more complicated in this case.

As in the other cases, the quantity to be minimized is related to the transition probability between the state $|\Psi\rangle$ and the rotated state $D^{(j)}(R_{\eta,\hat{n}})$, namely, the fidelity

$$F_{|\Psi\rangle}(\eta, \hat{n}) := |\langle\Psi|D^{(j)}(R_{\eta,\hat{n}})|\Psi\rangle|^2 \ . \tag{3.74}$$

The optimal rotosensor for a rotation by an angle η around an averaged axis corresponds to the state that minimizes the average of the fidelity over all the posible directions $\hat{n} = (\theta, \phi)$, i.e., the quantity to be minimized is

$$\mathcal{F}_{|\Psi\rangle}(\eta) := \frac{1}{4\pi}\int_{\mathcal{S}^2} F_{|\Psi\rangle}(\eta, \hat{n}) d\hat{n} \ . \tag{3.75}$$

Before to doing the integration, let us look at the integrand expressing the state in the block-diagonal basis

$$F_{|\Psi\rangle}(\eta, \hat{n}) = \left(\sum_{r=1} |z_r|^2 \langle\psi^{j_r}|D^{(j_r)}(R_{\eta,\hat{n}})|\psi^{j_r}\rangle\right)^2 \ , \tag{3.76}$$

where $D^{(j_r)}(R_{\eta,\hat{n}})$ can be expanded in terms of polarization operators as [61]

$$D^{(j_r)}(R_{\eta,\hat{n}}) = 2\sqrt{\pi}\sum_{L=0}^{2j_r}\frac{(-i)^L}{\sqrt{2j_r+1}}\chi_L^{(j_r)}(\eta)\sum_{M=-L}^{L}Y_{LM}^*(\theta,\phi)T_{LM}^{(j_r)}\ , \tag{3.77}$$

where the functions $\chi_L^{(j)}(\eta)$ are the generalized characters of order L of the irreducible representation of rank j, these functions are defined in terms of the characters of the irreducible representations by the relation [61]

$$\chi_L^{(j)}(\eta) = \sqrt{2j+1}\sqrt{\frac{(2j-L)!}{(2j+L+1)!}}(\sin\frac{\eta}{2})^L\left(\frac{d}{d\cos\frac{\eta}{2}}\right)^L\chi^{(j)}(\eta)\ , \tag{3.78}$$

where L is an integer, $0 \leq L \leq 2j$.

Then,

$$\begin{aligned}F_{|\Psi\rangle}(\eta,\hat{n}) =& 4\pi\sum_{r,q}\frac{|z_r z_q|^2}{\sqrt{(2j_r+1)(2j_q+1)}}\times \\ &\sum_{L,L'}\sum_{M,M'}\chi_L^{(j_r)}(\eta)\chi_{L'}^{(j_q)}(\eta)(-i)^{L+L'}Y_{LM}^*Y_{L'M'}^*\langle\psi^{(j_r)}|T_{LM}^{(j_r)}|\psi^{(j_r)}\rangle\langle\psi^{(j_q)}|T_{L'M'}^{(j_q)}|\psi^{(j_q)}\rangle\ ,\end{aligned}$$

integrating over the sphere and using the orthonormality of spherical harmonics,

$$\int_{\mathcal{S}^2}Y_{LM}Y_{L'M'}^*d\hat{n} = \delta_{LL'}\delta_{MM'}\ , \tag{3.79}$$

we conclude that the averaged fidelity is given by

$$\mathcal{F}_{|\Psi\rangle}(\eta) = \sum_{r,q}\frac{|z_r z_q|^2}{\sqrt{(2j_r+1)(2j_q+1)}}\sum_{L,M}\chi_L^{(j_r)}(\eta)\chi_L^{(j_q)}(\eta)\langle\psi^{(j_r)}|T_{LM}^{(j_r)}|\psi^{(j_r)}\rangle\langle\psi^{(j_q)}|T_{LM}^{(j_q)}|\psi^{(j_q)}\rangle\ , \tag{3.80}$$

the indices r and q run over the different blocks appearing in the decomposition, L goes from 0 to $\min(2r, 2q)$ because those are the non-vanishing terms when expanding in the polarization operator basis and M runs from $-L$ to L, as usual. Related quantities have been studied analytically and numerically in [59] and [62], respectively.

Example 22. *Average fidelity for* $\mathbf{3}^{\vee 2}$.

In the case of a state of 2 symmetrized qutrits, the corresponding block-diagonal decomposition corresponds to $\mathbf{3}^{\vee 2} = \mathbf{5}\oplus\mathbf{1}$, *hence we have a spin* 2 *and a spin* 0. *The average fidelity in this case is given by*

$$\mathcal{F}_{|\Psi\rangle}(\eta) = |z_0|^4 + \frac{2|z_0 z_2|^2\chi^{(2)}(\eta)}{5} + \frac{|z_2|^4}{5}\left(\frac{(\chi^{(2)}(\eta))^2}{5} + \sum_{L=1}^{4}(\chi_L^{(2)}(\eta))^2 w_L^2\right)\ , \tag{3.81}$$

where we used that $\chi_0^{(j)}(\eta) = \chi^{(j)}(\eta)$, $T_{00}^{(j)} = \frac{1}{2j+1}\mathbb{I}$ *and*

$$w_L^2 := \sum_{M=-L}^{L} \langle\psi^{(2)}|T_{LM}^{(2)}|\psi^{(2)}\rangle\langle\psi^{(2)}|T_{LM}^{(2)\dagger}|\psi^{(2)}\rangle \ . \tag{3.82}$$

Chapter 4

Geometry of antisymmetric multiqudit systems

In this chapter we will study the geometry of antisymmetric multiqudit systems, as in the symmetric case we will present an interesting way to understand and visualize the rotational properties of those states and we will also give a generalization of the Majorana representation, this will be useful to exhibit some particular classes of states with extremal properties and develop some applications.

The antisymmetrized states of multiple qudits appear in many physical scenarios, for example as Slater determinants in atomic and molecular physics or in some quantum information tasks. In particular, we will show that this kind of states can be used to build a topologically protected way to perform holonomic quantum computation.

4.1 Multiconstellations

As in the case of k-symmetric states of spin-s it is possible to assign a multiconstellation to a k-antisymmetric state by following an analogous procedure. Given a state in $\mathcal{H}_s^{\wedge k}$, we can find its spin components by looking at the block-diagonal basis that decomposes in irreducible blocks the matrices $D_{\wedge}^{(s,k)}$. In this case the $U_{s,k}$ matrices that perform that change of basis are not the same as in the symmetric case, but their construction is quite similar: we start

with the highest vector of spin s_{max} and make successive applications of the lowering operator and taking into account orthogonal states. The block-diagonalized state can be regarded as a collection of states of different spins, and we can define the multiconstellation of the state in $\mathcal{H}_s^{\wedge k}$ as the collection of Majorana constellations of those spin states appearing in each block, as in the symmetric case, the information of relative phases can be encoded in a spectator spin carrying the necessary extra information to projectively recover the original state in the block-diagonal basis from the multiconstellation.

In this particular case of antisymmetric states, the eigenvectors of $S_z^{(s,k)}$ can be found as wedge products of the eigenvectors of $S_z^{(s)}$, being the eigenvalue of this eigenstate the sum of the corresponding eigenvalues of $S_z^{(s)}$ involved in the product.

Because of the antisymmetry of the product in this case it is impossible to have repeated factors, hence, the (s,k)-plane[1] of maximal spin is $|s,s\rangle \wedge |s,s-1\rangle \wedge \cdots \wedge |s,s-(k-1)\rangle$, which has the maximal possible eigenvalue of $S_z^{(s,k)}$, s_{max}, which is also the maximal value of spin j that appear in the decomposition of $D^{(s,k)}$ into irreducible components, and it is equal to

$$s_{max} = s + (s-1) + \cdots + (s-(k-1)) = \frac{1}{2}k(2s+1-k) \ . \tag{4.1}$$

Applying to this (s,k)-plane the operator $S_-^{(s,k)}$, we find a state with eigenvalue $s_{max}-1$:

$$|s,s\rangle \wedge \cdots \wedge |s,s-(k-2)\rangle \wedge |s,s-k\rangle \ ,$$

applying a second time the lowering operator, to obtain the state corresponding to the eigenvalue $s_{max}-2$ we obtain not only one state, but a linear combination of two of them

$$\alpha|s,s\rangle \wedge \cdots \wedge |s,s-(k-1)\rangle \wedge |s,s-k\rangle + \beta|s,s\rangle \wedge \cdots \wedge |s,s-(k-2)\rangle \wedge |s,s-(k+1)\rangle \ . \tag{4.2}$$

With more applications we find the whole multiplet. On the other hand, having a combination of states for the eigenvalue $j = s_{max}-2$ it is possible to generate a new multiplet taking as highest weight vector, the vector that is orthogonal to the linear combination found above and

[1] With (s,k)-plane we denote a k-plane of spin-s states.

the remaining part of the multiplet can be generated in the same way, with more applications of lowering operator. In fact, this is a matter of convention, we could start with the minimal spin and build the required basis by successive applications of the raising operator. With this, we conclude that for all s and k, the representations with $j = s_{max}$ and $j = s_{max} - 2$ appear with multiplicity 1, while those with $j = s_{max} - 1/2, j = s_{max} - 3/2$ never appear. Continuing in the same way, we can find the basis of $\wedge^k \mathcal{H}$ that carries $D^{(s,k)}$ to the block-diagonal form. Let us see a simple example.

Example 23. *Multiconstellation of a* 2*-plane of spin* 2*.*

Consider the 2*-plane generated by the states*

$$|\psi_1\rangle = \frac{1}{\sqrt{2}}\left(|2,2\rangle + |2,0\rangle\right) \quad \text{and} \quad |\psi_2\rangle = \frac{1}{\sqrt{2}}\left(|2,1\rangle + |2,-2\rangle\right) \ . \tag{4.3}$$

This plane can be represented projectively as the following antisymmetric product

$$|\psi\rangle = |\psi_1\rangle \wedge |\psi_2\rangle \tag{4.4}$$

$$= |2,2\rangle \wedge |2,1\rangle + |2,2\rangle \wedge |2,-2\rangle + |2,0\rangle \wedge |2,1\rangle + |2,0\rangle \wedge |2,-2\rangle \ . \tag{4.5}$$

*Now we must pass to the block-diagonal basis to read the spins of the multiconstellation, according to the corresponding change of basis obtained with the above procedure which in this case turns out to be composed by a spin-*3 *part and another of spin-*1*. The matrix that gives us the change of basis is*

$$U_{(2,2)} = \begin{pmatrix} 1 & 0 & 0 & 0 & 0 & 0 & 0 & 0 & 0 & 0 \\ 0 & 1 & 0 & 0 & 0 & 0 & 0 & 0 & 0 & 0 \\ 0 & 0 & \sqrt{3/5} & 0 & \sqrt{2/5} & 0 & 0 & 0 & 0 & 0 \\ 0 & 0 & 0 & 1/\sqrt{5} & 0 & 2/\sqrt{5} & 0 & 0 & 0 & 0 \\ 0 & 0 & 0 & 0 & 0 & 0 & \sqrt{3/5} & \sqrt{2/5} & 0 & 0 \\ 0 & 0 & 0 & 0 & 0 & 0 & 0 & 0 & 1 & 0 \\ 0 & 0 & 0 & 0 & 0 & 0 & 0 & 0 & 0 & 1 \\ 0 & 0 & \sqrt{2/5} & 0 & -\sqrt{3/5} & 0 & 0 & 0 & 0 & 0 \\ 0 & 0 & 0 & 2/\sqrt{5} & 0 & -1(\sqrt{5} & 0 & 0 & 0 & 0 \\ 0 & 0 & 0 & 0 & 0 & 0 & \sqrt{2/5} & -\sqrt{3/5} & 0 & 0 \end{pmatrix} . \tag{4.6}$$

Changing the basis, our plane can be expressed as

$$|\psi\rangle = \frac{1}{2}\left(e_{(3,3)} - \sqrt{\frac{2}{5}}e_{(3,1)} + \frac{1}{\sqrt{5}}e_{(3,0)} + e_{(3,-2)} + \sqrt{\frac{3}{5}}e_{(1,1)} + \frac{2}{\sqrt{5}}e_{(1,0)}\right) . \tag{4.7}$$

*From this, we read a spin-*3 *state, a spin-*1*, namely*

$$|\psi^{(3)}\rangle = \left(\frac{1}{2}, 0, -\frac{1}{2}\sqrt{\frac{2}{5}}, \frac{1}{2\sqrt{5}}, 0, \frac{1}{2}, 0\right)^T \tag{4.8}$$

$$|\psi^{(1)}\rangle = \left(\frac{1}{2}\sqrt{\frac{3}{5}}, \frac{1}{\sqrt{5}}, 0\right)^T . \tag{4.9}$$

From these we can compute the spectator qubit, obtaining the following three normalized states that completely characterize rotationally the 2*-plane*

$$|\psi^{(3)}\rangle_N = \frac{1}{\sqrt{13}}\left(\sqrt{5}, 0, -\sqrt{2}, 1, 0, \sqrt{5}, 0\right)^T , \tag{4.10}$$

$$|\psi^{(1)}\rangle_N = \frac{1}{\sqrt{7}}\left(\sqrt{3}, 2, 0\right)^T , \tag{4.11}$$

and

$$|\psi_{spec}\rangle_N = \frac{1}{2\sqrt{5}}\left(\sqrt{13}, \sqrt{7}i\right)^T . \tag{4.12}$$

4.2 Multiplicities and characters

As in the symmetrized state case, the easiest way to compute the multiplicities of the irreducible representations that appear in the block-decomposition is through the machinery of characters.

Following a similar calculation [63] to that of equation (3.9) a formula can be found for $\chi^{(s,k)}(\alpha)$ in terms of the spin-s characters of different powers of the group element, namely

$$\chi^{(s,k)}(\alpha) = \sum_{M} \frac{(-1)^{k-\tilde{M}}}{z(M)} \left(\chi^{(s)}(\alpha)\right)^{m_1} \left(\chi^{(s)}(2\alpha)\right)^{m_2} \cdots \left(\chi^{(s)}(k\alpha)\right)^{m_k} , \tag{4.13}$$

where $\tilde{M} := m_1 + m_2 + \cdots + m_k$.

In this case there is also a formula derived from a generating function. The multiplicity $m_j^{(s,k)}$ corresponds to the x^i-coefficient in the Laurent expansion around zero of the function

$$\zeta_{s,k}(x) = (1 - x^{-1}) \prod_{r=1}^{k} \frac{x^{s+1} - x^{r-s-1}}{x^r - 1} ,$$

where terms outside the domain $0 \leq j \leq s_{max}$ must be dropped.

One must be careful when working with those expressions because the corresponding blocks are in fact different from those obtained in the symmetric case. For example, a 2-antisymmetric state of spin 2 has a block decomposition $\mathbf{5}^{\wedge 2} = \mathbf{7} \oplus \mathbf{3}$ but, in contrast, the 2-symmetric system of spin-2 decomposes as $\mathbf{5}^{\vee 2} = \mathbf{9} \oplus \mathbf{5} \oplus \mathbf{1}$. There exist a relation between the irreducible blocks of different values of (s, k) and even a relation of the appearing blocks in the symmetric case with those appearing in the antisymmetric case, but with different (s, k). This is the essential content of Murnaghan and Hermite isomorphisms, presented in the next section.

4.3 Hermite reciprocity and Murnaghan isomorphism

Hermite's law of reciprocity [64] is an interesting way to see a correspondence between the angular-momentum states of systems of different number of parties and spins given a statistics, or in a more intriguing version, a correspondence of many-boson and many-fermion systems or, more generally, multipartite symmetric and antisymmetric quantum systems. This relation

is studied as a part of a general problem known as *plethysm* in algebraic geometry and which we will illustrate in the following lines.

This theory is relevant for us because it gives us an explanation of why different (s,k) pairs lead to the same irreducible representations when computing the block-diagonal representation of the $SU(2)$ action on them. More specifically, Hermite's law of reciprocity implies the following relation for a double symmetrization

$$\vee^k(\vee^{2s}\mathcal{H}_{1/2}) \sim \vee^{2s}(\vee^k\mathcal{H}_{1/2}) \ , \tag{4.14}$$

where $\mathcal{H}_{1/2}$ denotes the Hilbert space of a spin-1/2 system. Now, notice that $\vee^{2s}\mathcal{H}_{1/2} \sim \mathcal{H}_s$ because there is an isomorphism between the space of totally symmetric products of $2s$ spins 1/2 and the space of a single spin-s, then there exists an isomorphism h such that

$$h : \vee^k\mathcal{H}_s \to \vee^{2s}\mathcal{H}_{k/2} \ , \tag{4.15}$$

then the number of parties and the spins give this interesting relation about how two different physical systems transform under rotations. In some sense, at least in what refers to rotational properties, can be seen as the same system. We have an intuition on this kind of results for example with 2 qubit systems which effectively behaves like a qutrit by making the associations

$$|++\rangle \to |1\rangle \ , \tag{4.16}$$

$$\frac{1}{\sqrt{2}}(|++\rangle + |--\rangle) \to |0\rangle \ , \text{and} \tag{4.17}$$

$$|--\rangle \to |-1\rangle \ . \tag{4.18}$$

In summary, we can think k-symmetric states of spin s as $2s$-symmetric states of spin $k/2$. This explains why $\mathbf{4}^{\vee 2}$ and $\mathbf{3}^{\vee 3}$ have the same irreducible blocks (in this case $\mathbf{7} \oplus \mathbf{3}$).

Related to Hermite's reciprocity law is the Murnaghan isomorphism [65]

$$m : \mathcal{H}_s^{\vee k} \to \mathcal{H}_{s+\frac{k-1}{2}}^{\wedge k} \ ,$$

that relates symmetric and antisymmetric products of different number of factors and spins. This explains why in the decomposition of $\mathbf{3}^{\vee 2}$ and $\mathbf{4}^{\wedge 2}$ appear the same irreducible blocks. In terms of rotations states of either space behave exactly in the same way.

These isomorphisms generalize the classical result of the equivalence under rotations between the symmetrized qubits and higher spin states.

4.4 Anticoherent planes

Given a $\wedge$-factorizable state in $\mathcal{H}_s^{\vee k}$ we can interpret it as a k-plane of spin-s states, that is, a point on the Grassmannian $Gr_{k,2s+1}(\mathbb{C})$. A particularly interesting class of planes is that of anticoherent planes that we define as follows:

If the plane is generated by $\{\psi\}_i$, we say that it is an 1-anticoherent plane of spin s if for all i, j occurs that $\langle\psi_i|\,\vec{S}\,|\psi_j\rangle = 0$. Similarly, a t-anticoherent plane can be defined as a collection of linearly independent states in which for any i, j occurs that $\langle\psi_i|\,(\hat{n}\cdot\vec{S})^m\,|\psi_j\rangle$ does not depend on the direction $\hat{n}$ for $m = 1, 2, \ldots, t$.

This naturally is a generalization of the notion of anticoherent states. Let us see some examples. We must start at spin 3/2 due to the lack of anticoherent planes for spin 1/2 and the triviality of those of spin 1.

Example. Families of anticoherent planes.

In this example we describe some families of anticoherent planes for all $s \geq 2$:

(i) For any integer spin $s \geq 2$, the state $|s, 0\rangle$ and $\frac{1}{\sqrt{2}}\left(|s, s\rangle + |s, -s\rangle\right)$ constitute an anticoherent 2-plane. Geometrically, this result indicates that the the state with s stars in north pole and s in the south pole and a state of $2s$ equidistant points on the equatorial circle[2] form an anticoherent plane.

(ii) For even spin, the states with s stars in both poles and s in the directions of $\hat{x}$ and $\hat{y}$ axes form an anticoherent 3-plane, this is the plane generated by $|\hat{x}; s, 0\rangle, |\hat{y}; s, 0\rangle, |s, 0\rangle$.

To see (i) simply notice that $|s, 0\rangle$ and $\frac{1}{\sqrt{2}}\left(|s, s\rangle \pm |s, -s\rangle\right)$ are anticoherent[3] and that

$$\langle s, 0|\hat{S}_x|s, s\rangle \pm \langle s, 0|\hat{S}_x|s, -s\rangle = \frac{1}{2}\sqrt{s(s+1)}\left(\delta_{0,s+1} + \delta_{1,s} \pm \delta_{0,-s+1} \pm \delta_{1,-s}\right) = 0\ . \tag{4.19}$$

Similarly, it can be verified that $\langle s, 0|\hat{S}_{y,z}|s, s\rangle \pm \langle s, 0|\hat{S}_{y,z}|s, -s\rangle = 0$.

[2] $\frac{1}{\sqrt{2}}\left(|s, s\rangle - |s, -s\rangle\right)$ corresponds to equidistributed points on the equator because its Majorana polynomial is $z^{2s} = 1$.

[3] We can take any of the two possible states, with + or −.

To verify (ii), note that the state with s stars in the positive and negative directions of $\hat{x}$ axis has a Majorana polynomial of the form $(z-1)^s(z+1)^s = (z^2-1)^s$. By the binomial theorem it is easy to see that this state can be expressed as

$$|x_s\rangle = \sum_{k=0}^{s}(-1)^k \frac{\binom{s}{k}}{\sqrt{\binom{2s}{2k}}}|s, 2k-s\rangle \ . \tag{4.20}$$

For the $\hat{y}$ y $\hat{z}$ axes, respectively, we have

$$|y_s\rangle = i^s \sum_{k=0}^{s} \frac{\binom{s}{k}}{\sqrt{\binom{2s}{2k}}}|s, 2k-s\rangle \tag{4.21}$$

and

$$|z_s\rangle = |s, 0\rangle \ . \tag{4.22}$$

Note that

$$\langle x_s|\hat{S}_x|z_s\rangle = \sum_{k=0}^{s}(-1)^k \frac{\binom{s}{k}}{\sqrt{\binom{2s}{2k}}}\langle s, 2k-s|\hat{S}_x|s, 0\rangle \tag{4.23}$$

$$= \sum_{k=0}^{s}(-1)^k \frac{\binom{s}{k}}{\sqrt{\binom{2s}{2k}}}\frac{1}{2}\sqrt{s(s+1)}\,(\delta_{2k-s,1} + \delta_{2k-s+1,0}) = 0 \ . \tag{4.24}$$

Similarly, $\langle x_s|\hat{S}_y|z_s\rangle = 0$. And $\langle x_s|\hat{S}_z|z_s\rangle = 0$ because $|z_s\rangle = |s, 0\rangle$. Therefore, we conclude that $\langle x_s|\vec{S}|z_s\rangle = 0$, and that $\langle y_s|\vec{S}|z_s\rangle = 0$.

Repeating for $\langle x_s|\vec{S}|y_s\rangle$, it is easy to see that $\langle x_s|\hat{S}_x|y_s\rangle = \langle x_s|\hat{S}_y|y_s\rangle = 0$.

And for the remaining component,

$$\begin{aligned}
\langle x_s|\hat{S}_z|y_s\rangle &= i^s \sum_{k=0}^{s}\sum_{l=0}^{s}(-1)^k \frac{\binom{s}{k}\binom{s}{l}}{\sqrt{\binom{2s}{2k}\binom{2s}{2l}}}\langle s, 2k-s|\hat{S}_z|s, 2l-s\rangle \\
&= i^s \sum_{k=0}^{s}\sum_{l=0}^{s}(-1)^k \frac{\binom{s}{k}\binom{s}{l}}{\sqrt{\binom{2s}{2k}\binom{2s}{2l}}}(2l-s)\delta_{k,l} \\
&= i^s \sum_{l=0}^{s}(-1)^l \frac{\binom{s}{l}^2}{\binom{2s}{2l}}(2l-s) = 0 \ .
\end{aligned}$$

The sum appearing in the last step of the computation is zero only in the case of even s, this result is related to particular properties of hypergeometric functions.

With this we conclude that the states of (ii) are an anticoherent 3-plane for all even s.

In the following sections we will explore some applications of the k-antisymmetric spin states. We will illustrate its potential to applications in holonomic quantum computation through the concept of geometric phase.

4.5 Toponomic Quantum Computation

In this section we discuss an application of this geometrical perspective to the understanding of antisymmetrized multiqudit states. In particular, some holonomies that are acquired by a plane that evolves under rotations will be used as quantum gates with interesting properties that make them robust under certain types of noise.

We will start with a discussion of the concept of geometric phase, which is the underlying key concept in this application. After this and a brief introduction to quantum computation and quantum gates, we will explore how geometric phases can be used to perform quantum operations. Finally, some examples are given. The geometric visualization of the antisymmetrized states will be relevant when setting the conditions to design the appropriate gate.

4.5.1 Geometric phases

In 1984 M. Berry noted that [66] when considering a cyclic and adiabatic evolution of a quantum system this returns to its initial state after some time and, in general, besides of the usual dynamical phase defined by the Hamiltonian that governs the evolution, the state acquires an additional phase with a very particular property: it only depends on the geometric structure of the parameter space of which the Hamiltonian is dependend and it does not depend on the time-parametrization of the evolution [67]. This is the well-known geometric or Berry phase.

After the appearance of Berry's discovery [67], some generalizations were presented: the Aharonov-Anandan phase [68] which does not use the adiabaticity condition, the Wilczek-Zee [69] phase which can be defined for systems of degenerated spectra and, among others, the Mukunda-Simon phase [70] that does not use the hypotheses of neither cyclicity nor adiabaticity. I will focus in the last one because it is the most general and highlights the fact

that geometric phase is a deep intrinsic concept of quantum systems.

The work of Mukunda and Simon in geometric phases [70], among other aspects, differs from the others because it defines a geometric phase associated to open curves in projective space, where total and dynamical phases can be distinguished, this phase is defined in a gauge invariant form and with invariance under reparametrizations of the curve, as will be explained below.

Consider a curve $\mathcal{C}_0 := \{\psi(s) \in \mathcal{S}(\mathcal{H}) | s \in [s1, s2] \subset \mathbb{R}\}$ in $\mathcal{H}$.

Applying the gauge transformation $\mathcal{C}_0 \to \mathcal{C}_0'$ given by

$$\psi'(s) = e^{i\alpha(s)}\psi, \ \ s \in [s_1, s_2] \ , \tag{4.25}$$

and using the fact that $\mathrm{Re}\langle\psi(s)|\dot{\psi}(s)\rangle = 0$ we infer that $\langle\psi(s)|\dot{\psi}(s)\rangle = i\mathrm{Im}\langle\psi(s)|\dot{\psi}(s)\rangle$, hence

$$\mathrm{Im}\langle\psi'(s)|\dot{\psi}'(s)\rangle = \mathrm{Im}\langle\psi(s)|\dot{\psi}(s)\rangle + \dot{\alpha}(s) \ . \tag{4.26}$$

With this at hand, a functional can be defined, from $\mathcal{C}_0$, which is gauge invariant and that gives the same values for $\mathcal{C}_0$ and $\mathcal{C}_0'$:

$$\arg\langle\psi'(s_1)|\psi'(s_2)\rangle - \mathrm{Im}\int_{s_1}^{s_2} ds\langle\psi'(s)|\dot{\psi}'(s)\rangle = \arg\langle\psi(s_1)|\psi(s_2)\rangle - \mathrm{Im}\int_{s_1}^{s_2} ds\langle\psi(s)|\dot{\psi}(s)\rangle \ . \tag{4.27}$$

Then, the geometric phase of the open curve can be defined at $\mathcal{C}_0$ as

$$\phi_g[\mathcal{C}_0] := \arg\langle\psi(s_1)|\psi(s_2)\rangle - \mathrm{Im}\int_{s_1}^{s_2} ds\langle\psi(s)|\dot{\psi}(s)\rangle \ . \tag{4.28}$$

Notice that now that in $\mathcal{P}(\mathcal{H})$ it happens that $\mathcal{C}_0$ and $\mathcal{C}_0'$ define the same curve C_0 and it results that the geometric phase associated to this curve in the projective space is

$$\phi_g[C_0] = \phi_{tot}[\mathcal{C}_0] - \phi_{dyn}[\mathcal{C}_0] \ , \tag{4.29}$$

where $\phi_{tot}[\mathcal{C}_0] := \arg\langle\psi(s_1)|\psi(s_2)\rangle$ is the total phase of $\mathcal{C}_0$ and $\phi_{dyn}[\mathcal{C}_0] := \mathrm{Im}\int_{s_1}^{s_2} ds\langle\psi(s)|\dot{\psi}(s)\rangle$ is the dynamic phase associated to the curve $\mathcal{C}_0$.

It is important to highlight that those two functionals are individually dependent on the curve $\mathcal{C}_0$, but their difference is a functional of C_0 on the projective space.

An interesting property of this geometric phase is that it vanishes for geodesics with respect to the natural metric for quantum states, as described in [70].

To explain this point, let $\mathcal{C}_0 = \{\psi(s)\}$ be a curve on the state space, at the point $\psi(s)$ of $\mathcal{C}_0$ the tangent to the curve is the velocity $u(s) := \dot{\psi}(s)$. The horizontal component[4] of $u(s)$ according to the connection $A_\psi(\phi) = \mathrm{Im}\langle\psi|\phi\rangle$ which is given by

$$u_\perp(s) = u(s) - \langle\psi(s)|u(s)\rangle\psi(s) \ . \tag{4.30}$$

Under the gauge transformation (4.25), mapping $\mathcal{C}_0$ a $\mathcal{C}_0^{'} = \{\psi'(s)\}$, we have that $u'_\perp(s) = e^{i\alpha(s)}u_\perp(s)$, this means that the horizontal component of the tangent vector is transformed in a similar way to ψ. In [70] it is shown that the norm of this horizontal component, $||u_\perp(s)||$, defines a metric on projective space.

Another important theoretical aspect is that this phase, despite being a property of the curve in the projective space given by the evolution of the state, it requires for its calculation a choice of lifting the curve in Hilbert space, that is, a continuous phase assignment at each point of the projective space in order to have an image of the curve in Hilbert space. It is possible to give an expression for the Mukunda-Simon phase in terms of only quantities of the projective space (without making any reference to a specific lift), see [70].

4.5.2 Quantum Computation

Since its appearance, more than a century ago, quantum mechanics has been a revolution in knowledge about nature and an inexhaustible source of invaluable technologies for progress, in areas as diverse as medicine, materials science, communications and a long etcetera. Within this long etcetera, I would like to emphasize that quantum mechanics can be used for the processing and transmission of information. The theory that studies these relationships between quantum mechanics and information theory is known as *quantum information* and it is precisely in this context that some of the results of this work may find a place in possible applications, this brief introduction to this topic is based mainly on [71, 72, 73].

[4]The notion of horizontality that we will use is the following : a vector $|\phi\rangle$, tangent at $|\psi\rangle$, is horizontal if $A_\psi(\phi) = 0$.

One of the main paradigms in quantum information is the quantum computer, an entity that is capable of carrying out the tasks of processing, storing and transmitting information in such a way that, without losing the advantages of classical computers, it allows to extend the range of applicability of computers and improve efficiency in the consumption of computing resources, usually time, energy, space and material resources.

There are several ways that look for a realization of a quantum computer, some of them are based on intrinsic properties of quantum systems, giving rise to what is known as *geometric computation* or *topological computation*. In this work I will present some advances and future proposals to advance the understanding of one of these paths towards quantum computation: holonomic quantum computation. This is, in a simple way, the application of non-abelian geometric phases to the processing of quantum information. It is a field that has been studied since its emergence in 1999 with Zanardi and Rasetti's celebrated article [74], which has led to interesting applications and experiments. Holonomic quantum computation is particularly attractive for approaching a realistic computational model since it is known to be particularly robust to a certain type of noise, known as *parametric noise* and there is also another source of robustness from the reparametrization invariance of geometric phase. In this work, some schemes will be proposed that allow the generation of quantum gates of geometric origin from various mechanisms, as will be explained later.

A brief introduction to quantum computation, in general, and holonomic quantum computation, in particular, will be given below, discussing some advantages and challenges of this field.

Quantum computing originated in the 80's when Feynman suggested that a computer based on quantum mechanics would be ideal for simulating quantum-mechanical systems [71]. The developments made in this field have shown that the advantages of quantum computation go far beyond this, since it has been shown that quantum computers, in principle, can efficiently solve problems that classically have high complexity. An example of this is the problem of factoring large prime numbers, which, using Shor's algorithm, can be efficiently solved in a quantum computer [75]. Another example of a complex problem in classical computing is the determination of the Jones polynomial of a knot, which has an exponential difficulty, however, in certain cases the problem can be solved efficiently using a quantum algorithm, precisely,

the algorithm of Aharonov, Jones and Landau [76].

The unit of quantum information is the *qubit* and essentially, a quantum computer is a many-qubit system. Physically, a qubit is a two level system, like a spin 1/2 particle, this can be realized in different ways: photons and their polarization, atoms and two energy levels, etc. Then a quantum computer is a many-qubit system whose evolution is controllable and a quantum operation corresponds to a unitary transformation that acts on the many-qubit state that describes the quantum computer.

It is important to highlight that quantum entanglement plays an important role in some protocols of quantum computation (but not in all cases), like superdense coding, that allows the transmission of two bits of classical information through the manipulation of only one of the two entangled qubits, or quantum teleportation, that allows the transmission of the information of a quantum state from one place to other even if it is very far. In modern experiments this has been verified up to the order of hundreds of kilometers [77].

As in the case of classical computation, there are many models of computation that have been translated into the quantum computation, as the model of Turing's machine or the circuit model, being the latter the most used in recent literature, maybe because of its simplicity. In this model of quantum computation there are three main steps to perform any computation

- Initialize the state,
- evolve state with quantum gates (unitary operations),
- measure the resulting quantum state.

Another matter of primary interest in quantum computing is the correction of errors, because there are errors in quantum computation of different origins, ranging from errors associated with coupling with the environment to decoherence effects such as errors associated with imprecision in the application of unit operations.

4.5.3 Holonomic Quantum Computation

Holonomic quantum computation consists in the use of non-abelian geometric phases as quantum logic gates [74]. The main advantage of this scheme is its robustness, guaranteed by the

fact that holonomies only depend on the paths in the space of external parameters of the systems and not on their particular parametrizations, this way to perform gate implementation is immune to variations in fine details of the dynamics of system, it is a robust implementation against noise and errors related with the control of the system. This made holonomic quantum computation a relevant model for its eventual realization. Nevertheless, a concrete realization requires to overcome some difficulties. A quantum computer working under this implementation should have the following properties [73]:

(i) Controllability: The quantum holonomic computer should have a great number of control parameters to generate arbitrary gates.

(ii) Enough degeneracy: Degeneracy of energy levels must be preserved during the evolution of the states in the computer. It is also important to have high-dimensional degenerated subspaces, this in order to work with systems of many qubits.

(iii) Adiabaticity: Following the Wilczek-Zee prescription, the computation must be slow enough to satisfy the requirements of adiabatic theorem, but fast enough to avoid decoherence effects. It is also important to vary control parameters to avoid undesirable transitions between different energy levels of the system. This balance of slow and fast times to obtain the appropriate holonomy is known as isoholonomic problem and optimal solutions to it have been studied [78].

Although many holonomic computer designs have been established, and even experimental implementations have been proposed [79], it remains a big problem to make one with a realistic implementation. Requirement (iii) seems to be under control, at least in a theoretical scheme. Requirements (i) and (ii) are of practical relevance and there is no theoretical proposal to solve them in a general way.

4.5.4 Toponomic gates

In this section we propose a way to generate gates for holonomic quantum computation using the non-abelian geometric factors obtained by the evolution of anticoherent k-planes under the action of $SU(2)$. This novel approach use the topological property of the acquired geometric phases to enhance the robustness of the generated gate. The robustness of our

gates are twofold: on the one hand they have the robustness under reparametrizations of the curve as in other schemes for holonomic quantum computation but also a robustness against variations of the curve in $SU(2)$ that implements the evolution of the plane, this is due to the particularities of the geometric phase of anticoherent states, as we explain below.

A k-plane $|\Pi\rangle = |\psi_1\rangle \wedge \cdots \wedge |\psi_k\rangle$ is called anticoherent if for all i, j we have $\langle\psi_i|\mathbf{S}|\psi_j\rangle = 0$.

If cyclic evolutions given by rotations are considered acting on anticoherent k-planes, the (non-abelian) geometric phase that is acquired is independent of the path in the space of rotations, with the corresponding identifications due to discrete symmetries.

The main idea of this result is based on a non-abelian extension of the Mukunda-Simon phase, reported in [80]. In this case, the statement of the problem in terms of fiber bundles is the following: The Grassmannian takes the role of base space (replacing the projective space in the Mukunda-Simon case) and over each point we associate a fiber, diffeomorphic to $U(k)$, hence, the total space is $S_{k,\mathbb{P}}$ which is the space of orthonormal k-frames[5] over the projective space $\mathbb{P}$. In this way, the non-abelian geometric phase of a curve $\mathcal{C}$ in a particular section in $S_{k,\mathbb{P}}$ can be written as

$$U_{geo}[\mathcal{C}] = Q_p[\mathcal{C}]F[\mathcal{C}] \ , \tag{4.31}$$

where

$$F[\mathcal{C}] \equiv P\exp\left[-\int_{s_1}^{s_2} A(s)ds\right] \ , \ A_{ij}(s) = \langle\phi_i(s)|\dot{\phi}_j(s)\rangle \ , \tag{4.32}$$

and Q_p is the unitary part of the matrix Q, with entries $Q_{ij} = \langle\phi_i(s_1)|\phi_j(s_2)\rangle$.

In [81] it has been shown that in the case of cyclic evolutions of anticoherent k-planes, given by rotations, $F \equiv \mathbb{I}$ and the geometric phase is given only by the unitary part of Q, which naturally generalizes the result we obtained for the geometric phase of anticoherent spin states under rotations, in Appendix B it is shown that the geometric phase of anticoherent spin states has a topological character. Then, for cyclic evolution of planes it can be easily noted that under an evolution by rotation the states evolve in such a way that $|\phi_j(s)\rangle \to R(s)|\phi_j(s_1)\rangle = e^{i\alpha\hat{n}\cdot\vec{S}}|\phi_j(s_1)\rangle$, then $A_{ij}(s) = i\alpha\hat{n}\cdot\langle\phi_i(s)|\vec{S}|\phi_j(s)\rangle$, therefore, for anticoherent planes $A_{ij} = 0$.

In intuitive terms, the Mukunda-Simon phase tells us that there is a part of the geometric

[5] $S_{k,\mathbb{P}}$ is known as Stiefel manifold.

phase that depends on the extreme points of the curve and another that depends on the entire curve, but in this case the result has a topological character due to which only has dependence on the extreme points, as we see in this case, the matrix Q only has information at the ends of the curve, while all the integration along the curve resides in F. This implies that U_{geo} is, rather than a geometric quantity, a topological quantity. Those holonomies can be used to carry out quantum operations as quantum logic gates as shown in the following examples.

Example 24. *CNOT gate*

Consider the following 4*-plane of spin-*8 *states:*

$$\Pi = \left\{ \frac{1}{\sqrt{2}} \left(|8,8\rangle + |8,-8\rangle \right), |8,0\rangle, \frac{1}{4} \left(|8,6\rangle + |8,3\rangle + |8,-3\rangle + |8,-6\rangle \right), \frac{1}{4} \left(|8,6\rangle - |8,3\rangle - |8,-3\rangle + |8,-6\rangle \right) \right\} .$$

It is easy to show that it is an anticoherent plane. When Π *evolves by a rotation along the z-axis by an angle of* π*, the plane after this evolution returns to itself but acquiring the following geometric phase:*

$$\phi(\Pi) = \begin{pmatrix} 1 & 0 & 0 & 0 \\ 0 & 1 & 0 & 0 \\ 0 & 0 & 0 & 1 \\ 0 & 0 & 1 & 0 \end{pmatrix} ,$$

which corresponds to a CNOT gate.

CNOT gate is an important 2*-qubit gate because it is part of many universal sets of quantum gates that are used as building blocks for more complex quantum gates (in fact, CNOT and rotation gates are enough to approximate any gate).*

The symmetry of the plane under $R_{(\hat{z},\pi)}$ *is easily recognizable from the symmetry of the constellations of the four vectors that span the plane.*

- *The state* $|8,0\rangle$ *has four stars at north pole and the remaining four at the south pole.*
- *The state* $\frac{1}{\sqrt{2}} \left(|8,8\rangle + |8,-8\rangle \right)$ *has eight stars at the vertices of an hexadecagon in the equatorial plane.*
- *The other two states have a polyhedral form (pentagons and squares in a symmetric configuration), one being a rotation of the other. Beyond figures, the block of 5 zeroes*

in the expression of the state in the standard S_z-basis indicates that the $\hat{z}$ axis is an axis of symmetry by rotations of $2\pi/(5+1) = \pi/3$ and therefore, there is a rotational symmetry under rotations along the $\hat{z}$ axis by rotations of π, as desired.

Example 25. *CCNOT=Toffoli gate*

Toffoli is a 3-qubit gate that has two controls before to apply the NOT operation, important in the context of universal quantum computation and in reversible computation (this gate in the classical context has the property that any reversible circuit can be written using only Toffoli gates).

In order to obtain a Toffoli gate we can consider the following anticoherent 8-plane in spin 16:

$$\Pi_2 = \left\{ \frac{1}{\sqrt{2}} \left(|16, r\rangle + |16, -r\rangle \right), |16, 0\rangle, \frac{1}{4} \left(|16, 6\rangle + |16, 3\rangle + |16, -3\rangle + |16, -6\rangle \right), \frac{1}{4} \left(|16, 6\rangle - |16, 3\rangle - |16, -3\rangle + |16, -6\rangle \right) \right\},$$

where $r \in \{8, 10, 12, 14, 16\}$.

Applying the same rotation of the last example, we obtain as geometric phase one of the permutations of the three-qubit Toffoli gate:

$$\phi(\Pi_2) = \begin{pmatrix} 1 & 0 & 0 & 0 & 0 & 0 & 0 & 0 \\ 0 & 1 & 0 & 0 & 0 & 0 & 0 & 0 \\ 0 & 0 & 1 & 0 & 0 & 0 & 0 & 0 \\ 0 & 0 & 0 & 1 & 0 & 0 & 0 & 0 \\ 0 & 0 & 0 & 0 & 1 & 0 & 0 & 0 \\ 0 & 0 & 0 & 0 & 0 & 1 & 0 & 0 \\ 0 & 0 & 0 & 0 & 0 & 0 & 0 & 1 \\ 0 & 0 & 0 & 0 & 0 & 0 & 1 & 0 \end{pmatrix}.$$

In this case the symmetry is also easy to see

- *The state $|16, 0\rangle$ has 16 stars at each pole.*
- *The state $\frac{1}{\sqrt{2}} \left(|16, 16\rangle + |16, -16\rangle \right)$ has 32 stars at the vertices of an 32-gon in the equatorial plane.*
- *The state $\frac{1}{\sqrt{2}} \left(|16, 14\rangle + |16, -14\rangle \right)$ has 30 stars at the vertices of an 30-gon in the equatorial plane, and one star at each pole.*

- *The state* $\frac{1}{\sqrt{2}}\left(|16,12\rangle + |16,-12\rangle\right)$ *has 28 stars at the vertices of an 28-gon in the equatorial plane, and two star at each pole (and now is clear the pattern of constellations of this class of states).*

- *The last two states have a polyhedral form (in a symmetric configuration as shown in the nb), one being a rotation of the other. Beyond figures, the block of 5 zeroes in the expression of the state in the standard* S_z*-basis indicates that the* $\hat{z}$ *axis is an axis of symmetry by rotations of* $2\pi/(5+1) = \pi/3$ *and therefore, there is a rotational symmetry under rotations along the* $\hat{z}$ *axis by rotations of* π*, as desired.*

Example 26. *r-CNOT gate*

Let us define the r-CNOT gate as $r+1$*-qubit gate* $\underbrace{\text{CC...C}}_{r \text{ times}}\text{NOT}$ *. CNOT is the gate corresponding to* $r = 1$ *and for* $r = 2$ *we have the TOFFOLI gate. I find this example interesting in our context because, despite not having the possibility of taking tensor products, we can infer some heuristic methods to extend our well known gates to multiqubit systems, as usually required in practice.*

With the examples above it is easy to see the general solution of the toponomic generation of the r-CNOT gate:

We need a $2^{r+1}-$*anticoherent plane of spin* 2^{r+2} *with the following states being a basis of the plane:*

- *The state* $|2^{r+2},0\rangle$ *whose constellation is an* 2^{r+3}*-gon in the equatorial plane*

- *Two states with* special *constellations with symmetry under rotations about* $\pi/3$ *along* $\hat{z}$ *(the symmetry is automatic because of the spacing between non-zero entries).*

- *The states* $\frac{1}{\sqrt{2}}\left(|2^{r+2},2^{r+2}-2k\rangle + |2^{r+2},-\left(2^{r+2}-2k\right)\rangle\right)$ *for* $k = 1,2,\ldots,2^{r+1}-4$*. The constellation of those states are* k *stars at each pole and the remaining stars are distributed in the vertices of a regular polygon in the equatorial plane.*

Chapter 5

Concluding remarks and future directions

Throughout this work we have explored some topics in the field of geometry of multipartite quantum systems and have developed various applications in areas such as quantum information, quantum computation and quantum metrology.

We reviewed some generalities of this field, beginning with the most fundamental properties of complex projective space, which constitutes the space where individual spin systems reside. In this part, the Majorana representation constitutes a powerful tool for the analysis of the rotational properties of this type of systems, in addition to the fact that, as we develop in section 1.3.3, this representation is defined operationally, which more than an abstract mathematical construction is a measurable feature of a quantum system.

At a theoretical level, we extended this representation to the case of symmetric and antisymmetric tensor powers of a Hilbert space, finding that more than a single constellation that carries all the rotational properties of the system, a set of constellations, i.e. a multiconstellation, is required to be able to codify all the required parameters. This analysis was carried out by analyzing the decompositions into irreducible representations of the representations of $SU(2)$ in the symmetrized or antisymmetrized tensor powers of a given Hilbert space.

Given the nature of these decompositions, we find that given an original system, only integer or

half-integer spins appear in its decomposition, and with multiplicities that can be determined without the need to find the corresponding decompositions, thanks to some results in character theory, as explained in sections 3.1.2 and 4.2. At a mathematical level, the classic problem of plethysm in algebraic geometry manifests itself in the fact that certain decompositions, and therefore multiconstellations, for different systems coincide.

In the domain of applications we can notice that through the introduction of the notion of anticoherent planes (see 4.4) we can study the non-abelian geometric factors coming from evolutions of factorizable antisymmetrized systems that produce, given the initial states and the appropriate evolutions , robust logic gates against noise, noise from reparametrizations of the curve in the rotation space that dictates the evolution (this is a property of the geometric phase) and noise from errors in the path traced by the curve in the space of rotations, which, at an experimental level, could be interpreted as robustness to variations in the magnetic field used to guide the evolution of the spin system. This second point comes from using an anticoherent plane.

The representation of states through multiconstellations is fundamental in the development of toponomic gates, since to solve the inverse problem involved in the design of a gate, intuition about the rotational symmetries of the system is necessary, which are understood thanks to this representation.

One advantage of this model for computation, apart from its topological robustness, is that it gives to us an idea about how to tackle the problem of extensibility in holonomic computation. As we studied in 4.5, the symmetry patterns make us able to extend the number of entries in the register of the quantum computer and therefore extend the holonomic gates by means of an increase in the dimensionality of the spin system. This is not a simplification nor a solution of the problem, but it makes a suggestion: we can increase the size of gates for more entries paying an increase on the dimensionality of the spin system involved on it.

In the metrological context we studied how our representation of states allows us understand how to use factorizable multiqudit systems in the problem of finding optimal quantum rotosensors. This kind of applications may be relevant in the field of magnetometry in which one looks for making precise measurements of small variations of a given magnetic field. This

point is important because in different fields it has been shown that the precision of measurements of physical parameters by means of quantum systems, instead of classical, may be considerably increased.

In terms of possible extensions of the multiconstellation formalism one may ask what happens if we have a spin system that is not symmetrized or antisymmetrized, but has a mixed symmetry? By mixed symmetry we mean antisymmetry in certain tensor factors and symmetry in others, with an underlying Young's diagram describing these symmetry relationships. Note that this is not necessarily a parastatistical system (systems that we do not seem to observe in nature), since the spin part of the wavefunction can have mixed symmetry and yet the total wavefunction be fully symmetric or antisymmetric.

To do this extension, it would be necessary to analyze the irreducible representations of $SU(2)$ in tensor powers with symmetry dictated by a specific Young diagram, and from this, generate the new multiconstellations.

In the domain of applications there are many topics to explore. Starting by finding the relationship between entanglement and the eigenvalues of the Gramian matrix in a more general situation than those described in this work.

It would also be interesting to study the geometric measures of entanglement in more general systems that are not necessarily factorizable. In this case, it may be that the description is much more complex since there is no direct mechanism to build the Gramian matrix, which is possibly a manifestation of the more general object that is really related to the geometric measures of entanglement.

We also studied through some examples the entanglement of factorizable systems of symmetrized multiqudits, finding interesting results, in particular, relationships between the geometric measure of entanglement and the eigenvalues of the Gramian matrix associated with the initial state, in which a curious relationship between the GHZ state and the W takes place, in a certain way, from the separable state we can arrive at one of the other, following a different geodesic.

Naturally, there are many aspects both in the theoretical part and in the applications that we did not develop but that constitute ideas for future progress in this direction.

Another aspect that will be interesting to explore are the properties of anticoherent states of multipartite systems. Probably the first step in this direction would be to find a precise definition of anticoherence of multipartite state that recover the notion of most quantum state as in the single particle case. These kinds of states, over the past 15 years, have given rise to many interesting applications that could possibly be extended to more general quantum systems. In this context probably the geometry of multiconstellations could be relevant to understand the anticoherent states.

Within the faithful representations of rotations of quantum systems, in addition to the Majorana representation, we have the Schwinger representation in which a spin state is associated with a certain wave function of the harmonic oscillator in such a way that if we rotate the state of spin by a rotation $D^{(s)}(R_{\hat{n},\alpha})$ then the squared modulus of the wave function of the associated oscillator rotates by the same rigid rotation $R_{\hat{n},\alpha}$. It would be interesting to explore if we can develop a similar representation for multipartite quantum systems and explore the information they give us about the system under study.

This is only a fraction within the vast field of geometry of multipartite quantum systems, whose understanding can take us from a greater comprehension of the most fundamental systems that constitute matter to the development of new quantum technologies that change the way in which we live.

.1

Geometric phases of anticoherent spin states

One aspect of anticoherent spin states that we have studied is the fact that in some cases they have a non-trivial symmetry group Γ such that the orbit of the anticoherent state in SO(3) is reduced in a non-trivial manner to the space $\mathrm{SO}(3)/\Gamma$. When one has a continuous sequence of rotations that reach one of those symmetry rotations, a cyclic evolution of the state is determined, thus, a geometric phase associated with this cyclic evolution. This geometric phase is a homotopic invariant in SO(3) and it is a one-dimensional representation of the fundamental group $\pi_1(\mathrm{SO}(3)/\Gamma)$, as we will show in this section. For a more detailed version see our work [82].

In that sense, the geometric phase that anticoherent spin states accumulate in those evolutions through rotations has a topological origin, as the phase that appears in the well-known example of Berry and Robbins [83].

Let us then compute the geometric phase acquired by an anticoherent spin state.

Consider a spin state $|\psi\rangle$ whose Majorana representation has a discrete rotational symmetry group Γ in SO(3) and a curve $g(\tau)$ in SO(3), $0 \leq \tau \leq 1$, such that $g(0) = e$ and $g(1) = \mathcal{R} \in \Gamma$, where e is the identity in SO(3).

Then, if $U(g)$ is a representation of $g \in \mathrm{SO}(3)$ acting in the Hilbert space of a spin j, the curve given by $U(g(\tau))$ is closed in the sense that $U(g(1))|\psi\rangle = U(s)|\psi\rangle = e^{i\chi^s}|\psi\rangle$ (closed in the space $\mathcal{P}(\mathcal{H})$).

For that reason, and not having the requirement of adiabatic evolution, we can compute the Aharonov-Anandan phase. To do this, one must consider the evolution in such a way there is no accumulation of total phase. Consider the evolution

$$|\Psi, \tau\rangle = e^{i\chi(\tau)} e^{-i\vec{J}\cdot\hat{n}\alpha(\tau)}|\psi\rangle \ , \tag{1}$$

that describes a continuous sequence of rotations along the instantaneous rotation axis $\hat{n}$ with angle $\alpha(\tau)$, such that at $\tau = 0$ there is no rotation and at $\tau = 1$ the state has rotated by s. The function $\chi(\tau)$ is used to absorb the total phase and it is any function that satisfies that $\chi(1) - \chi(0) = -\chi^s$.

Therefore, the geometric phase is given by

$$\phi_g^s = i \int_0^1 \langle \Psi, \tau | \left(\partial_\tau | \Psi, \tau \rangle \right) d\tau. \tag{2}$$

Using Leibniz rule, we obtain that

$$\langle \Psi, \tau | \left(\partial_\tau | \Psi, \tau \rangle \right) = \tag{3}$$

$$= \langle \psi | e^{-i\chi(\tau)} e^{i\mathbf{J}\cdot\mathbf{n}(\tau)\alpha(\tau)} \partial_\tau \left(e^{i\chi(\tau)} e^{-i\mathbf{J}\cdot\mathbf{n}(\tau)\alpha(\tau)} \right) | \psi \rangle \tag{4}$$

$$= i\partial_\tau \chi(\tau) + \langle \psi | e^{i\mathbf{J}\cdot\mathbf{n}(\tau)\alpha(\tau)} \partial_\tau \left(e^{-i\mathbf{J}\cdot\mathbf{n}(\tau)\alpha(\tau)} \right) | \psi \rangle. \tag{5}$$

If the state is anticoherent, the second term vanishes because $e^{i\mathbf{J}\cdot\mathbf{n}(\tau)\alpha(\tau)} \partial_\tau \left(e^{-i\mathbf{J}\cdot\mathbf{n}(\tau)\alpha(\tau)} \right)$ is an element of $\mathfrak{su}(2)$, which can be written as $\mathbf{X}(\tau)\cdot\mathbf{J}$,for a vector $\mathbf{X}(\tau)$, which has a vanishing expectation value for any anticoherent spin state. Thus, the geometric phase is given by

$$\varphi_g^s = -\int_0^1 \partial_\tau \chi(\tau) d\tau = \chi(0) - \chi(1) = \chi^s. \tag{6}$$

Resulting then that all the accumulated phase is the geometric phase. We conclude that *the geometric phase φ_g^s corresponding to a cyclic evolution of the state, associated with a symmetry s, is constant in the homotopy class of the curve in $SO(3)$*. Doing the corresponding lifting of the curve $g(\tau)$ to $SU(2)$, this result translates into a natural independence on the path in $SU(2)$. Notice the importance of the fact that $|\psi\rangle$ is 1-anticoherent, in terms of constellations the 1-anticoherence is manifested in the invariance of the states under some non-trivial discrete subgroups of the rotation group.

This independence on the path is what, in essence, reveals that this geometric phase has a topological origin. To clarify this, we will explore in more detail the geometry of the problem.

In the Mukunda-Simon formulation the geometric phase is a property of curves in projective space. From this perspective, given a curve $C(t) = [|\psi(t)\rangle]$ in $\mathcal{P}(\mathcal{H})$ we can associate with it a geometric phase which is, as we have shown, equal to the total phase in the case of evolutions by rotations if the state under consideration is anticoherent (I denoted by $[|\psi\rangle]$ the class of states that share the same projection as the representative $|\psi\rangle$). We might think that this curve is the path traced by a spin state during a sequence of rotations $R(t) \in SO(3)$,

$$|\psi(t)\rangle = D(R(t))|\psi(0)\rangle \ , \tag{7}$$

where $D(R(t))$ denotes the irreducible representation of rotations for spin s, where this is the spin of the state under consideration.

We will consider the special situation of the evolution of anticoherent states that have a discrete rotational symmetry group.

Consider, for example, a curve $R(t)$ that at $t = 0$ is on the identity of the group and at $t = 1$ in a symmetry rotation $R_m \in \Gamma \subset SO(3)$. As the Majorana constellation determines the state projectively and R_m is a symmetry of the constellation, we have that

$$D(R_m)|\psi(0)\rangle = e^{i\alpha_m}|\psi(0)\rangle \ ,$$

thus $[|\psi(1)\rangle]$=$[|\psi(0)\rangle]$, i.e., $[|\psi(t)\rangle]$ is a closed curve on the projective space. It is clear that for those curves the geometric phase is simply α_m, independently of the details of the curve $R(t)$. This is the case because the phase only depends on the homotopy class.

These phases, besides being unaffected by perturbation in the path traced in $SO(3)$, may be affected by imprecision in the location of the final point of the path, nevertheless, those variations are small being at most quadratic in the error of the rotation ϵ, this means that if we apply to the state $|\psi\rangle$ a rotation

$$R = e^{-i\epsilon\hat{n}\cdot\vec{S}}R_m \ , \tag{8}$$

where R_m is a symmetry rotation and the prefactor comes from the efect of noise, it is easy to note that

$$\langle\psi|R|\psi\rangle = e^{i\alpha_m}\left(1 + \mathcal{O}(\epsilon^2)\right). \tag{9}$$

In opposition to the case of any general state whose orbit under the action of $SO(3)$ is diffeomorphic to a copy of $SO(3)$, in the case of anticoherent states with a symmetry group Γ the orbit is reduced to a copy of the quotient space $SO(3)/\Gamma$.

This fact can be visualized by means of the representation of $SO(3)$ by a ball of radius π in which the axis of rotation is indicated by a direction on the sphere and the angle of the same is indicated by the distance to the origin of the point of the ball. If there is a symmetry rotation, a quotient space can be visualized as a cell in which lie the closest states to the symmetry rotation (this implies to give a notion of distance which is specific, as we explain

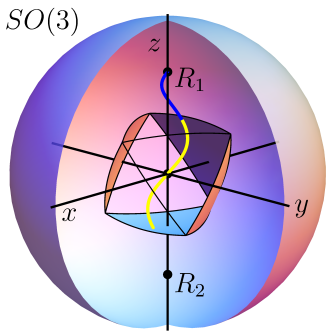

Figure 1: Cell in $SO(3)$ to represent $SO(3)/\Gamma$, taken from [82]. The curve in yellow starts at the identity and goes to a symmetry rotation of the tetrahedron, the rotation by $2\pi/3$ around the $\hat{z}$ axis, we can see that the blue part of the curve is outside the cell, but with the realized identifications the curve reappears from the bottom of the cell and reaches the identity.

in [82]). In the following figure one of those cells is represented (that which is around the identity operation) for the case in which Γ is the discrete subgroup of the symmetries of the tetrahedron.

These identifications make the orbit O_ψ under $SO(3)$ of an anticoherent spin state an object with a complex topology. A feature of this topology is that there can be curves in the orbit which are not homotopic, i.e., it can occur that there is no continuous map from one to the other maintaining fixed endpoints. We say that the two curves are in different homotopy classes. The curves on the orbit, taking concatenation as product, form a group known as *fundamental group*. The non-trivial topology is therefore encoded in this group.

Then, the phases $e^{i\alpha_m}$ that are acquired by the anticoherent state $|\psi\rangle$ evolving by rotations, starting on the identity and ending at a symmetry rotation $R_m \in \Gamma$, are a unidimensional representation of the fundamental group [1] $\pi_1(SO(3)/\Gamma)$ of the orbit O_ψ.

As an example, in the next table the geometric phases that we computed for platonic states are shown. Those states are characterized by having Majorana constellations corresponding to the sets of vertices of the respective solids.

[1] the fundamental group is commonly denoted by π_1 to indicate that it is the group of the equivalence classes of non-homotopic loops. There are homotopy groups of higher order that consist of topologically inequivalent classes of n-spheres, instead of loops. These groups are commonly denoted by π_2,π_3, etc.

Example 27. *Geometric phases of platonic states.*

	2	3	4	5
Tetrahedron	0	$\frac{2\pi}{3}$	-	-
Cube	0	0	0	-
Octahedron	π	0	π	-
Dodecahedron	0	0	-	0
Icosahedron	0	0	-	0

Table 1: Platonic states are those whose Majorana constellation is given by the set of vertices of a platonic solid. In table 1, the absolute values of the geometric phases, corresponding to symmetry rotations, are shown indicated by their order (i.e., by an angle $2\pi/n$, being n the order). The value of n is depicted in the top row of the table. ■

Bibliography

[1] A. Messiah, *Quantum Mechanics*. Dover Publications, 1999.

[2] R. Penrose, *Fashion, faith, and fantasy in the new physics of the universe*. Princeton University Press, 2016.

[3] I. Bengtsson and K. Życzkowski, *Geometry of Quantum States (2nd Ed.)*. Cambridge University Press, 2017.

[4] E. Majorana, "Atomi orientati in campo magnetico variabile," *Nuovo Cimento*, vol. 9, pp. 43–50, 1932.

[5] J. J. Sakurai, *Modern Quantum Mechanics (Revised Edition)*. Addison-Wesley, 1994.

[6] U. Fano and G. Racah, "Irreducible tensorial sets," *Irreducible tensorial sets*, 1959.

[7] C. Chryssomalakos, E. Guzmán-González, and E. Serrano-Ensástiga, "Geometry of spin coherent states," *J. Phys. A: Math. Theor.*, vol. 51, no. 16, p. 165202, 2018. `arXiv:1710.11326`.

[8] J. Zimba, "Anticoherent spin states via the majorana representation," *EJTP*, vol. 3, no. 10, pp. 143–156, 2006.

[9] L. Hanotel, "Constelaciones de Majorana, estados de espín arquimídeos y anticoherencia." Undergraduate thesis. Facultad de Ciencias, Universidad Nacional Autónoma de México, 2016.

[10] J. Crann, R. Pereira, and D. W. Kribs, "Spherical designs and anticoherent spin states," *J. Phys. A: Math. Theor.*, vol. 43, p. 255307, 2010.

[11] E. Bannai and M. Tagami, "A note on anticoherent spin states," *J. Phys. A: Math. Theor.*, vol. 44, p. 342002, 2011.

[12] P. Delsarte, J.-M. Goethals, and J. J. Seidel, "Spherical codes and designs," in *Geometry and Combinatorics*, pp. 68–93, Elsevier, 1991.

[13] D. Baguette, F. Damanet, O. Giraud, and J. Martin, "Anticoherence of spin states with point-group symmetries," *Phys. Rev. A*, vol. 92, p. 052333, Nov. 2015.

[14] R. Horodecki, P. Horodecki, M. Horodecki, and K. Horodecki, "Quantum entanglement," *Reviews of modern physics*, vol. 81, no. 2, p. 865, 2009.

[15] F. Mintert, C. Viviescas, and A. Buchleitner, "Basic concepts of entangled states," in *Entanglement and Decoherence*, pp. 61–86, Springer, 2009.

[16] E. Schrödinger, "Die gegenwärtige situation in der quantenmechanik," *Naturwissenschaften*, vol. 23, no. 49, pp. 823–828, 1935.

[17] A. Acín, A. Andrianov, L. Costa, E. Jané, J. Latorre, and R. Tarrach, "Generalized schmidt decomposition and classification of three-quantum-bit states," *Physical Review Letters*, vol. 85, no. 7, p. 1560, 2000.

[18] H. A. Carteret, A. Higuchi, and A. Sudbery, "Multipartite generalization of the schmidt decomposition," *Journal of Mathematical Physics*, vol. 41, no. 12, pp. 7932–7939, 2000.

[19] V. Vedral and M. B. Plenio, "Entanglement measures and purification procedures," *Physical Review A*, vol. 57, no. 3, p. 1619, 1998.

[20] T.-C. Wei and P. M. Goldbart, "Geometric measure of entanglement and applications to bipartite and multipartite quantum states," *Physical Review A*, vol. 68, no. 4, p. 042307, 2003.

[21] C. H. Bennett, D. P. DiVincenzo, J. A. Smolin, and W. K. Wootters, "Mixed-state entanglement and quantum error correction," *Physical Review A*, vol. 54, no. 5, p. 3824, 1996.

[22] J. Eisert, K. Audenaert, and M. Plenio, "Remarks on entanglement measures and nonlocal state distinguishability," *Journal of Physics A: Mathematical and General*, vol. 36,

no. 20, p. 5605, 2003.

[23] A. Shimony, "Degree of entanglement," *Ann. New York Acad. Scien.*, vol. 755, no. 1, pp. 675–679, 1995.

[24] F. Verstraete and H. Verschelde, "Fidelity of mixed states of two qubits," *Physical Review A*, vol. 66, no. 2, p. 022307, 2002.

[25] G. Vidal and R. Tarrach, "Robustness of entanglement," *Physical Review A*, vol. 59, no. 1, p. 141, 1999.

[26] R. Hübener, M. Kleinmann, T.-C. Wei, C. González-Guillén, and O. Gühne, "Geometric measure of entanglement for symmetric states," *Physical Review A*, vol. 80, no. 3, p. 032324, 2009.

[27] L. Chen, A. Xu, and H. Zhu, "Computation of the geometric measure of entanglement for pure multiqubit states," *Physical Review A*, vol. 82, no. 3, p. 032301, 2010.

[28] J.-L. Brylinski, "Algebraic measures of entanglement," in *Mathematics of quantum computation*, pp. 19–40, Chapman and Hall/CRC, 2002.

[29] A. Sawicki and V. V. Tsanov, "A link between quantum entanglement, secant varieties and sphericity," *Journal of Physics A: Mathematical and Theoretical*, vol. 46, no. 26, p. 265301, 2013.

[30] K. Smith, L. Kahanpää, P. Kekäläinen, and W. Traves, *An invitation to algebraic geometry*. Springer Science & Business Media, 2004.

[31] I. Bengtsson, S. Weis, and K. Życzkowski, "Geometry of the set of mixed quantum states: An apophatic approach," in *Geometric Methods in Physics*, pp. 175–197, Springer, 2013.

[32] K. Szymański, S. Weis, and K. Życzkowski, "Classification of joint numerical ranges of three hermitian matrices of size three," *Linear algebra and its applications*, vol. 545, pp. 148–173, 2018.

[33] O. Chterental and D. Z. Djokovic, "Normal forms and tensor ranks of pure states of four qubits," *arXiv preprint quant-ph/0612184*, 2006.

[34] I. Gelfand, M. Kapranov, and A. V. Zelevinsky, "Discriminants, resultants and multidimensional determinants. reprint of the 1994 edition. modern birkhäuser classics," 2008.

[35] L. H. Kauffman and S. J. Lomonaco, "Braiding operators are universal quantum gates," *New Journal of Physics*, vol. 6, no. 1, p. 134, 2004.

[36] J. E. Marsden and T. S. Ratiu, *Introduction to mechanics and symmetry: a basic exposition of classical mechanical systems*, vol. 17. Springer Science & Business Media, 2013.

[37] K. Karnas, K. Kowalczyk-Murynka, M. Kuś, T. Macikazek, M. Oszmaniec, and A. Sawicki, "Multipartite quantum correlations: symplectic and algebraic geometry approach," *arXiv preprint arXiv:1701.03536*, 2017.

[38] M. Walter, B. Doran, D. Gross, and M. Christandl, "Entanglement polytopes: multiparticle entanglement from single-particle information," *Science*, vol. 340, no. 6137, pp. 1205–1208, 2013.

[39] A. Sawicki, A. Huckleberry, and M. Kuś, "Symplectic geometry of entanglement," *Communications in mathematical physics*, vol. 305, no. 2, pp. 441–468, 2011.

[40] A. Sawicki, M. Oszmaniec, and M. Kuś, "Convexity of momentum map, morse index, and quantum entanglement," *Reviews in Mathematical Physics*, vol. 26, no. 03, p. 1450004, 2014.

[41] T. Macikazek and A. Sawicki, "Asymptotic properties of entanglement polytopes for large number of qubits," *Journal of Physics A: Mathematical and Theoretical*, vol. 51, no. 7, p. 07LT01, 2018.

[42] M. Aulbach, D. Markham, and M. Murao, "Geometric entanglement of symmetric states and the majorana representation," in *Conference on Quantum Computation, Communication, and Cryptography*, pp. 141–158, Springer, 2010.

[43] W. Fulton and J. Harris, *Representation theory: a first course*, vol. 129. Springer Science & Business Media, 2013.

[44] A. P. Polychronakos and K. Sfetsos, "Composition of many spins, random walks and

statistics," *Nuclear Physics B*, vol. 913, pp. 664–693, 2016.

[45] C. Chryssomalakos, L. Hanotel, E. Guzmán-González, D. Braun, E. Serrano-Ensástiga, and K. Życzkowski, "Symmetric multiqudit states: Stars, entanglement, and rotosensors," *Physical Review A*, vol. 104, no. 1, p. 012407, 2021.

[46] D. Baguette, T. Bastin, and J. Martin, "Multiqubit symmetric states with maximally mixed one-qubit reductions," *Phys. Rev. A*, vol. 90, p. 032314, 2014.

[47] T. Durt, B.-G. Englert, I. Bengtsson, and K. Życzkowski, "On mutually unbiased bases," *International journal of quantum information*, vol. 8, no. 04, pp. 535–640, 2010.

[48] S. Brierley, S. Weigert, and I. Bengtsson, "All mutually unbiased bases in dimensions two to five," *arXiv preprint arXiv:0907.4097*, 2009.

[49] T.-C. Wei and P. M. Goldbart, "Geometric measure of entanglement and applications to bipartite and multipartite quantum states," *Physical Review A*, vol. 68, no. 4, p. 042307, 2003.

[50] J. Martin, O. Giraud, P. Braun, D. Braun, and T. Bastin, "Multiqubit symmetric states with high geometric entanglement," *Physical Review A*, vol. 81, no. 6, p. 062347, 2010.

[51] M. Enríquez, I. Wintrowicz, and K. Życzkowski, "Maximally entangled multipartite states: a brief survey," in *Journal of Physics: Conference Series*, vol. 698, p. 012003, IOP Publishing, 2016.

[52] R. Hübener, M. Kleinmann, T.-C. Wei, C. González-Guillén, and O. Gühne, "Geometric measure of entanglement for symmetric states," *Physical Review A*, vol. 80, no. 3, p. 032324, 2009.

[53] J. Grabowski, M. Kuś, and G. Marmo, "Entanglement for multipartite systems of indistinguishable particles," *Journal of Physics A: Mathematical and Theoretical*, vol. 44, no. 17, p. 175302, 2011.

[54] K. C. Tan and H. Jeong, "Nonclassical light and metrological power: An introductory review," *AVS Quantum Science*, vol. 1, no. 1, p. 014701, 2019.

[55] B. Babadi, N. Kalouptsidis, and V. Tarokh, "Asymptotic achievability of the cramér–rao

bound for noisy compressive sampling," *IEEE Transactions on Signal Processing*, vol. 57, no. 3, pp. 1233–1236, 2008.

[56] M. G. Paris, "Quantum estimation for quantum technology," *International Journal of Quantum Information*, vol. 7, no. supp01, pp. 125–137, 2009.

[57] A. Z. Goldberg and D. F. James, "Quantum-limited euler angle measurements using anticoherent states," *Physical Review A*, vol. 98, no. 3, p. 032113, 2018.

[58] S. L. Braunstein and C. M. Caves, "Statistical distance and the geometry of quantum states," *Physical Review Letters*, vol. 72, no. 22, p. 3439, 1994.

[59] J. Martin, S. Weigert, and O. Giraud, "Optimal detection of rotations about unknown axes by coherent and anticoherent states," *Quantum*, vol. 4, p. 285, 2020.

[60] D. Baguette, T. Bastin, and J. Martin, "Multiqubit symmetric states with maximally mixed one-qubit reductions," *Physical Review A*, vol. 90, no. 3, p. 032314, 2014.

[61] D. Varshalovich, A. Moskalev, and V. Khersonskii, *Quantum Theory of Angular Momentum*. World Scientific, 1988.

[62] C. Chryssomalakos and H. Hernández-Coronado, "Optimal quantum rotosensors," *Physical Review A*, vol. 95, no. 5, p. 052125, 2017.

[63] C. Chryssomalakos, E. Guzmán-González, L. Hanotel, and E. Serrano-Ensástiga, "Stellar representation of multipartite antisymmetric states," *Commun. Math. Phys.*, vol. 381, pp. 735–764, 2021. `arXiv:1909.02592`.

[64] B. G. Wybourne, "Hermite's reciprocity law and the angular-momentum states of equivalent particle configurations," *Journal of Mathematical Physics*, vol. 10, no. 3, pp. 467–471, 1969.

[65] F. D. Murnaghan, "A generalization of hermite's law of reciprocity," *Proceedings of the National Academy of Sciences of the United States of America*, vol. 37, no. 7, p. 439, 1951.

[66] F. Berdjis, "A criterium for completeness of casimir operators," *J. Math. Phys.*, vol. 22, pp. 1850–1856, 1981.

[67] M. V. Berry, "Quantal phase factors accompanying adiabatic changes," *Proceedings of the Royal Society of London. A. Mathematical and Physical Sciences*, vol. 392, no. 1802, pp. 45–57, 1984.

[68] Y. Aharonov and J. Anandan, "Phase change during a cyclic quantum evolution," *Phys. Rev. Lett.*, vol. 58, pp. 1593–1596, Apr 1987.

[69] F. Wilczek and A. Zee, "Appearance of gauge structure in simple dynamical systems," *Phys. Rev. Lett.*, vol. 52, pp. 2111–2114, Jun 1984.

[70] N. Mukunda and R. Simon, "Quantum kinematic approach to the geometric phase. i. general formalism," *Annals of Physics*, vol. 228, no. 2, pp. 205–268, 1993.

[71] G. Benenti, G. Casati, and G. Strini, *Principles of quantum computation and information: Volume I: Basic Concepts*. World scientific, 2004.

[72] B. Field and T. Simula, "Introduction to topological quantum computation with non-abelian anyons," *Quantum Science and Technology*, vol. 3, no. 4, p. 045004, 2018.

[73] S. Tanimura, "Holonomic quantum computing and its optimization," in *Mathematical Aspects Of Quantum Computing 2007*, pp. 115–138, World Scientific, 2008.

[74] P. Zanardi and M. Rasetti, "Holonomic quantum computation," *Physics Letters A*, vol. 264, no. 2-3, pp. 94–99, 1999.

[75] P. W. Shor, "Algorithms for quantum computation: Discrete logarithms and factoring," in *Foundations of Computer Science, 1994 Proceedings., 35th Annual Symposium on*, pp. 124–134, Ieee, 1994.

[76] D. Aharonov, V. Jones, and Z. Landau, "A polynomial quantum algorithm for approximating the jones polynomial," *Algorithmica*, vol. 55, no. 3, pp. 395–421, 2009.

[77] X.-S. Ma, T. Herbst, T. Scheidl, D. Wang, S. Kropatschek, W. Naylor, B. Wittmann, A. Mech, J. Kofler, E. Anisimova, *et al.*, "Quantum teleportation over 143 kilometres using active feed-forward," *Nature*, vol. 489, no. 7415, pp. 269–273, 2012.

[78] S. Tanimura, M. Nakahara, and D. Hayashi, "Exact solutions of the isoholonomic problem and the optimal control problem in holonomic quantum computation," *Journal of*

mathematical physics, vol. 46, no. 2, p. 022101, 2005.

[79] L.-M. Duan, J. I. Cirac, and P. Zoller, "Geometric manipulation of trapped ions for quantum computation," *Science*, vol. 292, no. 5522, pp. 1695–1697, 2001.

[80] E. Sjöqvist, "Geometric phases in quantum information," *Intern. J. Quant. Chem.*, vol. 115, pp. 1311–1326, 2015.

[81] E. Serrano, *Shapes in Quantum Mechanics*. Tesis de Doctorado, UNAM, 2018.

[82] P. Aguilar, C. Chryssomalakos, E. Guzmán-González, L. Hanotel, and E. Serrano-Ensástiga, "When geometric phases turn topological," *arXiv preprint arXiv:1903.05022*, 2019.

[83] J. Robbins and M. Berry, "A geometric phase for m= 0 spins," *Journal of Physics A: Mathematical and General*, vol. 27, no. 12, p. L435, 1994.